UNIVERSIDADE FEDERAL DE SANTA CATARINA
PROGRAMA DE PÓS-GRADUAÇÃO EM ENGENHARIA DE AUTOMAÇÃO E SISTEMAS

Michael Klug

CONTROL OF NONLINEAR SYSTEMS USING N-FUZZY MODELS

Florianópolis

2015

Michael Klug

CONTROL OF NONLINEAR SYSTEMS USING N-FUZZY MODELS

A Thesis submitted to the Departament of Automation and Systems Engineering in partial fulfillment of the requirements for the degree of Doctor of Philosophy in Automation and Systems Engineering.
Supervisor: Dr. Eugênio de Bona Castelan Neto
Co-Supervisor: Dr. Daniel Ferreira Coutinho

Florianópolis

2015

Ficha de identificação da obra elaborada pelo autor,
através do Programa de Geração Automática da Biblioteca Universitária da UFSC.

Klug, Michael
Control of Nonlinear Systems Using N-fuzzy models / Michael Klug ; orientador, Eugênio de Bona Castelan Neto ; coorientador, Daniel Ferreira Coutinho. - Florianópolis, SC, 2015.
183 p.

Tese (doutorado) - Universidade Federal de Santa Catarina, Centro Tecnológico. Programa de Pós-Graduação em Engenharia de Automação e Sistemas.

Inclui referências

1. Engenharia de Automação e Sistemas. 2. T-S Fuzzy Models. 3. Nonlinear Systems. 4. Local Stability. 5. Disturbances. I. Castelan Neto, Eugênio de Bona . II. Coutinho, Daniel Ferreira. III. Universidade Federal de Santa Catarina. Programa de Pós-Graduação em Engenharia de Automação e Sistemas. IV. Título.

Michael Klug

CONTROL OF NONLINEAR SYSTEMS USING N-FUZZY MODELS

This Thesis is hereby approved and recommended for acceptance in partial fulfillment of the requirement for the degree of "Doctor of Philosophy in Automation and Systems Engineering".

Florianópolis, 7 December 2015.

Dr. Eugênio de Bona Castelan Neto
Supervisor

Dr. Daniel Ferreira Coutinho
Co-Supervisor

Dr. Rômulo Silva de Oliveira
Graduate Program Coordinator

Examining Comittee:

Dr. Eugênio de Bona Castelan Neto
Chair

Dr. Reinaldo Martinez Palhares

Dr. Ricardo Coração de Leão Fontoura de Oliveira

Dr. Alexandre Trofino Neto

Dr. Edson Roberto de Pieri

Dr. Hector Bessa Silveira

ABSTRACT

Takagi-Sugeno (T-S) fuzzy models have been extensively investigated over the last decade to develop the so-called fuzzy model based (FMB) control techniques, providing nonlinear control design methodologies with a systematic aspect and numerical solution. However, the actual T-S fuzzy modeling techniques, in general, only guarantee the convexity of the model and/or their accuracy of representation for a specific domain of the state space. Thus, for control strategies based on convexity properties, the stability of the closed-loop system composed of the nonlinear system and the fuzzy controller should be analyzed in a local context, being fundamental to determine stability regions for the closed-loop system. This inherent local characteristic is often not considered in most FMB control design results, which may lead to poor performance or even instability of the closed-loop system.

In this sense, this thesis aims to consider the regional validity of the T-S fuzzy models for the development of nonlinear discrete-time control systems analysis and design tools, to consider other physical constraints and to discuss the problems associated with the complexity of T-S fuzzy models. A modeling method based on the use of nonlinear local rules that provides a compact and accurate representation is presented, allowing also to handle with the dynamic output feedback control problem for systems with nonlinearities that may depend on unmeasurable states. Using fuzzy Lyapunov functions (FLF), closed-loop stability conditions are provided, which can be verified in terms of the feasibility of a set of linear matrix inequalities (LMIs). The proposed controllers are based on a state and sector nonlinearities feedback, for systems subject to disturbances bounded in energy or amplitude, and on a dynamic output feedback, for systems with saturating actuators. Numerical examples are presented throughout this document to illustrate the effectiveness of the proposed design methodologies. Further, aiming to assist students and engineers in the nonlinear control system design, an interactive computational tool is presented for fuzzy modeling and control. Practical aspects and a study of the digital implementation of fuzzy controllers are discussed using a Hardware-in-the-Loop (HIL) simulation with a Field Programmable Gate Array (FPGA) development board.

Keywords: nonlinear systems, local stability, T-S fuzzy models, disturbances.

RESUMO EXPANDIDO

CONTROLE DE SISTEMAS NÃO LINEARES UTILIZANDO MODELOS N-FUZZY

Palavras-chave: sistemas não lineares, estabilidade local, modelos fuzzy T-S, perturbações.

Introdução

A utilização de modelos fuzzy Takagi-Sugeno (T-S) tem sido extensivamente investigada no decorrer das últimas décadas, principalmente por propiciarem o desenvolvimento de metodologias de projeto de sistemas de controle não lineares que possuem caráter sistemático e solução numérica. Uma importante razão para isto é que os modelos T-S (TAKAGI; SUGENO, 1985) fornecem uma representação de plantas não lineares por uma combinação de submodelos lineares locais (ou afins) invariantes no tempo, também chamados de regras, permitindo estender e utilizar de forma natural e elegante alguns resultados e ferramentas comuns à teoria de controle robusto e de sistemas lineares com parâmetros variantes (LPV, do inglês *Linear Parameter Varying*) (MOZELLI; PALHARES, 2011b). Tal combinação de regras é controlada por funções peso-normalizadas, denominadas de funções de pertinência (GAO et al., 2012). Este conceito é mais amplo que a linearização da planta em um único ponto de interesse, pois possibilita a descrição em regiões mais distantes, formando um domínio de operação para o sistema.

Muito embora diversos resultados de análise de estabilidade e síntese de controladores sejam encontrados na literatura, existem questões com motivação prática que permanecem em aberto no contexto do controle fuzzy baseado em modelo (FMB, do inglês *Fuzzy Model Based*) (FENG, 2010). Em geral, as técnicas de modelagem fuzzy T-S atuais garantem a convexidade do modelo e/ou a sua precisão de representação somente para uma determinada região do espaço de estados. Desta forma, para estratégias de controle baseadas em propriedades de convexidade, a estabilidade do sistema de malha fechada formado pelo sistema não linear realimentado pela lei de controle fuzzy deve ser estudada no contexto de estabilidade local, sendo fundamental a determinação de regiões de estabilidade para o sistema de malha fechada.

Esta importante característica dos modelos fuzzy T-S raramente é considerada na literatura, podendo implicar em perda de desempenho e até mesmo instabilidade do sistema em malha fechada (KLUG et al., 2014). Outro problema inerente à utilização de modelos fuzzy T-S diz respeito ao aumento exponencial de complexidade do modelo com o número de não linearidades presentes no sistema (LAM, 2011), principalmente quando se busca descrever de forma exata a dinâmica do sistema a controlar, o que implica no aumento da complexidade numérica dos algoritmos para análise e projeto, assim como do aumento da complexidade de implementação de leis de controle.

Neste contexto, esta tese busca evidenciar a importância da consideração da validade regional dos modelos fuzzy de tipo T-S para o desenvolvimento de ferramentas de análise e síntese de sistemas de controle não lineares, assim como considerar outras restrições físicas presentes no sistema de controle como limites nos atuadores, e discutir a problemática associada à complexidade dos modelos fuzzy T-S.

Objetivos

De modo geral, um dos problemas que devem ser resolvidos no projeto de controladores fuzzy T-S aplicados a sistemas não lineares diz respeito à consideração das restrições impostas tanto pelo processo de modelagem, relacionado ao domínio de validade regional do modelo, quanto a restrições físicas comuns aos atuadores, e também na presença de sinais externos comumente encontrados em sistemas reais. Neste contexto, os seguintes objetivos específicos são estabelecidos:

- Definir um arcabouço de ferramentas teóricas e algorítmicas para a consideração do domínio de validade dos modelos fuzzy T-S no projeto de sistemas de controle não lineares, utilizando também da teoria de estabilidade de Lyapunov para a construção de conjuntos contrativos de forma a estimar a região de atração do sistema de malha fechada (calcular regiões de estabilidade);
- Formalizar um processo de modelagem com redução do número de regras que possibilite uma menor complexidade numérica, permitindo também a implementação de controladores por realimentação dinâmica de saídas com não linearidades que dependam de estados não mensuráveis do sistema. Este processo de modelagem é baseado na utilização de modelos fuzzy T-S com submodelos não lineares locais, denominados neste trabalho de modelos N-fuzzy;
- Desenvolver condições de análise de estabilidade e síntese de controladores com garantia de desempenho para sistemas não lineares

representados por modelos N-fuzzy, levando em consideração o domínio de validade regional com estimação de regiões de estabilidade e perturbações externas, como as de energia limitada e/ou as de amplitude limitada;

- Efetuar simulações Hardware-in-the-Loop (HIL) considerando que as plantas sejam emuladas virtualmente e os controladores implementados em uma plataforma programável real, a fim de analisar a complexidade de implementação digital de controladores fuzzy clássicos e N-fuzzy;
- Prover uma ferramenta interativa à comunidade científica relacionada com vistas a auxiliar estes usuáros no projeto de controle não linear usando técnicas fuzzy.

Contextualização

A lógica fuzzy foi introduzida pelo professor Lofti A. Zadeh da Universidade da Califórnia, a qual definiu uma nova teoria de conjuntos (ZADEH, 1965). O princípio fundamental desta lógica é que um determinado elemento pode pertencer, em um certo grau, a um conjunto e, em um outro grau, a um outro conjunto. Nota-se este tipo de relação de pertinência em várias situações da natureza e na vida cotidiana. Esta percepção foi relacionada posteriormente à similaridade com o comportamento humano na solução de problemas complexos, permitindo por exemplo, que o projetista utilize o conhecimento experimental para elaborar o projeto de controle do seu sistema. Desde então, a teoria de lógica fuzzy tem sido utilizada com sucesso em diversas aplicações de engenharia, e dentre as várias arquiteturas existentes, destaca-se o uso dos modelos fuzzy T-S (FENG, 2010).

Os modelos fuzzy T-S baseiam-se na utilização de um conjunto de regras fuzzy para descrever um sistema não linear em termos de submodelos lineares/afins invariantes no tempo e locais, conectados por funções de pertinência que controlam a lei de interpolação entre as regras. Esta representação facilita, através da utilização da teoria de Lyapunov, a descrição dos problemas de controle na forma de desigualdades matriciais lineares (LMIs, do inglês *Linear Matrix Inequalities*) (BOYD et al., 1994), e portanto a obtenção de solução numérica confiável. Um método comum é o uso de funções de Lyapunov quadráticas, ao qual porém, em geral, conduzem a resultados conservadores. Recentemente, funções de Lyapunov fuzzy (FLF, do inglês *Fuzzy Lyapunov Function*) tem sido utilizadas para se obter condições de projeto menos conservadores ao custo de um aumento da carga computacional (GUERRA; VERMEIREN, 2004).

Neste contexto, o número de regras para representação do modelo T-S pode tornar o problema de projeto de controle computacionalmente intratável, ao qual poucos estudos se destinam a reduzir o número de regras mantendo a descrição exata do sistema original. Excetuam-se os trabalhos de Dong, Wang & Yang (2009, 2010) e Klug & Castelan (2011), ao qual admitem que determinados termos não lineares pertencentes a setores limitados apareçam explicitamente nos submodelos locais. Isto é perfeitamente aplicável na prática, visto que uma grande classe de não linearidades verificam condições de setor ao menos localmente, além de trazer o mecanismo matemático desenvolvido para lidar com não linearidades de setor para o controle de sistemas FMB (LIBERZON, 2006).

Outros aspectos práticos estão relacionados com não linearidades inerentes aos atuadores, tais como saturação, zona morta e/ou histerese. Por exemplo, a presença de saturação (TARBOURIECH et al., 2011a) pode causar efeitos indesejados, como o surgimento de ciclos limites e pontos de equilíbrio, deterioração do desempenho e até mesmo instabilidade do sistema de malha fechada. Além disso, a importante característica de validade local de convexidade dos modelos fuzzy T-S normalmente não é considerada na literatura, podendo comprometer o uso dos controladores obtidos por estas metodologias, com a possibilidade do sistema de controle violar os limites seguros de operação, perder desempenho ou até mesmo instabilizar as trajetórias do sistema de malha fechada.

Contribuições da Tese

Dentre as contribuições da pesquisa realizada, no Capítulo 2 é apresentado a formalização de uma técnica de modelagem fuzzy baseada na utilização de submodelos não lineares que permite a redução do número de regras fuzzy sem comprometer a exatidão da representação. Esta metodologia pode ser uma importante fonte de redução de complexidade numérica, facilitando a obtenção de soluções factíveis ao problema de controle posteriormente definido. Além disso, a flebilidade proporcionada por esta metodologia permite ao projetista modificar a lei de controle convenientemente, para possuir ou não termos de realimentação do vetor de não linearidades de setor, tornando possível por exemplo a implementação de controladores por realimentação dinâmica de saídas de sistemas que possuam não linearidades que dependam de estados não mensuráveis do sistema. Nos Capítulos 3, 4 e 5, partindo da utilização de funções de Lyapunov fuzzy para definir condições de estabilidade para o sistema em malha fechada, obtém-se ferramentais baseados em desigualdades matriciais lineares, aos quais são utilizados para o projeto de controladores. Os controladores propostos são baseados na realimentação de estados e do vetor de não linearidades de setor, ao qual são consideradas perturbações limitadas em energia ou amplitude, e na realimentação dinâmica de saídas, para sistemas não perturbados com atuadores saturantes ou para sistemas sujeitos a perturbações persistentes. Em todos os casos a importante característica local da modelagem fuzzy T-S é levada em consideração na fase de projeto, ao qual através de uma condição de inclusão garante-se que as trajetórias do sistema de malha fechada evoluam apenas no interior do domínio garantido de validade de convexidade do modelo fuzzy T-S.

Além disso, objetivando auxiliar estudantes, engenheiros e pesquisadores na análise e projeto de controle de sistemas não lineares, apresenta-se no Capítulo 6 o desenvolvimento de uma ferramenta computacional interativa para a modelagem e controle fuzzy. Complementarmente, aspectos práticos e um estudo da complexidade de implementação digital de controladores fuzzy são discutidos através de uma simulação *Hardware-in-the-Loop* (HIL) com utilização de uma placa de desenvolvimento FPGA (do inglês *Field Programmable Gate Array*).

Conclusão

Nesta tese, novas abordagens para o projeto de controladores aplicados a sistemas não lineares em tempo discreto que possam ser representados por modelos fuzzy T-S são desenvolvidas. Considera-se um método alternativo de modelagem baseado no uso de regras não lineares locais, que possibilita os seguintes benefícios: i) redução do número de regras em relação a abordagem clássica, que conduz a uma diminuição da complexidade numérica mantendo a exatidão da representação e ii) flexibilidade no controle, permitindo o projeto e implementação prática de controladores por realimentação dinâmica de saídas na presença de não linearidades que dependam de estados não mensuráveis do sistema. Além disso, os resultados propostos consideram os problemas inerentes ao projeto de controle, tais como a validade regional dos modelos fuzzy T-S, restrições físicas nos atuadores, e a presença de sinais externos usualmente encontrados em sistemas reais. Exemplos numéricos são apresentados ao longo do trabalho com o objetivo de ilustrar a eficiência dos métodos propostos.

LIST OF FIGURES

LIST OF TABLES

ABBREVIATIONS

NOTATIONS

$\subset (\subseteq)$	Subset (subset or equal)
$\in$	Included
$\notin$	Not included
$\forall$	For all
$\Re$	Set of real numbers
$\Re^+$	Set of non-negative real numbers
$\mathbb{Z}^+$	Set of non-negative integer numbers
$\Re^n$	n-dimensional real vector space
$\Re^{n \times m}$	$n \times m$-dimensional real matrix
$x_{(i)}$	i^{th} element of vector x
$X_{\{i\}}$	i^{th} row of matrix X
A' (a')	Transpose of a matrix (vector) A (a)
A^{-1}	Inverse of a matrix A
$\|\|A\|\|$	Euclidean norm of a matrix A
$A > B$	For two matrices, $A - B$ is positive definite
$A \geq B$	For two matrices, $A - B$ is positive semi-definite
$\text{diag}\{A, B\}$	Block diagonal matrix, with main diagonal blocks A and B
$S[0, \Omega]$	Cone sector condition
$\mathcal{N}(N)$	Null space (kernel) of N
I (0)	Identity (zero) matrix with appropriate dimension
I_n (0_n)	n-dimensional identity (zero) matrix
$\star$	Symmetric block with respect to the main diagonal of a matrix
$\bullet$	Element that has no influence on the development

CONTENTS

1 INTRODUCTION

The control of nonlinear systems by means of fuzzy models has become quite popular over the last decades, attracting the attention of many researchers in Brazil and abroad. In particular, among the various studies and applications of Fuzzy Model Based (FMB) control techniques, the Takagi-Sugeno (T-S) fuzzy models (TAKAGI; SUGENO, 1985) have emerged as a successful approach. An important reason for this is that the T-S models can represent nonlinear systems in terms of local linear (or affine) time-invariant submodels, smoothly connected by means of nonlinear fuzzy membership functions (KOSKO, 1997; GAO et al., 2012) allowing the application of well-established Lyapunov and Linear Matrix Inequality (LMI) based tools for parameter varying control systems (MOZELLI; PALHARES, 2011b; KLUG; CASTELAN, 2012). This modeling technique is more comprehensive than the linearization of the plant at a single equilibrium point, since it allows a more accurate description at distant regions, forming a wider operating domain for the system. Figure 1 represents a fuzzy description of a certain class of nonlinear systems to be studied in this thesis.

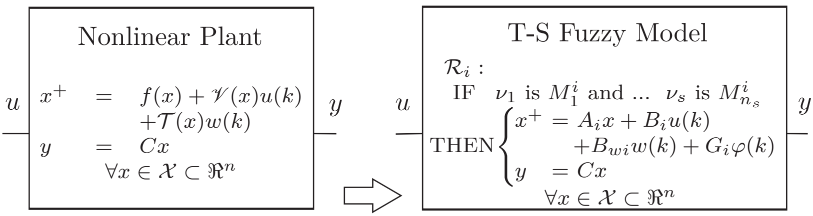

Figure 1 – T-S fuzzy models for nonlinear systems

A key issue when applying a T-S fuzzy representation for control purposes is the model accuracy, since T-S models can exactly or approximately represent the original nonlinear system to be controlled. In the exact description, the number of submodels, also known as fuzzy rules, increase exponentially with the number of nonlinearities, consequently increasing the numerical complexity of the control algorithms and complicating their implementation (LAM, 2011). To prevent a large number of rules, approximate models as described in Teixeira & Zak (1999) might be employed, which add some model inaccuracy, and may result in the loss of performance or even the instability of the closed-loop system.

Even though the exact T-S fuzzy representation has identical dynamics[1] to the original nonlinear system, the convexity of the model can only be guaranteed in a specific domain of the state space. Thus, for control strategies based on convex properties, the performance and dynamic behavior of the control system composed of the feedback interconnection of the nonlinear plant and the fuzzy controller may deteriorate if the system states evolve outside this domain. This inherent local characteristic of the fuzzy model should be taken into account when using fuzzy controllers applied to nonlinear plants, whether in the design phase, as considered in this work, or in subsequent analysis. This important aspect, which directly affects the practical results, is rarely considered in literature, and imposes the use of local stability concepts that, in consequence, can be dealt with the definition of contractive sets. The notion of contractive sets is basic to determine asymptotic stability regions for nonlinear systems, usually performed using Lyapunov functions. In this way, regions of admissible initial conditions that asymptotically converge to the origin are found (OLIVEIRA et al., 2011), and can be used as estimates of the domain of attraction of the closed-loop system (KHALIL, 2003).

In recent works, such as the articles Chadli & Guerra (2012), Li et al. (2014) and Zhu et al. (2015), a numerical complexity reduction of the control algorithms is obtained by decreasing the number of LMIs to be solved using the representation of nonlinear plants by descriptor systems. However, this approach does not effectively reduce the number of rules in the T-S fuzzy model, and few studies commit to maintaining the exact description of the original system. Some exceptions are the works Dong, Wang & Yang (2009, 2010), nevertheless without considering the T-S fuzzy models local characteristic, and the works Klug & Castelan (2011) and Klug, Castelan & Coutinho (2013), in which it is possible to reduce the number of fuzzy rules without compromising the model exactness by applying the technique referred to as N-fuzzy modeling. In this approach, some nonlinear sector bounded terms may explicitly appear in the T-S fuzzy models at the cost of losing the linearity of classical fuzzy modeling. This is perfectly reasonable in practice, since a large class of nonlinearities, as well as sensors and actuators limitations, can be considered as sector bounded functions, at least locally. In spite of losing the linearity of the fuzzy model, the N-fuzzy approach is quite interesting since the well-established mathematical machinery developed to handle sector bounded nonlinearities (such as the abso-

[1]Identical dynamics refers to the trajectories of the nonlinear system and its respective fuzzy model having the same behavior.

lute stability theory (KHALIL, 2003; LIBERZON, 2006)) can be applied to FMB control design.

At this point, it is worth mentioning that the research about the use of the nonlinear fuzzy models cited in the last paragraph was initiated by the author during the development of his master's thesis: "Realimentação Dinâmica de Saídas com Parâmetros Variantes e Aplicação aos Sistemas Fuzzy Takagi-Sugeno", UFSC, December 2010, which launched the basis for developing this doctoral thesis.

Considering the aforementioned context, this thesis seeks to: (i) demonstrate the importance of considering the regional validity of T-S fuzzy models for the development of analysis and synthesis tools for nonlinear control systems; (ii) develop algorithms for stability analysis and control design applied to nonlinear plants represented by T-S fuzzy models with a reduced number of rules; (iii) consider inherent restrictions on the system to be controlled and on the actuators, as well as the presence of external disturbances; and (iv) execute hardware-in-the-loop simulations in order to analyze the complexity of the digital implementation of classical and N-fuzzy controllers.

1.1 RELATED WORKS AND CONTEXTUALIZATION

The term "fuzzy logic" was introduced by Professor Lofti A. Zadeh at the University of California (ZADEH, 1965) in his definition of a new set theory. The fundamental principle of this logic is that an element can belong, with a certain degree, to a set, and with another degree, to another set. It is possible to see this type of membership relation in many situations in nature and daily life. This perception was subsequently related to human behavior in solving complex problems, allowing the use of experimental knowledge in control design (MAMDANI, 1974). Since then, the theory of fuzzy logic has been used in numerous control engineering applications, power systems, telecommunications, information processing, pattern recognition, signal processing, and economics, among others.

The main motivations for the study of fuzzy theory are the possibility to process uncertain or qualitative information and the ability of fuzzy models to serve as a universal approximator (FENG, 2010). Several different architectures of fuzzy control have been developed, suitable for different types of applications, such as Mamdani models (MAMDANI; ASSILIAN, 1975; MAMDANI, 1977). Among these, the use of T-S models has been prominent in the last decades, due to a higher formalism and mathematical rigor of this technique.

The T-S fuzzy systems are based on the use of a set of fuzzy rules to describe a nonlinear system in terms of local linear (or affine) time-invariant submodels, blended by membership functions that control the law of interpolation between the rules (ALATA; DEMIRLI; BULGAK, 1999; FENG, 2010). This is a more general concept in relation to the linearization of a nonlinear system at a single point of interest, which probably cannot adequately describe the dynamic behavior of the system over the entire operating range, as it is not possible to predict the corresponding domain of attraction. Moreover, the classical linearization method can be considered as a particular case of the T-S fuzzy model consisting of only one local submodel. It should also be emphasized that the T-S fuzzy representation allows the application of the theoretical and algorithmic background used in robust control and systems with varying parameters for analysis and design of controllers. In particular, it can be verified close relations between the control design and implementation techniques using T-S models with the ones defined for Linear Parameter Varying (LPV) systems (MOZELLI; PALHARES, 2011b; KLUG; CASTELAN, 2012).

Most of FMB control design results consist of formulating analysis and synthesis conditions as convex optimization problems (FENG, 2006; GUERRA; KRUSZEWSKI; LAUBER, 2009; WU et al., 2011; YANG; YANG, 2012; GUERRA et al., 2012a) described in terms of LMIs (BOYD et al., 1994). A popular method is the use of a common quadratic Lyapunov function (TANAKA; WANG, 2001) because of the simplicity in deriving numerical and tractable conditions. However, a common quadratic Lyapunov function may lead to conservative results, in general terms, since a single Lyapunov matrix should be found for all T-S local submodels. Recently, Fuzzy Lyapunov Functions (FLF) have been used to obtain less conservative design conditions at the cost of extra computations, as proposed, for instance, in Guerra & Vermeiren (2004). Another possibility is the use of piecewise Lyapunov functions, among others, commonly applied to a control scheme called Parallel Distributed Compensation (PDC) (FENG, 2010). Alternative structures have also been used, such as the non-PDC (GUERRA; VERMEIREN, 2004) and the switched-PDC control (DONG; YANG, 2008).

In this context, the number of local submodels required for the T-S model representation may make the FLF-FMB control design problem computationally intractable, which is partly related to the modeling error. For example, in the application of an exact description to complex systems, the excessive number of rules can make it difficult to find feasible solutions for the control algorithms, which also complicates the implementation of the obtained controllers. In this case, it is possible to consider the use of approximate fuzzy models, such as the method in Teixeira & Zak (1999). However, the closed-loop system composed of the designed fuzzy controller and the original nonlinear system may not meet the control specifications, causing a loss of performance or even instability due to the model inaccuracy. In Daruichi (2003), optimization based techniques for obtaining the fuzzy models with the minimization of modeling error are presented. Alternative approaches for rule reduction consist of using uncertain T-S models (TANIGUCHI et al., 2001). Nevertheless, researchers have made little progress obtaining fuzzy models with a reduced number of rules and maintaining the exact description.

Based on the aforementioned issue, and allowing certain nonlinear terms belonging to bounded sectors to explicitly appear in local submodels, it is possible to obtain an exact fuzzy description with a reduced number of rules. From a practical point of view this is perfectly reasonable, since a large class of nonlinearities verifies, at least locally, bounded sector conditions, as polynomial terms with odd degree, some trigonometric functions, saturation, dead-zone, hysteresis, among others (KHALIL, 2003). A graphic description of a global and a local bounded sector nonlinearity is shown in Figure 2.

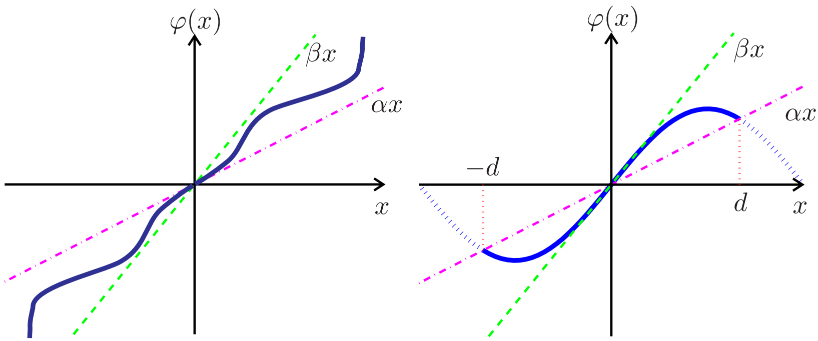

Global Sector: $\varphi(.) \in S[\alpha, \beta], \forall x \in \Re$ Local Sector: $\varphi(.) \in S[\alpha, \beta]$ for $|x| \leq d$

Figure 2 – Sector nonlinearities

The fuzzy model composed of nonlinear local submodels, or simply N-fuzzy model, can be viewed as a linear parameter varying system with a sector bounded nonlinearity in the feedback loop. Although the linearity of fuzzy rules is lost, the counterpart may be positive, since all the mathematical machinery developed to handle sector bounded nonlinearities can be applied for FMB control design, such as the absolute stability theory (LIBERZON, 2006).

Notwithstanding the many stability analysis and synthesis conditions that have been extensively developed in the past years, there are some practical motivated issues that remain open, or that were not fully solved yet in the context of FMB control systems. Some of them may compromise the stability analysis and synthesis conditions used nowadays. Among them, one may first cite the region of operation of a plant or the regional validity of the model used in the FMB control system. This inherent local characteristic of T-S modeling techniques is often not considered in most FMB control design results (see, e.g., Chang & Yang (2014), Figueredo et al. (2014), Qiu, Feng & Gao (2013), Chang (2012), Golabi, Beheshti & Asemani (2012), Su et al. (2012)), which may lead to poor performance or even instability of the actual nonlinear closed-loop system (consisting of the original nonlinear plant and the designed fuzzy controller). The local stability issue in T-S fuzzy models may also be related to the natural existence of constraints in the state variables of real systems, due, for example, to safe operational conditions, physical limitations or some desired level of energy consumptions, as discussed in Klug et al. (2014); or related to the presence of time-derivatives of the membership functions in the stability analysis when dealing with continuous-time systems, as in Guerra et al. (2012b) and Tognetti, Oliveira & Peres (2013).

Recently, in Tanaka et al. (2012a), fuzzy polynomial models that allow a global representation of the nonlinear plant are used. However, this approach is too restrictive as it requires that the nonlinearities are of the polynomial type or belonging to a global sector, limiting its application to real systems. Also, aiming for a lower conservatism of the control algorithms solution, several techniques based on relaxed LMIs conditions have been proposed, as can be seen in Montagner, Oliveira & Peres (2010), Tognetti, Oliveira & Peres (2011) and Faria, Silva & Oliveira (2013), still not considering the issue of model validity, for instance.

Another practical aspect is related to the actuators nonlinearities, such as saturation, relay, dead-zone and/or hysteresis. For example, the saturation is one of the most common nonlinearities in control and automation engineering practice, and usually derives from physical limitations imposed by the actuation devices. The presence of saturation may cause undesired effects, such as the appearance of limit cycles and multiple equilibrium points, potentially causing performance degradation and even instability of the closed-loop system. Thus, considering saturation in the analysis and design of control systems is a subject of theoretical and practical importance (TARBOURIECH et al., 2011a). It can be observed a graphic description of some typical nonlinearities in Figure 3.

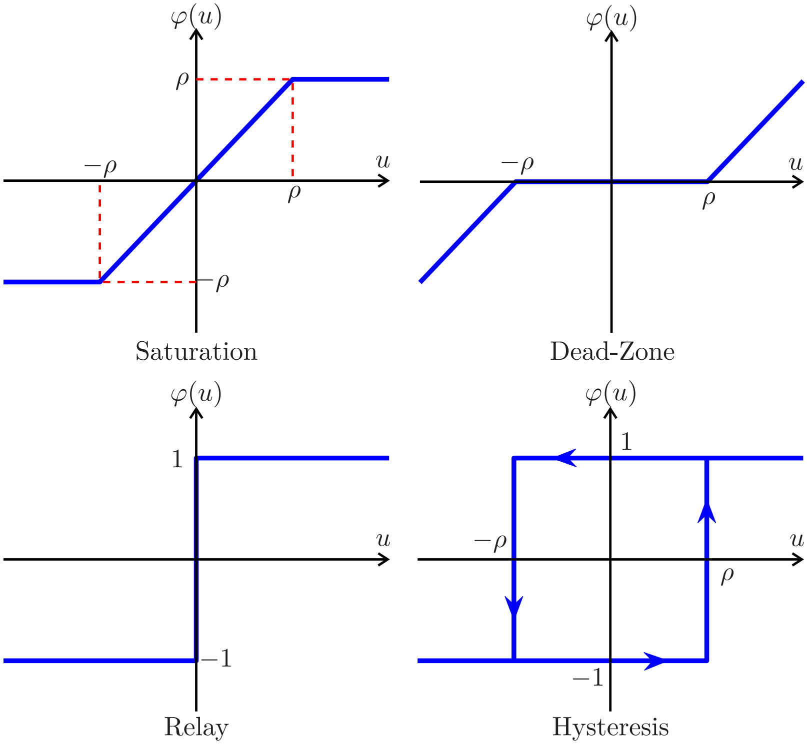

Figure 3 – Typical nonlinearities

Another topic of fuzzy systems research corresponds to the consideration of nonlinear plants subject to exogenous disturbance signals (MONTAGNER; OLIVEIRA; PERES, 2010) and time-delay systems (WU et al., 2011; HUANG; HE; ZHANG, 2011; TANAKA et al., 2012b). In the first case, most of the FMB results are concentrated on continuous-time systems, such as in Wang & Liu (2013), Lee, Joo & Tak (2014) and Wang et al. (2015). The discrete-time counterpart has been recently addressed in Klug, Castelan & Coutinho (2013), for the input-to-state (ISS) stabilization problem, and in an enhanced version in Klug, Castelan & Coutinho (2015a) an input-to-output performance criterion was also considered. Both articles consider energy bounded disturbances and the local behavior of the design conditions. It should be emphasized that in the presence of amplitude bounded disturbances, the asymptotic stability of the origin cannot be guaranteed and, in this case, the concept of ultimate bounded (UB) stability is considered (i.e., the state trajectory is guaranteed to converge to a region in the vicinity of the system origin). This problem is handled in the work Klug, Castelan & Coutinho (2015).

On the other hand, some recent results have addressed the FMB dynamic output feedback control problem such as in Zhang, Jiang & Staroswiecki (2010), Yoneyama (2014) and Nguyen, Dequidt & Dambrine (2015), considering the premise variables to be available online to the controller. This assumption is noticeably restrictive, since the premise variables vector is, in general, a nonlinear function of measurable and unmeasurable states (ASEMANI; MAJD, 2013). In Tognetti, Oliveira & Peres (2012) the problem of reduced-order dynamic output feedback control design for continuous-time systems is considered, using a line-integral fuzzy Lyapunov function, allowing the membership functions to vary arbitrarily. The controller is obtained in a two-stage LMI procedure with multi-simplex approach.

Finally, it is also important to highlight that the use of T-S fuzzy models allows the systematic design with a numerical solution of nonlinear control systems, whereas other techniques, such as feedback linearization, sliding-mode control, backstepping, passivity-based control, among others, usually requires that the equations of the plant are presented in a particular way and/or are only applied to a specific class of systems, besides having only analytic solutions. Thus, T-S fuzzy models provide an interesting framework for dealing with the fundamental issues in modern control theory for complex nonlinear systems.

1.2 OBJECTIVES

Overall, a fundamental issue that must be solved in T-S fuzzy controller design applied to nonlinear systems is concerning the restrictions imposed either by the modeling process, related to the regional validity of the model, or by the inherent physical constraints of actuators. Also, the presence of external signals usually found in real systems should be considered. In this context, the following specific objectives can be established:

- Define a theoretical and algorithmic framework to take into account the regional validity of the T-S fuzzy models in the nonlinear control systems design, using the Lyapunov stability theory for building contractive sets in order to estimate the domain of attraction of the closed-loop system (compute stability regions);

- Standardize a modeling process that provides a reduced number of rules and consequently a decrease in the numerical complexity of the control algorithms, allowing also to handle the dynamic output feedback control problem for systems with nonlinearities that may depend on unmeasurable states. This modeling process is based on the use of T-S fuzzy models with nonlinear local rules, referred to in this work as N-Fuzzy models;

- Develop conditions to synthesize controllers with guaranteed performance for nonlinear systems represented by N-fuzzy models, considering their regional validity and providing estimates of the stability region and admissible disturbance set, such as the ones bounded in energy and/or bounded in amplitude;

- Perform Hardware-in-the-Loop (HIL) simulations considering the physical plant virtually emulated using a computer and the controllers embedded in a real programmable platform, in order to analyze the complexity of digital implementation of classical and N-fuzzy controllers; and

- Provide an interactive tool for the scientific community of the related area aiming to assist those users in the nonlinear control design using fuzzy strategies.

Specifically this thesis considers only nonlinear discrete-time systems, not covering the discretization process for obtaining it. This important aspect is a future perspective of this work in order to perform real implementations of the obtained theoretical results.

1.3 STRUCTURE OF THE THESIS

This document is organized as follows:

In Chapter 2 some fundamental concepts are presented on Takagi-Sugeno fuzzy systems with nonlinear local rules, as well as the associated modeling process, discussions concerning the regional validity and a comparison of the numerical complexity involving classical and N-fuzzy models. It is important to emphasize the flexibility provided by N-fuzzy modeling, allowing the control designer to conveniently modify the control law in relation to the vector of sector nonlinearities, enabling for instance the practical implementation of fuzzy dynamic controllers.

Chapters 3, 4 and 5 are composed of the main contributions of this thesis, the results of which have been published or submitted in national and international conferences and journals. These chapters deal with, respectively: i) dynamic output feedback control design for nonlinear systems with saturating actuators represented by T-S fuzzy models; ii) the input-to-state stabilization problem with a certain input-to-output performance for nonlinear systems subject to energy bounded disturbances; and iii) ultimate bounded stabilization for nonlinear systems subject to amplitude bounded disturbances using state and dynamic output feedback in a special configuration that allows the presence of unmeasurable nonlinearities. In all cases the inherent local characteristic of T-S modeling technique is taken into consideration in the design phase, ensuring that the closed-loop trajectories evolve only in the T-S domain of validity.

Chapter 6 deals with the development of a user-friendly stability analysis and control design tool with interactive properties. This allows the user to, in a few steps, obtain a reasonable controller for a known nonlinear system that meets some desired closed-loop performance requirements. This chapter also presents practical aspects for implementing T-S fuzzy controllers, analyzed from hardware-in-the-loop simulations using a Field Programmable Gate Array (FPGA) development board.

In Chapter 7 some conclusions and recommendations for future research are discussed. The appendices present some additional information which complements the understanding of the preceding chapters.

2 T-S FUZZY MODELS, RULE REDUCTION AND REGIONAL VALIDITY

The objectives of this chapter are: formalize the mathematical description of the T-S fuzzy models and present the N-fuzzy modeling process; compare the numerical complexity of the control algorithms and the number of rules required in exact modeling for classical and N-fuzzy approaches; and analyze the modeling error and convexity on the exterior of the domain of validity. It is important to emphasize that the classical T-S fuzzy models described in Tanaka & Wang (2001) and Feng (2010) can be seen as a particular case of the N-fuzzy technique addressed in this work, which will be explained later. Finally, it is presented the N-fuzzy models of some nonlinear plants used in the remainder of this document, whose modeling process are show in Appendix B.

2.1 T-S FUZZY REPRESENTATION

The T-S fuzzy model, originally proposed by Takagi & Sugeno (1985), represents a nonlinear dynamic system by means of a fuzzy dynamic model. This model consists of a set of local linear (or affine) submodels that are connected using membership functions. In this section, the discrete-time representation with nonlinear local submodels, also referred to as N-fuzzy, will be used. The modeling procedure and notation are based in the article Klug & Castelan (2011).

Consider the class of nonlinear systems with state space representation affine in the input and disturbance signals, defined by the following equation

$$\begin{array}{rcl} x(k+1) & = & f(x(k)) + \mathscr{V}(x(k))u(k) + \mathcal{T}(x(k))w(k) \\ y(k) & = & Cx(k) \end{array} \tag{2.1}$$

where $x(k) \in \mathcal{X} \subset \Re^{n_x}$, $u(k) \in \mathcal{U} \subset \Re^{n_u}$, $y(k) \in \mathcal{Y} \subset \Re^{n_y}$ and $w(k) \in \mathcal{W} \subset \Re^{n_w}$ are respectively the state, the control input, the system output and the exogenous disturbance vectors. The functions $f(\cdot) : \Re^{n_x} \longrightarrow \Re^{n_x}$, with $f(0) = 0$, $\mathscr{V}(\cdot) : \Re^{n_x} \longrightarrow \Re^{n_x \times n_u}$ and $\mathcal{T}(\cdot) : \Re^{n_x} \longrightarrow \Re^{n_x \times n_w}$ are continuous and bounded for all $x(k) \in \mathcal{X}$, with $\mathcal{X}$ being a region belonging to the state space domain containing the origin which will be defined later in this chapter. Furthermore, in order to obtain numerically tractable conditions, the output vector $y(k)$

is considered to be linear, that is $C \in \Re^{n_y \times n_x}$ is a constant matrix.

For a given nonlinear system as in (2.1), the N-fuzzy model is represented by a description of IF-THEN fuzzy rules that express local dynamics by nonlinear local submodels, having $\mathcal{R}_1, \ldots, \mathcal{R}_{n_r}$ fuzzy rules defined as follows

$$\underset{i=1,\ldots,n_r}{\mathcal{R}_i} : \begin{cases} \text{IF} & \nu_{(1)}(k) \text{ is } M_1^i, \nu_{(2)}(k) \text{ is } M_2^i, \ldots, \nu_{(n_s)}(k) \text{ is } M_{n_s}^i \\ \text{THEN} & \begin{array}{rcl} x(k+1) & = & A_i x(k) + B_i u(k) + B_{wi} w(k) + G_i \varphi(k) \\ y(k) & = & Cx(k) \end{array} \end{cases} \tag{2.2}$$

with $\nu(k) := [\nu_{(1)}(k), \nu_{(2)}(k), ..., \nu_{(n_s)}(k)]$ representing the premise variables, M_j^i, $j = 1, \ldots, n_s$, representing the fuzzy sets, and $(A_i, B_i, B_{wi}, G_i, C)$ representing the matrices that define the fuzzy local submodels. The vector $\varphi(k) = \varphi(\pi(k)) \in \Re^{n_\varphi}$, with $\pi(k) = Lx(k)$, $\varphi(0) = 0$ and $L \in \Re^{n_\varphi \times n_x}$, is a known nonlinear function of $x(k)$ satisfying a (local) cone sector condition $\varphi(\cdot) \in S[0, \Omega]$ for all $x(k) \in \mathcal{X} \subset \Re^{n_x}$, i.e., a matrix $0 < \Omega = \Omega' \in \Re^{n_\varphi \times n_\varphi}$ exists such that

$$\varphi^{'}(k)\Delta^{-1}[\varphi(k) - \Omega Lx(k)] \leq 0, \ \forall \ x(k) \in \mathcal{X} \tag{2.3}$$

where $\Delta \in \Re^{n_\varphi \times n_\varphi}$ is any positive diagonal matrix, that is, $\Delta \triangleq \text{diag}\{\delta_f\}$, $\delta_f > 0$, $f = 1, \ldots, n_\varphi$. Ω is assumed to be a known parameter. From the definition of Δ, if (2.3) is verified then n_φ independent classical conditions, $\varphi'_{(f)}(k)[\varphi(k) - \Omega Lx(k)]_{(f)} \leq 0$, are also assured (JUNGERS; CASTELAN, 2011). Thus, Δ represents a degree of freedom for the purpose of design and optimization. Notice that if $\varphi(k) = 0$, then the rules $\mathcal{R}_1, \ldots, \mathcal{R}_{n_r}$ recover the classical definition of T-S fuzzy models (TAKAGI; SUGENO, 1985).

Let $\mu_j^i(\nu_{(j)}(k))$ be the "weight" of the fuzzy set M_j^i associated to the premise variable $\nu_{(j)}(k)$, and $\omega^i(\nu(k)) = \prod_{j=1}^{n_s} \mu_j^i(\nu_{(j)}(k))$. Considering $\mu_j^i(\nu_{(j)}(k)) \geq 0$, it follows that

$$\omega^i(\nu(k)) \geq 0, \quad \forall \ i = 1, ..., n_r \ \text{ and } \ \sum_{i=1}^{n_r} \omega^i(\nu(k)) > 0.$$

Furthermore, the normalized weight of each rule, $h_{(i)}(k)$, also referred to as the membership function of i^{th} local submodel, satisfies:

$$h_{(i)}(k) = h(\nu_{(i)}(k)) = \frac{\omega^i(\nu(k))}{\sum_{i=1}^{n_r} \omega^i(\nu(k))}, \quad \forall\, i = 1, ..., n_r, \qquad (2.4)$$

and it is limited in the unit simplex

$$\Xi = \left\{ h \in \Re^{n_r}; \sum_{i=1}^{n_r} h_{(i)} = 1, h_{(i)} \geq 0, i = 1, ..., n_r \right\}.$$

As will be clarified in the next section, the domain $\mathcal{X}$ and the simplex Ξ are associated by the relation: $x(k) \in \mathcal{X} \Rightarrow h_{(i)}(k) \in \Xi$.

Thus, given $(x(k), u(k), w(k), \varphi(k), \nu(k))$, the resulting fuzzy system is obtained as the weighted average of the local submodels (LEEKWIJCK W. V. AMD KERRE, 1999), also known as the center of gravity defuzzification method. Therefore, it is obtained

$$\begin{array}{rcl} x(k+1) & = & A(h(k))x(k) + B(h(k))u(k) + B_w(h(k))w(k) + G(h(k))\varphi(k) \\ y(k) & = & Cx(k) \end{array} \qquad (2.5)$$

with the structure of the matrices given by

$$\left[\, A(h(k)) \;\, B(h(k)) \;\, B_w(h(k)) \;\, G(h(k)) \,\right] = \sum_{i=1}^{n_r} h_{(i)}(k) \left[\, A_i \;\, B_i \;\, B_{wi} \;\, G_i \,\right].$$

Notice that the fuzzy model (2.5) is equivalent to the representation of a *Lur'e* type parameter varying system, referred to in this work as Nonlinear Parameter Varying (NPV) system, with polytopic uncertainties and cone bounded sector nonlinearities. This fact allows for stability analysis and control design techniques, originally proposed for associated parameter varying systems, to be adapted for the use in nonlinear systems that can be modeled using the N-fuzzy approach.

2.2 CONSTRUCTION OF THE FUZZY MODEL

In order to synthesize a fuzzy controller for a nonlinear plant, it is first necessary to obtain a T-S fuzzy model of this system. Therefore, the construction of a fuzzy model represents an important and basic procedure when using Fuzzy Model Based (FMB) techniques. In general, there are two approaches for this purpose (TANAKA; WANG, 2001):

1. identification using input-output data, and
2. derivation from given nonlinear system equations.

The approach using identification is suitable for plants that are unable or too difficult to be represented by analytical and/or physical models. On the other hand, when the nonlinear analytical equations are well-defined, for example in mechanical systems obtained by the Lagrange method or Newton-Euler method, the second approach is used. This work focuses on the second case, using the exact modeling.

For the construction of approximate models, as in the method shown in Teixeira & Zak (1999) (see Appendix A), the control designer should define operating points in the state space (based on the real behavior of the nonlinear plant to be analyzed), which will be associated with local linear submodels. These submodels can be determined by optimization methods or by Taylor series. However, it should be emphasized that control systems designed using approximate models cannot guarantee the performance and stability requirements initially established when applied to the original nonlinear plant, unless the discrepancies between the model and the plant are possible to be taken into account in the design process or by further analysis.

2.2.1 Class of Nonlinear Systems

For the demonstration of the fuzzy modeling process, the class of nonlinear system affine in the input and disturbance signals will be used, represented in the state space by the equation (2.1). This choice is due to the realistic fact that the great majority of nonlinear plants can be represented in this manner.

Consider that the nonlinear vector function $f(x(k))$ of (2.1) can be rewritten as[1]:

$$f = f_a + G\bar{\varphi} \tag{2.6}$$

with $\bar{\varphi} = \bar{\varphi}(Lx(k))$ belonging to the bounded sector $\bar{\varphi}(\cdot) \in S[\Omega_1, \Omega_2]$ (a mesh transformation will later be performed to match with (2.3)) at least locally in the domain of validity $\mathcal{X}$, to be defined for the model.

From (2.6), the i^{th} element of $f_a = f_a(x(k))$ is computed as

$$f_{a(i)} = \sum_{j=1}^{n_x} \bar{f}_{(i,j)} x_{(j)}. \tag{2.7}$$

[1] For convenience, and from this point on, the dependence of the sample-time or between variables can be suppressed.

Applying a similar procedure to $\mathscr{V}u = \mathscr{V}(x(k))u(k)$, $\mathcal{T}w = \mathcal{T}(x(k))w(k)$ and $G\bar{\varphi} = G(x(k))\bar{\varphi}(k)$, the following is obtained

$$(\mathscr{V}u)_{(i)} = \sum_{\kappa=1}^{n_u} v_{(i,\kappa)} u_{(\kappa)}, \quad (\mathcal{T}w)_{(i)} = \sum_{l=1}^{n_w} t_{(i,l)} w_{(l)}$$
$$\text{and} \quad (G\bar{\varphi})_{(i)} = \sum_{o=1}^{n_\varphi} g_{(i,o)} \bar{\varphi}_{(o)}. \tag{2.8}$$

Substituting equations (2.6), (2.7) and (2.8) into (2.1), leads to the following equivalent i^{th} system dynamics for $i = 1, ..., n_x$

$$x_{(i)}(k+1) = \sum_{j=1}^{n_x} \bar{f}_{(i,j)} x_{(j)} + \sum_{\kappa=1}^{n_u} v_{(i,\kappa)} u_{(\kappa)} + \sum_{l=1}^{n_w} t_{(i,l)} w_{(l)} + \sum_{o=1}^{n_\varphi} g_{(i,o)} \bar{\varphi}_{(o)} \tag{2.9}$$

In the next section, the nonlinear system (2.9), which is analogous to the system (2.1), will be modeled as a T-S fuzzy system with nonlinear local submodels in the considered domain of validity $\mathcal{X}$.

2.2.2 T-S Fuzzy Modeling

For the modeling method addressed in this work, the nonlinear local submodels are obtained using the maximum and minimum values of the nonlinear functions that compose the system in a specific domain of the state space (TANAKA; WANG, 2001; FENG, 2010). In the literature, this procedure is usually referred to as Sector Nonlinearity Approach (SNA), although it would be more appropriate to refer it as Min-Max Approach, for the reasons becoming clear from the context below. Therefore, once the domain $\mathcal{X}$ is determined, the following variables are considered:

$$\begin{array}{llllll} a_{ij1} & = & \max\limits_{x(k)\in\mathcal{X}} \{\bar{f}_{(i,j)}\}, & a_{ij2} & = & \min\limits_{x(k)\in\mathcal{X}} \{\bar{f}_{(i,j)}\} \\ b_{i\kappa 1} & = & \max\limits_{x(k)\in\mathcal{X}} \{v_{(i,\kappa)}\}, & b_{i\kappa 2} & = & \min\limits_{x(k)\in\mathcal{X}} \{v_{(i,\kappa)}\} \\ c_{il1} & = & \max\limits_{x(k)\in\mathcal{X}} \{t_{(i,l)}\}, & c_{il2} & = & \min\limits_{x(k)\in\mathcal{X}} \{t_{(i,l)}\} \\ d_{io1} & = & \max\limits_{x(k)\in\mathcal{X}} \{g_{(i,o)}\}, & d_{io2} & = & \min\limits_{x(k)\in\mathcal{X}} \{g_{(i,o)}\} \end{array} \tag{2.10}$$

It should be noted that the maximum and minimum values of each nonlinear function should be computed for the region $\mathcal{X}$ (GUERRA; KRUSZEWSKI; LAUBER, 2009). Then, it can be shown through (2.10) that it is possible to represent $\bar{f}_{(i,j)}$, $v_{(i,\kappa)}$, $t_{(i,l)}$ and $g_{(i,o)}$ as

$$\begin{aligned} \bar{f}_{(i,j)} &= \sum_{\ell^a=1}^{2} \alpha_{ij\ell^a}(x(k))a_{ij\ell^a} \quad & v_{(i,\kappa)} &= \sum_{\ell^b=1}^{2} \beta_{i\kappa\ell^b}(x(k))b_{i\kappa\ell^b} \\ t_{(i,l)} &= \sum_{\ell^c=1}^{2} \gamma_{il\ell^c}(x(k))c_{il\ell^c} \quad & g_{(i,o)} &= \sum_{\ell^d=1}^{2} \delta_{io\ell^d}(x(k))d_{io\ell^d} \end{aligned} \tag{2.11}$$

with

$$\begin{aligned} \alpha_{ij1} &= \frac{\bar{f}_{(i,j)} - a_{ij2}}{a_{ij1} - a_{ij2}} \quad , \quad & \alpha_{ij2} &= \frac{a_{ij1} - \bar{f}_{(i,j)}}{a_{ij1} - a_{ij2}}, \\ \beta_{i\kappa1} &= \frac{v_{(i,\kappa)} - b_{i\kappa2}}{b_{i\kappa1} - b_{i\kappa2}} \quad , \quad & \beta_{i\kappa2} &= \frac{b_{i\kappa1} - v_{(i,\kappa)}}{b_{i\kappa1} - b_{i\kappa2}}, \\ \gamma_{il1} &= \frac{t_{(i,l)} - c_{il2}}{c_{il1} - c_{il2}} \quad , \quad & \gamma_{il2} &= \frac{c_{ij1} - t_{(i,l)}}{c_{il1} - c_{il2}}, \\ \delta_{io1} &= \frac{g_{(i,o)} - d_{io2}}{d_{io1} - d_{io2}} \quad \text{and} \quad & \delta_{io2} &= \frac{d_{io1} - g_{(i,o)}}{d_{io1} - b_{io2}}. \end{aligned} \tag{2.12}$$

Notice that

$$\sum_{\ell^a=1}^{2} \alpha_{ij\ell^a} = \sum_{\ell^b=1}^{2} \beta_{i\kappa\ell^b} = \sum_{\ell^c=1}^{2} \gamma_{il\ell^c} = \sum_{\ell^d=1}^{2} \delta_{io\ell^d} = 1. \tag{2.13}$$

It is also observed that ℓ^a, ℓ^b, ℓ^c and ℓ^d are associated with the extremum points (maximum and minimum) of nonlinear functions in the domain $\mathcal{X}$. Substituting (2.11) into (2.9), leads to

$$\begin{aligned} x_{(i)}(k+1) = &\sum_{j=1}^{n_x}\sum_{\ell^a=1}^{2} \alpha_{ij\ell^a}(x(k))a_{ij\ell^a}x_{(j)} + \sum_{\kappa=1}^{n_u}\sum_{\ell^b=1}^{2} \beta_{i\kappa\ell^b}(x(k))b_{i\kappa\ell^b}u_{(\kappa)} \\ &+ \sum_{l=1}^{n_w}\sum_{\ell^c=1}^{2} \gamma_{il\ell^c}(x(k))c_{il\ell^c}w_{(l)} + \sum_{o=1}^{n_\varphi}\sum_{\ell^d=1}^{2} \delta_{io\ell^d}(x(k))d_{io\ell^d}\bar{\varphi}_{(o)} \end{aligned}$$

$\forall\ i = 1, ..., n_x$. Hence, the following state space representation is obtained:

$$x(k+1) = \tilde{A}x(k) + \tilde{B}u(k) + \tilde{B}_w w(k) + \tilde{G}\bar{\varphi}(k) \tag{2.14}$$

with

$$\mathscr{N} = \begin{bmatrix} \sum\limits_{\ell^n=1}^{2} \eta_{11\ell^n} n_{11\ell^n} & \cdots & \sum\limits_{\ell^n=1}^{2} \eta_{1n_x\ell^n} n_{1n_x\ell^n} \\ \vdots & \ddots & \vdots \\ \sum\limits_{\ell^n=1}^{2} \eta_{n_x1\ell^n} n_{n_x1\ell^n} & \cdots & \sum\limits_{\ell^n=1}^{2} \eta_{n_xn_x\ell^n} n_{n_xn_x\ell^n} \end{bmatrix}$$

where the tuple $(\mathscr{N}, \eta, n, \ell^n)$ represents either $\left(\tilde{A}, \alpha, a, \ell^a\right)$, $\left(\tilde{B}, \beta, b, \ell^b\right)$, $\left(\tilde{B}_w, \gamma, c, \ell^c\right)$ or $\left(\tilde{G}, \delta, d, \ell^d\right)$.

From the summation property in (2.13), the expression (2.14) can be conveniently rewritten by swapping the summations indices as follows

$$x(k+1) = \sum_{p_{11}=1}^{2} \ldots \sum_{p_{n_xn_x}=1}^{2} \sum_{q_{11}=1}^{2} \ldots \sum_{q_{n_xn_u}=1}^{2} \sum_{r_{11}=1}^{2} \ldots \sum_{r_{n_xn_w}=1}^{2} \sum_{s_{11}=1}^{2} \ldots \sum_{s_{n_xn_\varphi}=1}^{2} h_{p,q,r,s}(\bar{A}_p x + \bar{B}_q u + \bar{B}_{wr} w + \bar{G}_s \bar{\varphi}) \tag{2.15}$$

with

$$\bar{A}_p = \begin{bmatrix} a_{11p_{11}} & \cdots & a_{1n_xp_{1n_x}} \\ \vdots & \ddots & \vdots \\ a_{n_x1p_{n_x1}} & \cdots & a_{n_xn_xp_{n_xn_x}} \end{bmatrix},$$

$$\bar{B}_q = \begin{bmatrix} b_{11q_{11}} & \cdots & b_{1n_uq_{1n_u}} \\ \vdots & \ddots & \vdots \\ b_{n_x1q_{n_x1}} & \cdots & b_{n_xn_uq_{n_xn_u}} \end{bmatrix},$$

$$\bar{B}_{wr} = \begin{bmatrix} c_{11r_{11}} & \cdots & c_{1n_wr_{1n_w}} \\ \vdots & \ddots & \vdots \\ c_{n_x1r_{n_x1}} & \cdots & c_{n_xn_wr_{n_xn_w}} \end{bmatrix},$$

$$\bar{G}_s = \begin{bmatrix} d_{11o_{11}} & \cdots & d_{1n_\varphi o_{1n_\varphi}} \\ \vdots & \ddots & \vdots \\ d_{n_x1o_{n_x1}} & \cdots & d_{n_xn_\varphi o_{n_xn_\varphi}} \end{bmatrix},$$

and

$$h_{p,q,r,s} = \alpha_{11p_{11}} \ldots \alpha_{n_xn_xp_{n_xn_x}} \beta_{11q_{11}} \ldots \beta_{n_xn_uq_{n_xn_u}} \gamma_{11r_{11}} \cdots \gamma_{n_xn_wq_{n_xn_w}} \delta_{11r_{11}} \ldots \delta_{n_xn_\varphi q_{n_xn_\varphi}}.$$

Then, aggregating the summations and performing a mesh transformation (see Appendix C) with the nonlinearity $\bar{\varphi}$ leads to

$$x(k+1) = \sum_{i=1}^{2^{\varpi}} h_{(i)}(k)\left\{A_i x(k) + B_i u(k) + B_{wi} w(k) + G_i \varphi(k)\right\}, \quad (2.16)$$

where $h_{(i)}(k) = h_{p,q,r,s}$, $\varpi = n_x n_x + n_x n_u + n_x n_w + n_x n_\varphi$, $A_i = \bar{A}_i + G_i \Omega_1 L$, $B_i = \bar{B}_i$, $B_{wi} = \bar{B}_{wi}$, $G_i = \bar{G}_i$ e $\varphi = \bar{\varphi} - \Omega_1 L x$, with $\varphi(.) \in S[0 \ \ \Omega]$.

The equation (2.16) represents the T-S fuzzy model with nonlinear local rules described in (2.5), where A_i, B_i, B_{wi} and G_i are dependent on the extremum values $a_{ij\ell^a}$, $b_{i\kappa\ell^b}$, $c_{il\ell^c}$ and $d_{io\ell^d}$ of the nonlinearities of the system. The membership functions $h_{(i)}(k)$ are dependent on the functions $\alpha_{ij\ell^a}(x(k))$, $\beta_{i\kappa\ell^b}(x(k))$, $\gamma_{il\ell^c}(x(k))$ and $\delta_{io\ell^d}(x(k))$ defined in (2.12), and correspond to time-varying parameters for a NPV polytopic system.

Based on the aforementioned N-fuzzy modeling technique, and in other methods found in literature, an important issue usually not considered by researchers is that to obtain numerically tractable solutions for the stability analysis and control design of nonlinear systems, the available T-S fuzzy modeling techniques can only locally guarantee the stability properties of the original nonlinear system. Notice when deriving a T-S fuzzy model that a normalizing step is used in the defuzzification process, which requires that the premise variables are bounded in some chosen compact set, i.e. the positiveness of the functions in (2.12), and consequently of the membership functions $h_{(i)}(k)$, it is only guaranteed if $x(k) \in \mathcal{X}$.

In light of the above, there exists a bounded region $\mathcal{X}$ of state space containing the origin such that $x(k) \in \mathcal{X} \Rightarrow h_{(i)}(k) \in \Xi$. Hence, when applying convex methods to solve fuzzy based stability conditions on the Ξ space, it is necessary to take into account that the stability conditions hold only if the state trajectory of the original nonlinear system does not leave $\mathcal{X}$. From this reasoning, we refer to the region $\mathcal{X}$ as the *T-S domain of validity*. In this work, the domain $\mathcal{X}$ will be defined by means of the following polyhedral set

$$\mathcal{X} = \{x(k) \in \Re^{n_x} : |Nx(k)| \preceq \phi\}, \quad (2.17)$$

where $\phi \in \Re^{n_\phi}$ and $N \in \Re^{n_\phi \times n_x}$ are given constants. Also, ϕ represents the bounds of the associated states, and $n_\phi \leq n_x$ represents the number of constraints characterizing the region $\mathcal{X}$. For example, considering a generic nonlinear system with $x(k) \in \Re^3$, and the limits $\left|x_{(1)}(k)\right| \leq 2$

and $\left|x_{(2)}(k)\right| \leq 3$, with the free state $x_{(3)}(k)$, the domain $\mathcal{X}$ in (2.17) can be characterized by

$$N = \begin{bmatrix} 1 & 0 & 0 \\ 0 & 1 & 0 \end{bmatrix} \text{ and } \phi = \begin{bmatrix} 2 \\ 3 \end{bmatrix}.$$

This domain of validity should be taken into account in any control design or stability analysis that assumes the description (2.16) instead of (2.1) and is based on convex properties of the N-fuzzy model. Specifically, loss of performance or even instability may occur when the state trajectory evolves outside the domain of validity of the model (2.16).

Remark 2.1 *For the classical T-S fuzzy modeling described in Tanaka & Wang (2001), the vector of sector nonlinearities $\bar{\varphi}$ does not explicitly appear in the model equation (2.16). Otherwise, these nonlinearities should be handled and indirectly included in the system state matrix, as shown in the sequel. Let the unidimensional discrete-time nonlinear system*

$$x(k+1) = f_a(x(k)) + 0.7\bar{\varphi}(k) + u(k) + 0.2w(k),$$

with $\bar{\varphi} = \bar{\varphi}(Lx) = \sin(x)$, $L = 1$, and $f_a = x^2 = \bar{f}x \Rightarrow \bar{f} = x$. Considering that the trajectories are restricted to the state space domain defined by $|x| \leq \pi/2$, it is possible to rewrite $\bar{f}$, following the steps (2.10), (2.11) and (2.12), by $\bar{f} = \sum_{\ell^a=1}^{2} \alpha_{\ell^a} a_{\ell^a}$, with $a_1 = \pi/2$, $a_2 = -\pi/2$, $\alpha_1 = \dfrac{x - a_2}{a_1 - a_2}$ and $\alpha_2 = \dfrac{a_1 - x}{a_1 - a_2}$. It can also be observed that the nonlinearity $\bar{\varphi}$ is bounded in the sector $\bar{\varphi} \in S[\Omega_1, \Omega_2]$, with $\Omega_1 = 2/\pi$ and $\Omega_2 = 1$. Thus, the T-S fuzzy model with nonlinear local rules is given by

$$x(k+1) = \sum_{\ell^a=1}^{2} \alpha_{\ell^a}(k) \left\{ a_{\ell^a} x(k) + u(k) + 0.2w(k) + 0.7\bar{\varphi}(k) \right\}. \quad (2.18)$$

with the membership functions $h_{(i)}(k) = \alpha_{(i)}(k)$, $i = 1, 2$, depicted in Figure 4.

In another way, it is possible to rewrite the nonlinearity $\bar{\varphi}$, in the considered state space domain, as

$$\bar{\varphi} = \sin(x) = \left(\sum_{\ell^e=1}^{2} \epsilon_{\ell^e} \Omega_{\ell^e} \right) x, \quad (2.19)$$

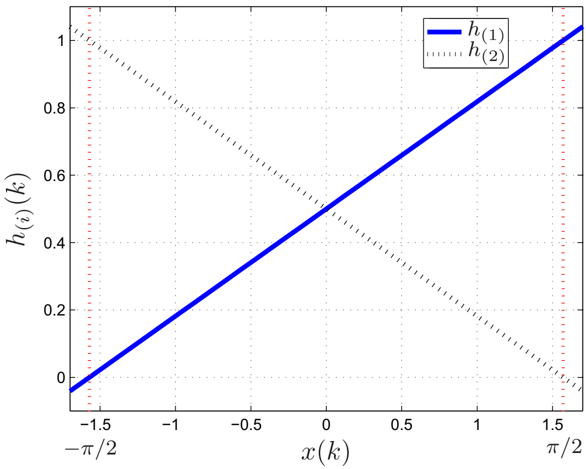

Figure 4 – Membership functions $h_{(i)}(k)$ for N-fuzzy model

where $\epsilon_{\ell^e} = \epsilon_{\ell^e}(x(k))$, $\ell^e = 1, 2$, *are any functions that satisfy (2.19) and respect the properties* $\epsilon_1 + \epsilon_2 = 1$ *and* $\epsilon_{\ell^e} \geq 0$, $\ell^e = 1, 2$, $\forall\ x(k) \in \mathcal{X}$. *One possibility is to choose*

$$\epsilon_1 = \begin{cases} \dfrac{\sin(x) - \Omega_1 x}{x(\Omega_2 - \Omega_1)}, & x \neq 0 \\ 1, & x = 0 \end{cases} \quad \text{and } \epsilon_2 = \begin{cases} \dfrac{\Omega_2 x - \sin(x)}{x(\Omega_2 - \Omega_1)}, & x \neq 0 \\ 0, & x = 0 \end{cases}$$

Hence, it has the following classical T-S fuzzy model with linear local rules

$$\begin{aligned} x(k+1) &= \sum_{\ell^a=1}^{2} \sum_{\ell^e=1}^{2} \alpha_{\ell^a}(k)\epsilon_{\ell^e}(k) \left\{ (a_{\ell^a} + 0.7\Omega_{\ell^e})x(k) + u(k) + 0.2w(k) \right\} \\ &= \sum_{i=1}^{4} h_{(i)}(k) \left\{ A_i x(k) + u(k) + 0.2w(k) \right\} \end{aligned} \tag{2.20}$$

with $A_i = a_{\ell^a} + 0.7\Omega_{\ell^e}$ *and* $h_{(i)}(k) = \alpha_{\ell^a}(k)\epsilon_{\ell^e}(k)$, *for* $i = \ell^e + 2(\ell^a - 1)$ *and* $\ell^a, \ell^e = 1, 2$. *It is worth noting that the term* Ω_{ℓ_e} *in (2.20), related to the sector nonlinearity, appears attached to the system state matrix. Furthermore, the treatment of* $\bar{\varphi}$ *implies an additional summation, and consequently an increase in the number of local submodels. This factor will be further explored in the next subsection.*

In Figure 5 the membership functions $h_{(i)}(k)$ *for the model (2.20) are depicted. As in the Figure 4, the reader can notice that the mem-*

bership functions $h_{(i)}(k)$ do not belong to the simplex Ξ outside the T-S domain of validity ($|x| \leq \pi/2$).

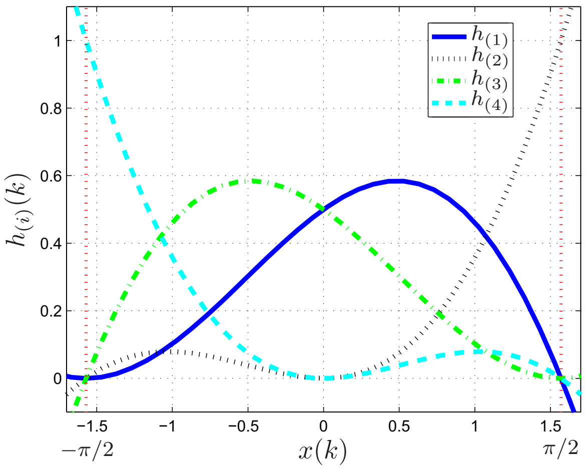

Figure 5 – Membership functions $h_{(i)}(k)$ for classical model

2.2.3 Comparison of the Number of Rules

It is important to highlight that a nonlinearity for each position of the state, control input, and disturbance matrices, as represented in the generalized model (2.15), does not necessarily exist. In this case, linear or null terms are not considered in the summations, consequently reducing the number of submodels in the fuzzy representation. In general, for the classical modeling of Tanaka & Wang (2001), there is a ratio of 2^{n_s} rules for the exact representation (TANIGUCHI et al., 2001), where n_s is the number of premise variables associated to the number of nonlinearities to be handled.

From another point of view, the definition of the vector φ eliminates functions that would also be represented by summations, contributing to a reduction in the number of local submodels. In this case it has a ratio of $2^{n_s - n_\varphi}$ rules for the exact representation of the model. Therefore, using the N-fuzzy approach can be important to reduce the numerical complexity, making easier the feasibility of the control algorithms and their implementation.

In Figure 6, it is shown a graphic comparison between the number of rules for classical T-S fuzzy models ($n_\varphi = 0$), having linear submodels, and the N-fuzzy model in two cases ($n_\varphi = 1$ and $n_\varphi = 2$).

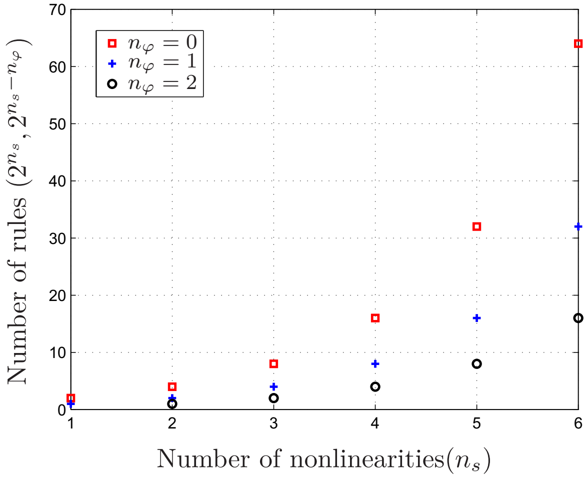

Figure 6 – Comparison of the number of rules

Notice that the larger is the size of the vector φ, the greater is the reduction of rules, after all $2^{n_s - n_\varphi} = 2^{n_s}/2^{n_\varphi}$. This relation allows to check a division factor of 2^{n_φ} in relation to the classical T-S fuzzy model.

2.3 MODELING ERROR ANALYSIS AND REGIONAL VALIDITY

An important issue when dealing with the T-S fuzzy models considered in the present work is that the convexity can only be guaranteed in a specific region of the state space, referred to as the domain of validity $\mathcal{X}$. The exception is for systems whose sector nonlinearities can be globally encompassed and/or a global maximum/minimum can be found. Otherwise, it is necessary to assign a confined region to compute the extremum points and/or to find a local bounded sector for the nonlinearities of the system. However, provided that the stability conditions are properly handled, this may not be a serious problem, because most real systems already have physical limitations which naturally constraint the excursion of the states.

Nonetheless, the inherent local characteristic of T-S modeling techniques is often not considered in most FMB control design results, as can be observed in Tognetti & Oliveira (2009), Andrea et al. (2008), Yang & Yang (2012), Mozelli & Palhares (2011a) and in references therein. Hence, the synthesized control laws in these references based on convex methods may lead to trajectories of the controlled nonlinear system evolving outside the domain of validity, thus representing a source of performance degradation or even instability of the corresponding closed-loop system.

As previously discussed, the loss of model convexity is associated with the positiveness of the membership functions, which is only ensured for the domain $\mathcal{X}$. A common strategy employed to avoid $h(k) \notin \Xi, \forall\, x(k) \notin \mathcal{X}$ is to partition the membership functions $h_{(i)}(k)$ in order to saturate them, i.e. $h_{(i)}(k) \in [0, 1]$. In other words, if the value of $h_{(i)}(k)$ is greater than 1, it is set ("clipped") to 1, if the value of $h_{(i)}(k)$ is lower than 0, it is set ("clipped") to 0. This strategy, despite its success when applied to the T-S fuzzy model, introduces modeling errors that might result in similar issues observed for the loss of model convexity case, when applied to the original nonlinear system. To sum up, in practical applications either the membership function are clipped, in which the model convexity is preserved at the cost of modeling errors, or not clipped, in which the model convexity is lost but the fuzzy model is exact. The following examples aim to demonstrate the involved problematic.

Example 2.2 (Modeling Error) *Let the nonlinear function $\bar{f}(x) = x\sin^2(x)$, with $x \in \Re$. It is desired to obtain an exact T-S fuzzy model of the function using the procedures described in the subsection 2.2.2. For this purpose, the domain of validity is considered (for example due to physical limitations) as $\mathcal{X} = \{x \in \Re : \ |x| \leq \pi/3\}$. Computing the maximum and minimum values of the nonlinear function $\bar{f}(x)$ for $\mathcal{X}$ leads to*

$$a_1 = \max_{x\in\mathcal{X}} \left\{\bar{f}(x)\right\} = 0.7854, \text{ and } a_2 = \min_{x\in\mathcal{X}} \left\{\bar{f}(x)\right\} = -0.7854.$$

Thus, it is possible to rewrite $\bar{f}(x)$, using (2.11) and (2.12), as the following equivalent T-S fuzzy model

$$\bar{f}(x) = \sum_{\ell^a=1}^{2} \alpha_{\ell^a}(\bar{f}(x))a_{\ell^a}, \ \forall\, x \in \mathcal{X}, \tag{2.21}$$

with

$$\alpha_1(\bar{f}(x)) = \begin{cases} \dfrac{\bar{f}(x) - a_2}{a_1 - a_2}, & a_2 \leq \bar{f}(x) \leq a_1 \\ 1, & \bar{f}(x) > a_1 \\ 0, & \bar{f}(x) < a_2 \end{cases} \quad \text{and}$$

$$\alpha_2(\bar{f}(x)) = \begin{cases} \dfrac{a_1 - \bar{f}(x)}{a_1 - a_2}, & a_2 \leq \bar{f}(x) \leq a_1 \\ 0, & \bar{f}(x) > a_1 \\ 1, & \bar{f}(x) < a_2 \end{cases} . \tag{2.22}$$

The membership functions are also depicted in Figure 7.

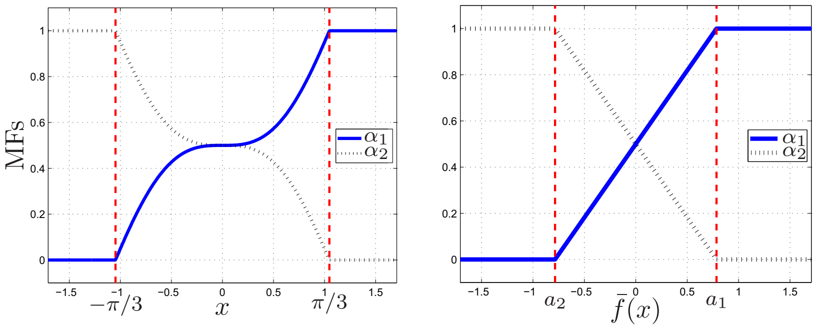

Figure 7 – Membership functions (MFs): $\alpha_1(x)$ and $\alpha_2(x)$

It should be emphasized that $\mathcal{X}$ is represented by vertical dashed lines in red, where $|x| \leq \pi/3 \Rightarrow a_2 \leq \bar{f}(x) \leq a_1$. In this region the properties $\sum_{\ell^a=1}^{2} \alpha_{\ell^a} = 1$ and $\alpha_{\ell^a} \geq 0$, $\ell^a = 1, 2$, by definition, are always verified. Otherwise, outside this domain there is no such guarantee, and positiveness is ensured by clipping the membership functions between 0 *and* 1*, as shown in (2.22).*

In Figures 8 and 9, the graph of the nonlinear function $\bar{f}(x)$ and its corresponding T-S fuzzy model, described in equation (2.21) are observed, respectively. The existing modeling error is shown in Figure 10.

Notice that there is no modeling error within the domain of validity $\mathcal{X}$, and thus the dynamic of the T-S fuzzy model is equivalent to the nonlinear function $\bar{f}(x)$ in this region. However, for $x \notin \mathcal{X}$, the fuzzy model can no longer represent the original function, having a discrepancy between the function and its fuzzy representation.

In light of the above example, modeling errors are introduced when considering the membership functions constrained between $[0, 1]$. In this case, and regarding a fuzzy model representing a nonlinear system and a fuzzy controller designed to satisfy stability and performance requirements, if the state vector achieves regions of the state space where the T-S model no longer accurately represents the dynamics of

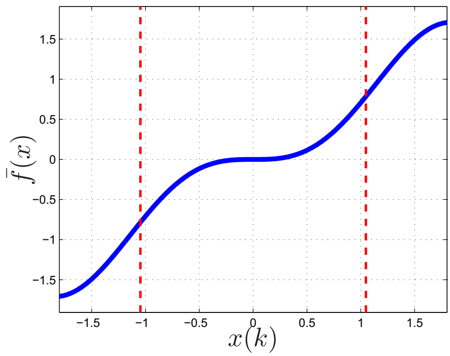

Figure 8 – Nonlinear function

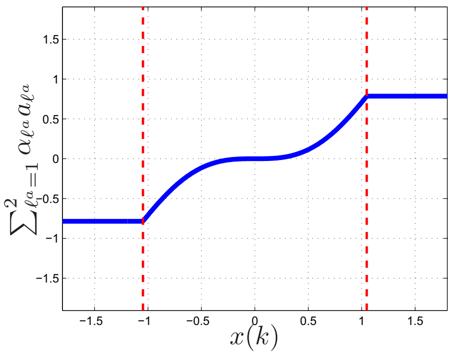

Figure 9 – T-S fuzzy representation

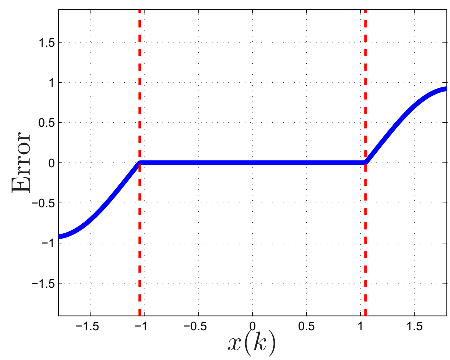

Figure 10 – Modeling error when MFs are clipped for $x(k) \notin \mathcal{X}$

the original plant, the desired stability and performance may not be guaranteed for the original system.

In the following, an illustrative example aims to demonstrate the problems that may occur in practice when the inherent local characteristic of T-S modeling techniques are not considered in control design, either by modeling error introduced when restricting the membership functions, or because of the loss of model convexity outside the domain $\mathcal{X}$.

Example 2.3 (Local Stability) *For simplicity, consider the following unidimensional nonlinear discrete-time system without control saturation constraints (KLUG et al., 2014)*

$$x(k+1) = x^3(k)+\sin(x(k))+(0.2+x^2(k))u(k) \quad , \quad y(k) = x(k) \quad (2.23)$$

and assume as premise variables $\nu_{(1)}(k) = y^2(k)$ and $\nu_{(2)}(k) = \sin(y(k))$. By considering the domain of validity (2.17), with $N = 1$ and $\phi = 5\pi/12$ (or simply $|x(k)| \leq 5\pi/12$), and using the techniques described in Remark 2.1 (FENG, 2010), a classical fuzzy T-S model based on four linear local submodels is obtained, i.e. with $G_i = 0 \; \forall \; i = 1,..,4$:

$$\begin{gathered} A_1 = [\ 2.7135\ ]\ ;\ A_2 = [\ 2.4514\ ]\ ;\ ,A_3 = [\ 1\ ]\ ;\ ,A_4 = [\ 0.7379\ ]\ ; \\ B_1 = [\ 1.9135\ ]\ ;\ B_2 = [\ 1.9135\ ]\ ;\ B_3 = [\ 0.2000\ ]\ ;\ B_4 = [\ 0.2000\ ]\,. \end{gathered} \quad (2.24)$$

The respective four membership functions are depicted in Figure 11 for the considered domain of validity where the convexity property of set (3.2) holds true.

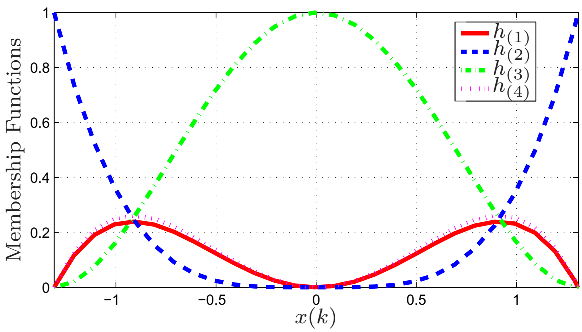

Figure 11 – Nonlinear membership functions $h_{(i)}(k), \forall \; i = 1, ..., 4$

.

These functions are the binary product between functions $\hat{M}_j^i$, $j = \{1, 2\}$ *and* $i = \{1, 2\}$, *defined as:*

$$\hat{M}_1^1 = \frac{x^2}{1.7135}, \ \hat{M}_2^1 = \frac{-x^2}{1.7135}, \quad and$$

$$\hat{M}_1^2 = \begin{cases} \dfrac{\sin(x) - 0.7379x}{x(0.2621)}, & x \neq 0 \\ 1, & x = 0 \end{cases}, \ \hat{M}_2^2 = \begin{cases} \dfrac{x - \sin(x)}{x(0.2621)}, & x \neq 0 \\ 0, & x = 0 \end{cases}.$$

Figure 12(a) depicts the estimated basin of attraction obtained by simulations of the two dimensional closed-loop system composed of the nonlinear system (2.23) and a dynamic output feedback fuzzy controller (adapted from Theorem 8.10 *in (FENG, 2010), with conditions described in Appendix D) computed to globally stabilize the T-S model (2.24). The dashed lines in this figure indicate the boundary of the domain of validity of the fuzzy T-S model. The points marked with* $\times$ *correspond to unstable initial conditions, that is, points not belonging to the basin of attraction. The points marked with* $\circ$ *belong to the considered basin of attraction but part of the corresponding trajectories evolve outside the domain of validity of the T-S fuzzy model. The other unmarked points complete the basin of attraction for the considered range of closed-loop initial conditions. Figure 12(b) depicts state trajectories corresponding to initial conditions chosen in the three mentioned regions of Figure 12(a),* $\xi(0) = [0.75\ 0]$ *symbolized by* $\square$, *and* $\xi(0) = [1\ 0]$ *symbolized by* $\circ$, *being stable conditions, and* $\xi(0) = [-1.2\ 0]$ *symbolized by* $\times$, *an unstable condition.*

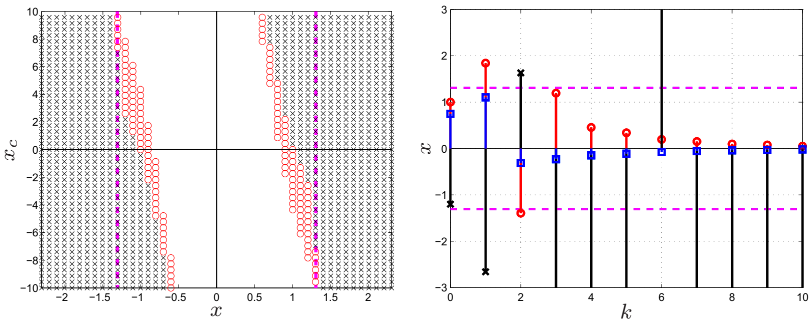

(a) Basin of Attraction (b) State Trajectory

Figure 12 – Regions and trajectories for motivating example

It is remarkable, as shown in Figures 12, that a compensator that in theory globally stabilizes the fuzzy T-S closed-loop system may yield unstable trajectories even though the initial conditions are inside the domain of validity when applied in the original nonlinear system (2.23). On the other hand, the use of some adequate techniques taking into account the domain of validity issue prevents unstable initial conditions inside a sub-region of $\mathcal{X}$*, as will be seen in the following chapters.*

In this sense, the local stabilization of nonlinear systems using T-S fuzzy models is an important contribution of this work, in which efforts were devoted to estimate a safe domain of attraction, i.e. a region of admissible initial conditions that asymptotically converge to the origin, for the closed-loop system.

2.4 CONCLUDING REMARKS

In this chapter some general concepts of T-S fuzzy systems theory were presented. A generalized process of modeling with the use of nonlinear local submodels, referred to as N-fuzzy modeling, was described. The objective is to obtain an exact representation of the nonlinear plant with the least possible number of rules, reducing the numerical complexity and consequently making easier the feasibility of the subsequently developed control algorithms and their practical implementation. A comparative study of the number of rules for classical and N-fuzzy models was also performed. The important issue of regional validity was discussed, generally disregarded by researchers in this area. At last, examples of nonlinear systems modeled by T-S fuzzy models are detailed in Appendix B, and an analysis of the numerical complexity of control algorithms is presented in Appendix D .

3 DYNAMIC OUTPUT FEEDBACK CONTROL DESIGN

In this chapter a control design technique for discrete-time nonlinear systems that can be represented by the N-Fuzzy model described in Chapter 2 is presented. The control law considered is a dynamic output feedback with some particularities which will be described later. Basically, the objective is to propose a systematic method for obtaining the matrices of the controller, dealing with some key practical issues such as the saturation of the actuators and the regional validity of the T-S fuzzy model.

The proposed dynamic compensator is full-order and dependent on the fuzzy membership functions that are assumed to be available online to the controller. Additionally, anti-windup gains are added as an attempt to mitigate the undesired effects of saturation, and a performance index based on the λ-contractivity of the level set, associated with the Lyapunov function, is used in order to ensure a certain rate of temporal convergence of the closed-loop system trajectories. The results presented here are enhanced versions of the works Klug & Castelan (2012) and Klug et al. (2014).

The numerical results described in the present chapter and in the next ones, were obtained using the following computational tools:

1. Yalmip (LöFBERG, 2004): an interface for the mathematical description of the considered LMI-optimization problem and management of the *SDP-solver* to be used;

2. SeDuMi (STURM, 1999) and SDPT3 (TOH; TUTUNCU; TODD, 2004): *SDP-solvers* which are used to search for feasible solutions of the LMI-based control algorithms;

3. Simulink: a graphical programming environment for modeling, simulating and analyzing multidomain dynamic systems.

3.1 PROBLEM FORMULATION

Consider the class of undisturbed nonlinear systems that can be modeled by the process demonstrated in section 2.2, described using the defuzzification method by center of gravity as follows:

$$\begin{array}{rcl} x(k+1) & = & A(h(k))x(k) + B(h(k))sat(u(k)) + G(h(k))\varphi(k) \\ y(k) & = & Cx(k) \end{array} \tag{3.1}$$

where $x(k) \in \mathcal{X} \subset \Re^{n_x}$, $u(k) \in \mathcal{U} \subset \Re^{n_u}$ and $y(k) \in \mathcal{Y} \subset \Re^{n_y}$ are respectively the state, the control input and the system output vectors. $h(k) \subset \Re^{n_r}$ is a vector of time-varying membership functions, and limited, $\forall\ x(k) \in \mathcal{X}$, in the unit simplex

$$\Xi = \left\{ h \in \Re^{n_r}; \sum_{i=1}^{n_r} h_{(i)} = 1, h_{(i)} \geq 0, i = 1, ..., n_r \right\}. \tag{3.2}$$

The function $sat(.) : \Re^{n_u} \to \Re^{n_u}$ represents the saturation of the control inputs, defined by the standard decentralized saturation function

$$sat(u_{(\ell)}(k)) = sign(u_{(\ell)}(k))min(\rho_{(\ell)}, \left|u_{(\ell)}(k)\right|), \quad \forall\ \ell = 1, ..., n_u \tag{3.3}$$

where $\rho_{(\ell)} > 0$ denotes the symmetric amplitude bound relative to the i^{th}control input.

Complementing the fuzzy model description (3.1), the vector of sector nonlinearities $\varphi(k) = \varphi(\pi(k)) \in \Re^{n_\varphi}$, with $\pi(k) = \bar{L}y(k) = Lx(k)$, $L = \bar{L}C \in \Re^{n_\varphi \times n_x}$, and $\bar{L}$ with appropriate dimensions, verifies (at least locally) the sector condition (2.3). This definition is required for control purposes.

The matrix structure is given by

$$\left[\begin{array}{ccc} A(h(k)) & B(h(k)) & G(h(k)) \end{array}\right] = \sum_{i=1}^{n_r} h_{(i)}(k) \left[\begin{array}{ccc} A_i & B_i & G_i \end{array}\right]. \tag{3.4}$$

Once the premise variables vector $\nu(k)$ is assumed to be a function of the measurable states, i.e., $\nu(k) = \nu(y(k))$, the vector of membership functions can be reconstituted in real-time from these signals. In other words, $h(k) = h(\nu(y(k))) = h(y(k))$. This assumption is necessary to implement any output feedback controller based on the PDC strategy, in which the membership functions are shared between the fuzzy model and controller. Notice that many works in literature do not clarify this important property, even using examples that can not be implemented in practice.

In light of the above, the following full-order nonlinear fuzzy

(N-fuzzy) dynamical output feedback compensator is investigated:

$$\begin{array}{rcl} x_c(k+1) & = & A_c(h(k))x_c(k) + B_c(h(k))y(k) + G_c(h(k))\varphi(Lx(k)) \\ & & -E_c(h(k))\Psi(u(k)) \\ u(k) & = & C_c(h(k))x_c(k) + D_c(h(k))y(k) + F_c(h(k))\varphi(Lx(k)) \end{array} \tag{3.5}$$

where $x_c(k) \in \Re^{n_x \times n_x}$ and $\Psi(.) : \Re^{n_u} \to \Re^{n_u}$ is the dead-zone nonlinearity given by:

$$\Psi(u(k)) = u(k) - sat(u(k)), \tag{3.6}$$

and the controller matrices are as follows

$$\begin{array}{l} \left[\begin{array}{ccc} A_c\left(h(k)\right) & B_c\left(h(k)\right) & G_c\left(h(k)\right) \end{array} \right] = \\ \qquad \displaystyle\sum_{i=1}^{n_r} \sum_{j=i}^{n_r} (1+\varsigma_{ij}) h_{(i)}(k) h_{(j)}(k) \left[\begin{array}{ccc} \frac{A_{cij}}{2} & \frac{B_{cij}}{2} & \frac{G_{cij}}{2} \end{array} \right] \\ \left[\begin{array}{cccc} C_c\left(h(k)\right) & D_c\left(h(k)\right) & F_c\left(h(k)\right) & E_c\left(h(k)\right) \end{array} \right] = \\ \qquad \displaystyle\sum_{i=1}^{n_r} h_{(i)}(k) \left[\begin{array}{cccc} C_{ci} & D_{ci} & F_{ci} & E_{ci} \end{array} \right], \end{array} \tag{3.7}$$

with ς_{ij} a binary variable such that

$$\varsigma_{ij} = \left\{ \begin{array}{lll} 1 & \text{if} & i \neq j, \\ 0 & & \text{otherwise.} \end{array} \right. \tag{3.8}$$

As assumed in Arcak, Larsen & Kokotovic (2003), the feedback controller (3.5) requires either the knowledge of $\varphi(\cdot)$ or its availability as a signal whenever $G_c(h(k)) \neq 0$ or $F_c(h(k)) \neq 0$. In addition, $E_c(h(k))$ is a fuzzy anti-windup gain matrix that helps to mitigate the effects of the saturation. It is worthwhile to say that such anti-windup gain is usually addressed as a constant and the present proposal may improve the closed-loop behavior, once it may contains the time-invariant gain, $E(h(k)) = E_c$, as a special case.

Considering the augmented state vector $\xi(k) = [x^{'}(k) \;\; x_c^{'}(k)]^{'} \in \Re^{2n_x}$, the closed-loop system can be described by:

$$\begin{array}{rcl} \xi(k+1) & = & \mathbb{A}(h(k))\xi(k) + \mathbb{G}(h(k))\varphi(\mathbb{L}\xi(k)) \\ & & -\mathbb{B}(h(k))\Psi\Big(\mathbb{K}(h(k))\xi(k) + F_c(h(k))\varphi(\pi(k))\Big) \end{array} \tag{3.9}$$

with

$$\mathbb{A}(h(k)) = \begin{bmatrix} A(h(k)) + B(h(k))D_c(h(k))C & B(h(k))C_c(h(k)) \\ B_c(h(k))C & A_c(h(k)) \end{bmatrix},$$

$$\mathbb{B}(h(k)) = \begin{bmatrix} B(h(k)) \\ E_c(h(k)) \end{bmatrix},\ \mathbb{G}(h(k)) = \begin{bmatrix} G(h(k)) + B(h(k))F_c(h(k)) \\ G_c(h(k)) \end{bmatrix},$$

$$\mathbb{K}(h(k)) = \begin{bmatrix} D_c(h(k))C & C_c(h(k)) \end{bmatrix}, \text{ and } \mathbb{L} = \begin{bmatrix} L & 0 \end{bmatrix}.$$

In view to the regional validity defined by (2.17), the T-S domain of validity is redefined in terms of the augmented space:

$$\mathcal{X}^{\{a\}} = \{\xi(k) \in \Re^{2n_x} : |\mathbb{N}\xi(k)| \preceq \phi\}, \tag{3.10}$$

where $\mathbb{N} = [\, N \quad 0_{n_\phi \times n_x} \,] \in \Re^{n_\phi \times 2n_x}$.

Thus, the problem of designing a controller (3.5) such that the closed-loop system remains stable requires handling the validity domain (3.10) besides a region of initial conditions $\xi(0)$ such that the allowed amplitudes of control signals are sufficient to assure the origin of (2.1) as an asymptotically stable equilibrium point. Such region of initial conditions is noted here as $\mathcal{S}_0$ and consists of a subset of the domain of attraction of the resulting nonlinear closed-loop system (2.1) (KHALIL, 2003, Sec. 8.2). As discussed in Tarbouriech et al. (2008), the basin of attraction can be defined as the set of all $\xi(k)$ such that for all $\xi(0)$ belonging to such set the corresponding system's trajectory converges asymptotically to the origin. It is noteworthy that an exact characterization of such set is in general not possible. This problem is formalized in the sequel:

Problem 3.1 *Determine the parameters of the controller (3.5), and a region $\mathcal{S}_0 \subseteq \Re^{2n_x}$, as large as possible, such that the origin of the closed-loop system (3.9) is asymptotically stable and for any initial condition $\xi(0) \in \mathcal{S}_0$, the corresponding trajectories of the closed-loop system remain in $\mathcal{X}^{\{a\}}$.*

Remark 3.2 *The differentiated structure (3.7), proposed to matrices $A_c(\cdot)$, $B_c(\cdot)$ and $G_c(\cdot)$, is required for obtaining the gains of the controller (3.5) from stabilizing conditions that will be proposed in the form of LMIs. Adopting a simplified structure, in this case, would invalidate this procedure, but could be used for the design of a controller with $C_c(h(k)) = C_c$, $D_c(h(k)) = D_c$ and $F_c(h(k)) = F_c$.*

Remark 3.3 *An alternative to the structure (3.7) was used in the works Klug & Castelan (2012) and Klug et al. (2014). This structure is based in a split of summations, generically represented by matrix $J(.)$ as*

$$J\left(h(k)\right) = \sum_{i=1}^{n_r} h_{(i)}(k)^2 J_i + \sum_{i=1}^{n_r-1} \sum_{j=i+1}^{n_r} h_{(i)}(k)h_{(j)}(k)J_{ij}$$

However, comparing the above representation with (3.7), it can be concluded that there exists an equivalence between the two structures in respect to the number of controller matrices and to the numerical complexity of the subsequent control algorithms. Thus, for convenience, it was used (3.7), since this provides a more compact representation.

It should be emphasized that the closed-loop matrices in (3.9) can be rewritten, by using the special structure (3.7) of the fuzzy compensator and some summation properties, as

$$\begin{bmatrix}\mathbb{A}(h_k) & \mathbb{G}(h_k)\end{bmatrix} = \sum_{i=1}^{n_r}\sum_{j=i}^{n_r}(1+\varsigma_{ij})h_{(i)}(k)h_{(j)}(k)\begin{bmatrix}\frac{\mathbb{A}_{ij}}{2} & \frac{\mathbb{G}_{ij}}{2}\end{bmatrix}$$

with

$$\mathbb{A}_{ij} = \begin{bmatrix} A_i + A_j + (B_iD_{cj} + B_jD_{ci})C & B_iC_{cj} + B_jC_{ci} \\ B_{cij}C & A_{cij}\end{bmatrix} \text{ and}$$

$$\mathbb{G}_{ij} = \begin{bmatrix} G_i + G_j + B_iF_{cj} + B_jF_{ci} \\ G_{cij}\end{bmatrix}.$$

3.2 PRELIMINARIES AND STABILITY ANALYSIS

Consider a fuzzy Lyapunov function (FLF) depending on the membership function $h(k) \in \Xi$, with Ξ given in (3.2), such that

$$V(\xi(k), h(k)) : \Re^{2n_x} \times \Xi \to \Re^+, \quad V(0, h(k)) = 0.$$

The level set associated with $V(\xi(k), h(k))$ is given by $\mathcal{E}_V \triangleq \{\xi(k) \in \Re^{2n_x};\ V(\xi(k), h(k)) \leq 1,\ h(k) \in \Xi\}$. Based on the definition of contractive sets provided in Khalil (2003), the λ-contractivity index given in what follows is used to improve the performance of the closed-loop system (3.9), being considered at the design stage of the fuzzy compensator (3.5):

Definition 3.4 *Consider a real scalar $\lambda \in (0, 1]$. The level set $\mathcal{E}_V$ is* λ-contractive, *with respect to the trajectories solutions of system (3.9), if*

$$\Delta V_\lambda(\xi(k), h(k)) \triangleq V(\xi(k+1), h(k+1)) - \lambda V(\xi(k), h(k)) < 0, \\ \forall\ \xi(k) \in \mathcal{E}_V, \forall\ h(k) \in \Xi. \tag{3.11}$$

From (3.11), it follows that for all $k > 0$ there exists $0 < \lambda_k < \lambda$ such that

$$V(\xi(k), h(k)) = \lambda_k V(\xi(k-1), h(k-1)). \tag{3.12}$$

Considering the definitions of $\mathcal{E}_V$ and (3.12), $\bar{k} > 0$ being any discrete-time instant and defining $\bar{\lambda} \triangleq \max_{1 \leq k \leq \bar{k}} \lambda_k$, it follows that

$$V(\xi(\bar{k}), h(\bar{k})) = \left(\prod_{k=1}^{\bar{k}} \lambda_k \right) V(\xi(0), h(0)) \leq \bar{\lambda}^{\bar{k}},$$

for any initial condition $\xi(0) \in \mathcal{E}_V$ and for any sequence $h(k)$, $k = 0, 1, \ldots, \bar{k}$, with $h(k) \in \Xi$. Thus, by letting $k \to \infty$, because $\bar{\lambda} < 1$ it follows from Definition 3.4 that any closed-loop trajectory of system (3.9) starting from $\mathcal{E}_V$, asymptotically converges to the origin of $\Re^{2n_x}$ with a speed of convergence associated with the contractivity coefficient λ. Furthermore, it can be deduced that the smaller $\lambda \in (0, 1]$ is, the faster is the asymptotic convergence to the origin.

The following FLF candidate is considered:

$$V(\xi(k), h(k)) = \xi^{'}(k) \mathbb{Q}^{-1}(h(k)) \xi(k) \tag{3.13}$$

where $\mathbb{Q}(h(k)) = \sum_{i=1}^{n_r} h_{(i)}(k) \mathbb{Q}_i,\ 0 < \mathbb{Q}_i = \mathbb{Q}_i' \in \Re^{2n_x \times 2n_x}$. The level set obtained from (3.13) is given by the intersection of ellipsoidal sets (HU; Z., 2003; JUNGERS; CASTELAN, 2011):

$$\mathcal{E}_V \triangleq \bigcap_{i \in \{1, \ldots n_r\}} \mathcal{E}(\mathbb{Q}_i^{-1}), \text{ with } \mathcal{E}(\mathbb{Q}_i^{-1}) = \left\{ \xi(k) \in \Re^{2n_x};\ \xi'(k) \mathbb{Q}_i^{-1} \xi(k) \leq 1 \right\}. \tag{3.14}$$

The desired asymptotic stability properties for the closed-loop system (3.9) is guaranteed by first assuring that the λ-contractive set relative to the system (3.1), $\mathcal{E}_V$, is inside the domain $\mathcal{X}^{\{a\}}$ given in (3.10). Recall that $\mathcal{X}^{\{a\}}$ is the set where, by hypothesis, the nonlinear closed-loop dynamical behaviour is well represented (convexly) by the fuzzy closed-loop system (3.9).

Lemma 3.5 *Consider matrix $\mathbb{N}$ in (3.10) and the respective vector ϕ. If there exist symmetric positive definite matrices $\mathbb{Q}_i \in \Re^{2n_x \times 2n_x}$, $i = 1, \ldots, n_r$, and a matrix $\mathbb{U} \in \Re^{2n_x \times 2n_x}$ such that*

$$\begin{bmatrix} -\mathbb{Q}_i + \mathbb{U}' + \mathbb{U} & \mathbb{U}'\mathbb{N}'_{\{\ell\}} \\ \star & \phi^2_{\{\ell\}} \end{bmatrix} \geq 0 \quad \forall\ i = 1, ..., n_r \text{ and } \ell = 1, ..., n_\phi, \tag{3.15}$$

then $\mathcal{E}_V \subseteq \mathcal{E}(\mathbb{Q}_i^{-1}) \subset \mathcal{X}^{\{a\}}$, $\forall\ i = 1, ..., n_r$.

Proof *Note that owing to the positivity of* $\mathbb{Q}_i$, $\mathbb{U}$[1] *is regular whenever (3.15) is verified. Now, consider (3.15) multiplied by* $h_{(i)}(k)$ *and summed up on* $i = 1, \ldots, n_r$. *By using the fact*

$$(\mathbb{U}' - \mathbb{Q}(h(k)))\mathbb{Q}^{-1}(h(k))(\mathbb{U} - \mathbb{Q}(h(k))) \geq 0,$$

the block $(1, 1)$ *can be overbounded by* $\mathbb{U}'\mathbb{Q}^{-1}(h(k))\mathbb{U}$. *The obtained inequality can be pre-multiplied by* $\mathrm{diag}\{\left(\mathbb{U}^{-1}\right)', I_r\}$ *and post-multiplied by its transpose, and applying Schur's Complement* (BOYD *et al.*, *1994) it yields* $\forall\ \ell = 1, ..., n_\phi$:

$$\begin{bmatrix} \mathbb{Q}^{-1}(h(k)) & \mathbb{N}'_{\{\ell\}} \\ \star & \phi^2_{\{\ell\}} \end{bmatrix} \geq 0 \Leftrightarrow \xi'(k)\mathbb{N}'_{\{\ell\}}\frac{1}{\phi^2_{\{\ell\}}}\mathbb{N}_{\{\ell\}}\xi(k) \leq \xi'(k)\mathbb{Q}^{-1}(h(k))\xi(k).$$

This implies that $\mathcal{E}(\mathbb{Q}^{-1}(h(k))) \subseteq \mathcal{X}^{\{a\}}$ *(see, for instance, Boyd et al. (1994), Jungers & Castelan (2011)).*

As a consequence of Lemma 3.5, if $\mathcal{E}_V \triangleq \bigcap_i \left\{\mathcal{E}(\mathbb{Q}_i^{-1})\right\}$ is λ-contractive, then every trajectory initiated in it remains in $\mathcal{X}^{\{a\}}$ and asymptotically converges to the origin.

Next, to consider that the control inputs may saturate, one can use the modified sector condition associated with the dead-zone nonlinearity $\Psi(u(k))$ (Gomes da Silva Jr.; TARBOURIECH, 2005). This modified sector condition is, in general, locally verified in a polyhedral set $\mathtt{S}(\rho, h(k))$, that for the present control fuzzy problem can be defined by:

$$\mathtt{S}(\rho, h(k)) = \big\{\xi(k) \in \Re^{2n_x} \text{ and } \\ |\left(\mathbb{K}(h(k)) - \mathbb{Y}(h(k))\,\xi(k)\right| \leq \rho, \forall\ h(k) \in \Xi\big\}, \quad (3.16)$$

with

$$\mathbb{K}(h(k)) = \sum_{i=1}^{n_r} h_{(i)}(k)\mathbb{K}_i = \sum_{i=1}^{n_r} h_{(i)}(k)\left[D_{ci}C \quad C_{ci}\right] \text{ and } \\ \mathbb{Y}(h(k)) = \sum_{i=1}^{n_r} h_{(i)}(k)\mathbb{Y}_i. \quad (3.17)$$

[1]Matrix $\mathbb{U}$ is chosen constant to avoid practical implementation issues.

Lemma 3.6 *Consider matrix* $\mathbb{K}_i$ *given in (3.17) and the vector* ρ *with the symmetric amplitude bounds relative to the control input. If there exist symmetric positive definite matrices* $\mathbb{Q}_i \in \Re^{2n_x \times 2n_x}$ *and* $\mathbb{H}_i \in \Re^{n_u \times 2n_x}$, $i = 1, \ldots, n_r$, *and matrix* $\mathbb{U} \in \Re^{2n_x \times 2n_x}$ *such that*

$$\begin{bmatrix} -\mathbb{Q}_i + \mathbb{U}' + \mathbb{U} & \mathbb{U}'\mathbb{K}'_{i\{\ell\}} - \mathbb{H}'_{i\{\ell\}} \\ \star & \rho^2_{\{\ell\}} \end{bmatrix} \geq 0, \quad \forall i = 1, \ldots, n_r \text{ and } \ell = 1, \ldots, n_u. \tag{3.18}$$

then, by setting $\mathbb{Y}_i = \mathbb{H}_i \mathbb{U}^{-1}$, *one has the inclusion* $\mathcal{E}_V \subseteq \mathtt{S}(\rho, h(k))$. *Furthermore, the following modified sector condition holds true for all* $\xi(k) \in \mathcal{E}\left(\mathbb{Q}^{-1}(h(k))\right)$:

$$\Psi'(u(k))S^{-1}\left(\Psi(u(k)) - \mathbb{Y}(h(k))\xi(k) - F_c(h(k))\varphi(\pi(k))\right) \leq 0, \tag{3.19}$$

for any diagonal positive definite matrix $S \in \Re^{n_u \times n_u}$.

Proof *The inclusion* $\mathcal{E}(\mathbb{Q}^{-1}(h(k))) \subseteq \mathtt{S}(\rho, h(k))$ *is similar to the inclusion considered in Lemma 3.5 and can be proven likewise. Thus, by following similar steps as in the proof of Lemma* 1 *in Gomes da Silva Jr. & Tarbouriech (2005), it can be shown that the sector condition (3.19) holds true for all* $\xi(k) \in \mathtt{S}(\rho, h(k))$. *Hence, it also holds true for all* $\xi(k) \in \mathcal{E}\left(\mathbb{Q}^{-1}(h(k))\right) \subseteq \mathtt{S}(\rho, h(k))$.

Note that the sector condition (3.19) can be viewed as an extension of the modified sector condition used in Castelan, Tarbouriech & Queinnec (2008), allowing the dependency on the membership function $h(k)$ to be taken into account. In the sequel are presented the results concerning the local asymptotic (LA) stability analysis of the closed-loop system (3.9).

Lemma 3.7 *(*LA-Stability Analysis*) Let* A_{cij}, B_{cij}, G_{cij}, E_{ci}, C_{ci}, D_{ci}, *and* F_{ci} *be given matrices that form structure (3.7) of compensator (3.5) and consider a given real scalar* $\lambda \in (0, 1]$. *If there exist symmetric positive definite matrices* $\mathbb{Q}_i \in \Re^{2n_x \times 2n_x}$, *positive definite diagonal matrices* $\Delta \in \Re^{n_\varphi \times n_\varphi}$ *and* $S \in \Re^{n_u \times n_u}$, *and matrices* $\mathbb{U} \in \Re^{2n_x \times 2n_x}$, $\mathbb{H}_i \in \Re^{n_u \times 2n_x}$ *verifying inequalities (3.15), (3.18), and*

$$\begin{bmatrix} -\mathbb{Q}_q & \frac{\mathbb{A}_{ij}}{2}\mathbb{U} & \frac{\mathbb{G}_{ij}}{2}\Delta & -\left(\frac{\mathbb{B}_i+\mathbb{B}_j}{2}\right)S \\ \star & \lambda^{-1}\left(\frac{\mathbb{Q}_i+\mathbb{Q}_j}{2}\right)-\mathbb{U}-\mathbb{U}' & \mathbb{U}'\mathbb{L}'\Omega & \frac{\mathbb{H}_i'+\mathbb{H}_j'}{2} \\ \star & \star & -2\Delta & \Delta\left(\frac{F_{ci}'+F_{cj}'}{2}\right) \\ \star & \star & \star & -2S \end{bmatrix} < 0$$

$$\forall\ q,i=1,\ldots,n_r \text{ and } j=i,\ldots,n_r \tag{3.20}$$

then, the set $\mathcal{E}_V \triangleq \bigcap_i \left\{\mathcal{E}(\mathbb{Q}_i^{-1})\right\}$ *is* λ*-contractive and verifies* $\mathcal{E}_V \subseteq \mathcal{X}^{\{a\}} \bigcap \mathtt{S}(\rho, h(k))$.

Proof *Assume that (3.20) is verified for all* $q,i=1,\ldots,n_r$ *and* $j=i,\ldots,n_r$. *Multiply the inequalities successively by* $h_{(i)}(k)$, $h_{(j)}(k)$ *and* $h_{(q)}(k+1)$, *and sum up on* $i,q=1,\ldots,n_r$ *and* $j=i,\ldots,n_r$. *Thus, the inequality* $\mathbb{M}(h(k))<0$ *holds if* $h(k)\in\Xi$ *with*

$$\mathbb{M}(h) = \begin{bmatrix} -\mathbb{Q}(h^+) & \mathbb{A}(h)\mathbb{U} & \mathbb{G}(h)\Delta & -\mathbb{B}(h)S \\ \star & -\lambda\mathbb{U}'\mathbb{Q}^{-1}(h)\mathbb{U} & \mathbb{U}'\mathbb{L}'\Omega & \mathbb{U}'\mathbb{Y}'(h) \\ \star & \star & -2\Delta & \Delta F_c'(h) \\ \star & \star & \star & -2S \end{bmatrix},$$

and the shorthands $h=h(k)$ *and* $h^+=h(k+1)$. *Note that the matrices* $\mathbb{Q}(h)$, $\mathbb{B}(h)$, $\mathbb{H}(h)$ *and* $F_c(h)$ *can be written as* (SILVA et al., 2014)

$$\begin{bmatrix} \mathbb{Q}(h) \\ \mathbb{B}(h) \\ \mathbb{H}(h) \\ F_c(h) \end{bmatrix} = \sum_{i=1}^{n_r}\sum_{j=i}^{n_r}(1+\varsigma_{ij})h_{(i)}(k)h_{(j)}(k)\left(\frac{1}{2}\begin{bmatrix} \mathbb{Q}_i+\mathbb{Q}_j \\ \mathbb{B}_i+\mathbb{B}_j \\ \mathbb{H}_i+\mathbb{H}_j \\ F_{ci}+F_{cj} \end{bmatrix}\right),$$

and that $\lambda\mathbb{U}'\mathbb{Q}^{-1}(h)\mathbb{U} \geq -\lambda^{-1}\mathbb{Q}(h)+\mathbb{U}'+\mathbb{U}$ *(see the proof of Lemma 3.5 for a similar one) is verified since* U *is full rank from the* $(2,2)$ *block of the left-hand side of (3.20). It is also observed that* h *and* h^+ *are handled independently, which may be a source of conservativeness of the presented technique, as well as the fact that solutions are valid for any sequence of* $h(k)$.

Pre- and post-multiplication of $\mathbb{M}(h)$ *by* $\operatorname{diag}\{I,(\mathbb{U}')^{-1},\Delta^{-1},S^{-1}\}$ *and its transpose, respectively, yield a matrix inequality that can be reformulated by Schur's complement as:*

$$\mathbb{M}_S(h) = \begin{bmatrix} \mathbb{A}'(h) \\ \mathbb{G}'(h) \\ -\mathbb{B}'(h) \end{bmatrix} \mathbb{Q}^{-1}(h^+) \begin{bmatrix} \mathbb{A}'(h) \\ \mathbb{G}'(h) \\ -\mathbb{B}'(h) \end{bmatrix}' + \begin{bmatrix} -\lambda\mathbb{Q}^{-1}(h) & \mathbb{L}'\Omega\Delta^{-1} & \mathbb{Y}'(h)S^{-1} \\ \Delta^{-1}\Omega\mathbb{L} & -2\Delta^{-1} & F_c'(h)S^{-1} \\ S^{-1}\mathbb{Y}(h) & S^{-1}F_c(h) & -2S^{-1} \end{bmatrix} < 0.$$

Thus, by defining $\vartheta(k) = \begin{bmatrix} \xi'(k) & \varphi'(k) & \Psi'(u(k)) \end{bmatrix}'$, *one gets:*

$$\vartheta'(k)\mathbb{M}_s(h)\vartheta(k) = \Delta V_\lambda(\xi(k), h(k)) - 2\varphi'(\pi(k))\Delta^{-1}\left(\varphi(\pi(k)) - \Omega\mathbb{L}\xi(k)\right) - 2\Psi'(u(k))S^{-1}\left(\Psi(u(k)) - \mathbb{Y}(h(k))\xi(k) - F_c(h(k))\varphi(\pi(k))\right) < 0, \quad (3.21)$$

which is valid for all $h(k) \in \Xi$.

Next, recall from Lemmas 3.5 and 3.6 that conditions (3.15) and (3.18) guarantee $\mathcal{E}(\mathbb{Q}^{-1}(h(k))) \subseteq \mathcal{X}^{\{a\}}$ *and* $\mathcal{E}(\mathbb{Q}^{-1}(h(k))) \subseteq \mathtt{S}(\rho, h(k))$, *respectively. Thus,* $\forall\xi(k) \in \mathcal{E}(\mathbb{Q}^{-1}(h(k))) \subseteq \mathcal{X}^{\{a\}} \bigcap \mathtt{S}(\rho, h(k))$ *one has by definition, that the nonlinearity* $\varphi(\pi(k))$ *verifies the sector condition (2.3) and, from Lemma 3.6, the nonlinearity* $\Psi(u(k))$ *verifies the modified sector condition (3.19). Hence, inequality (3.21) implies that relation (3.11) is verified for* $\mathcal{E}_V = \mathcal{E}(\mathbb{Q}^{-1}(h(k)))$ *and, by Definition 3.4, it is possible to conclude that this level set is* λ*-contractive, thereby completing the proof.*

3.3 STABILIZATION CONDITIONS

Considering the main objective previously formulated, i.e. define a method for the dynamic output feedback control design, the conditions presented in Lemma 3.7 are not adequate, which may only be used for stability analysis. Therefore, to compute the controller, inspired from the work in Scherer, Gahinet & Chilali (1997), it is possible to define the n_x-dimensional real square matrices X, Y, P, and Z (see Castelan et al. (2010)) and

$$\mathbb{U} = \begin{bmatrix} X & \bullet \\ Z & \bullet \end{bmatrix}, \ \mathbb{U}^{-1} = \begin{bmatrix} Y & \bullet \\ P & \bullet \end{bmatrix}, \ \Theta = \begin{bmatrix} Y & I_n \\ P & 0 \end{bmatrix}. \quad (3.22)$$

One has that: $\mathbb{U}\Theta = \begin{bmatrix} I_n & X \\ 0 & Z \end{bmatrix} \implies \hat{\mathbb{U}} = \Theta'\mathbb{U}\Theta = \begin{bmatrix} Y' & T' \\ I_n & X \end{bmatrix}$, where:

$$T' = Y'X + P'Z. \tag{3.23}$$

Furthermore, using the partitioning $\mathbb{Q}_i = \begin{bmatrix} Q_{11i} & Q_{12i} \\ \star & Q_{22i} \end{bmatrix}$, one can set:

$$\hat{\mathbb{Q}}_i = \Theta'\mathbb{Q}_i\Theta = \begin{bmatrix} Y'Q_{11i}Y + P'Q_{12i}'Y + & Y'Q_{11i} + \\ Y'Q_{12i}P + P'Q_{22i}P & P'Q_{12i}' \\ \star & Q_{11i} \end{bmatrix} = \begin{bmatrix} \hat{Q}_{11i} & \hat{Q}_{12i} \\ \star & \hat{Q}_{22_i} \end{bmatrix}. \tag{3.24}$$

Thus, from Lemma 3.7, and by using the above definitions, it is possible to propose the following convex synthesis condition that provides a solution to Problem 3.1.

Theorem 3.8 (LA-Stabilization) *Consider the system (3.1)-(3.4) and a given real scalar $\lambda \in (0, 1]$. If there exist symmetric positive definite matrices $\hat{\mathbb{Q}}_i$, positive diagonal matrices S and Δ, matrices X, Y, T, $\hat{A}_{ij}$, $\hat{B}_{ij}$, $\hat{G}_{ij}$, $\hat{E}_i$, $\hat{C}_i$, $\hat{D}_i$, $\hat{F}_i$ of appropriate dimensions, and $\hat{H}_{1i} \in \Re^{n_u \times n_x}$ and $\hat{H}_{2i} \in \Re^{n_u \times n_x}$, $i = 1, \ldots, n_r$ and $j = i, \ldots, n_r$, verifying the LMIs conditions (3.25)-(3.27) and the nonsingular matrices Z and P such that* (3.23) *is verified, then, the controller (3.5) structured as in (3.7) with matrices given in (3.28) (see next page) and the set $\mathcal{S}_0 \triangleq \mathcal{E}(\mathbb{Q}^{-1}(h(k))) = \bigcap_{i=1,\ldots,n_r} \mathcal{E}\left(\mathbb{Q}_i^{-1}\right)$ are solutions to Problem 3.1.*

$$\left[\begin{array}{c:c:c:c} -\hat{\mathbb{Q}}_q & \Pi_{ij}^1 & \begin{matrix} \dfrac{\hat{G}_{ij}}{2} \\ \dfrac{(G_i + G_j)\Delta + B_i\hat{F}_j + B_j\hat{F}_i}{2} \end{matrix} & \begin{matrix} -\dfrac{\hat{E}_i + \hat{E}_j}{2} \\ -\left(\dfrac{B_i + B_j}{2}\right)S \end{matrix} \\ \hdashline \star & \Pi_{ij}^2 & \begin{matrix} L'\Omega \\ X'L'\Omega \end{matrix} & \begin{matrix} \dfrac{\hat{H}_{1i}' + \hat{H}_{1j}'}{2} \\ \dfrac{\hat{H}_{2i}' + \hat{H}_{2j}'}{2} \end{matrix} \\ \hdashline \star & \star & -2\Delta & \dfrac{\hat{F}_i' + \hat{F}_j'}{2} \\ \hdashline \star & \star & \star & -2S \end{array}\right] < 0,$$

$$\forall\ q, i = 1, ..., n_r \text{ and } j = i, ..., n_r \tag{3.25}$$

$$\left[\begin{array}{c:c} -\hat{\mathbb{Q}}_i + \hat{\mathbb{U}} + \hat{\mathbb{U}}' & \begin{array}{c}(\hat{D}_{i\{\ell\}}C)' - \hat{H}'_{1i\{\ell\}} \\ \hat{C}'_{i\{\ell\}} - \hat{H}'_{2i\{\ell\}}\end{array} \\ \hdashline \star & \rho^2_{\{\ell\}} \end{array}\right] > 0,$$

$$\forall\ i = 1,...,n_r \ \ and\ \ell = 1,...,n_u \tag{3.26}$$

$$\left[\begin{array}{c:c} -\hat{\mathbb{Q}}_i + \hat{\mathbb{U}} + \hat{\mathbb{U}}' & \begin{array}{c}N'_{\{\ell\}} \\ (NX)'_{\{\ell\}}\end{array} \\ \hdashline \star & \phi^2_{\{\ell\}} \end{array}\right] > 0,$$

$$\forall\ i = 1,...,n_r \ \ and\ \ell = 1,...,n_\phi \tag{3.27}$$

with

$$\begin{aligned}
\Pi^1_{ij} &= \left[\begin{array}{cc} \dfrac{Y'(A_i + A_j) + \hat{B}_{ij}C}{2} & \dfrac{\hat{A}_{ij}}{2} \\ \dfrac{A_i + A_j + (B_i\hat{D}_j + B_j\hat{D}_i)C}{2} & \dfrac{(A_i + A_j)X + B_i\hat{C}_j + B_j\hat{C}_i}{2} \end{array}\right], \\
\Pi^2_{ij} &= \lambda^{-1}\left(\frac{\hat{\mathbb{Q}}_i + \hat{\mathbb{Q}}_j}{2}\right) - \hat{\mathbb{U}} - \hat{\mathbb{U}}'.
\end{aligned}$$

$$\left.\begin{aligned}
&D_{ci} = \hat{D}_i\ ,\ C_{ci} = (\hat{C}_i - D_{ci}CX)Z^{-1}, \\
&E_{ci} = (P')^{-1}(\hat{E}_iS^{-1} - Y'B_i),\ F_{ci} = \hat{F}_i\Delta^{-1}, \\
&B_{cij} = (P')^{-1}\left[\hat{B}_{ij} - Y'(B_iD_{cj} + B_jD_{ci})\right], \\
&G_{cij} = (P')^{-1}\left[\hat{G}_{ij}\Delta^{-1} - Y'(G_i + G_j + B_iF_{cj} + B_jF_{ci})\right], \\
&A_{cij} = (P')^{-1}\big[\hat{A}_{ij} - Y'(A_i + A_j)X - \hat{B}_{ij}CX \\
&\qquad\quad -Y'(B_iC_{cj} + B_jC_{ci})Z\big]Z^{-1}\ ,
\end{aligned}\right\} \tag{3.28}$$

Proof *Suppose there exists a solution to* (3.25)-(3.27) *for all* $q, i = 1, \ldots, n_r$ *and* $j = i, \ldots, n_r$. *Then, from the* $(2, 2)$ *block of (3.25), it follows that* $\hat{\mathbb{U}} > 0$. *Hence, in view of* (3.23), *the matrices* X, Y *and* $(T' - Y'X)$ *are nonsingular. As a result, for any nonsingular* P, *the matrices defined in (3.28) are well-defined.*

Next, consider (3.24), define the change of variables $\hat{D}_i$, $\hat{C}_i$, $\hat{F}_i$, $\hat{E}_i$, $\hat{B}_{ij}$, $\hat{G}_{ij}$ *and* $\hat{A}_{ij}$, *according to* (3.28), *and consider* $\mathbb{H}_i = \begin{bmatrix}\hat{H}_{1i} & \hat{H}_{2i}\end{bmatrix}$. *Thus, pre- and post-multiplication the inequality (3.20) by* $\mathrm{diag}\{\Theta', \Theta', I, I\}$ *and its transpose, respectively, leads to be concluded* *that the verification of* (3.25) *is equivalent to the verification of* (3.20). *Likewise, pre- and post-multiplication of both inequalities* (3.15) *and* (3.18) *by* $\text{diag}\{\Theta', 1\}$ *and its transpose, respectively, shows their equivalence with* (3.26) *and* (3.27). *Thus, Lemma 3.7 can be applied to conclude the proof.*

3.4 SYNTHESIS OF THE DYNAMIC CONTROLLER

For solving Problem 3.1 different criteria can be used to optimize the size of the set S_0. Among them, a shape set approach can be adopted to optimize the size of S_0 according to the shape of the domain of validity $\mathcal{X}^{\{a\}} \in \Re^{2n_x}$. For this purpose, define the set $\mathcal{V} \subset \Re^{2n_x}$,

$$\mathcal{V} = Co\left\{ \bar{v}_\sigma \in \Re^{2n_x} \; ; \; \bar{v}_\sigma = \begin{bmatrix} v_\sigma \\ 0 \end{bmatrix} \; , \; \sigma = 1, \dots, n_\sigma \right\},$$

where the set of vectors $\{v_\sigma \in \Re^{n_x}\}$ contains the information necessary to characterize the shape of $\mathcal{X} \subset \Re^{n_x}$, the primary domain of validity for the open-loop T-S fuzzy model. For instance, if $\mathcal{X}$ is a polytope (closed and bounded polyhedron), *i.e.*, $n_\phi = n_x$, then each v_σ is a vertex of $\mathcal{X}$. Otherwise, $n_\phi < n_x$ implies that $\mathcal{X}$ is unbounded along the null space of N, and the vectors v_σ can then be defined from the vertices of the projection of $\mathcal{X}$, along the null space of N, into the image of N.

For example, if $N = \begin{bmatrix} -1 & 2 & 0 \\ 2 & 3 & 0 \end{bmatrix}$ and $\phi = \begin{bmatrix} 1 & 2 \end{bmatrix}'$, one has that $n_\phi = 2$, $n_x = 3$ and $\mathcal{X}$ is defined by the set of vectors $\pm\frac{1}{7}\begin{bmatrix} 1 & 4 & 0 \end{bmatrix}'$ and $\pm\begin{bmatrix} 1 & 0 & 0 \end{bmatrix}'$, being not constrained along the direction of $\mathcal{N}(N) = \begin{bmatrix} 0 & 0 & 1 \end{bmatrix}'$. Then, in this case one has $v_1 = \frac{1}{7}\begin{bmatrix} 1 & 4 \end{bmatrix}'$, $v_2 = -v_1$, $v_3 = \begin{bmatrix} 1 & 0 \end{bmatrix}'$ and $v_4 = -v_3$.

Thus, for the purposes of synthesis the objective will be to maximize $\beta > 0$ such that the inclusion $\beta\mathcal{V} \subseteq S_0$ is also verified. Considering $\mu = 1/\beta^2$, this inclusion reads:

$$\begin{bmatrix} \mu & \bar{v}_\sigma' \\ \star & \mathbb{Q}_i \end{bmatrix} \geq 0 \; , \quad \begin{array}{l} \forall i = 1, \dots, n_r \\ \forall \sigma = 1, \dots, n_\sigma \end{array} \; ,$$

which, by pre- and post-multiplication by $\text{diag}\{1, \Theta'\}$ and its transpose, respectively, is equivalent to:

$$\left[\begin{array}{c|cc} \mu & v_\sigma^{'} Y & v_\sigma^{'} \\ \hline \star & \multicolumn{2}{c}{\hat{\mathbb{Q}}_i} \end{array}\right] \geq 0,\ i = 1, \ldots, n_r,\ \sigma = 1, \ldots, n_\sigma. \tag{3.29}$$

In this way, by using Theorem 3.8 and condition (3.29), the following convex optimization problem to synthesize the controller gains can be proposed:

$$\begin{array}{c} \min\limits_{\substack{\bar{Q}_{11i}, \bar{Q}_{12i}, \bar{Q}_{22i}, \hat{A}_{ij}, \hat{G}_{ij}, X, Y, T, \Delta, S, \\ \hat{B}_{ij}, \hat{C}_i, \hat{D}_i, \hat{E}_i, \hat{F}_i, \hat{H}_{11i}, \hat{H}_{12i}, \hat{H}_{2i}}} \mu \\ subject\ \ to \\ LMIs\ \ (3.25),\ \ (3.26),\ \ (3.27)\ \ and\ \ (3.29). \end{array} \tag{3.30}$$

3.5 EXPERIMENTS

3.5.1 Illustrative Example Continued

For this experiment it is considered the system of the Illustrative Example 2.3 (see Chapter 2, section 2.3), now subject to amplitude bound control input

$$x(k+1) = x^3(k) + \sin(x(k)) + (0.2 + x^2(k))sat(u(k)) \quad , \qquad y(k) = x(k) \tag{3.31}$$

Although (3.31) represents a unidimensional system, its application here is interesting in terms of comparison and for graphical representation (the augmented space belongs to $\Re^2$).

Now, defining the sector nonlinearity $\varphi(y(k)) = \sin(y(k)) \in S\,[0,1]$, and considering the domain of validity defined by $|x| \leq 5\pi/12$, it is obtained a N-Fuzzy model with two local nonlinear rules, with matrices given by:

$$A_1 = [\ 1.7135\ ]\ ;\ A_2 = [\ 0\ ]\ ;\quad B_1 = [\ 1.9135\ ]\ ;\ B_2 = [\ 0.2000\ ]$$
$$G_1 = G_2 = [\ 1\ ]\ ;\quad L = 1\ ;\quad \Omega = 1. \tag{3.32}$$

This illustrates how the use of N-fuzzy models can effectively reduce the number of rules w.r.t. the classical fuzzy modeling used in (2.24). The two nonlinear membership functions

$$h_{(1)}(k) = \frac{y^2(k)}{1.7135} \text{ and } h_{(2)}(k) = 1 - \frac{y^2(k)}{1.7135},$$

are shown in Figure 13 for the considered domain of validity.

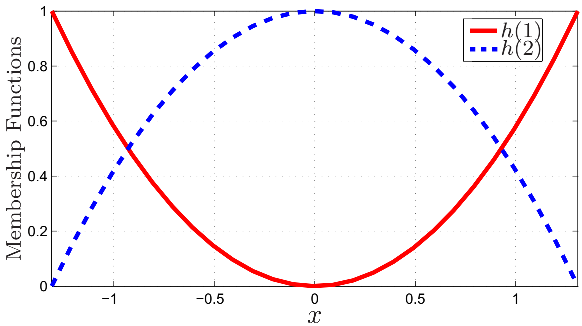

Figure 13 – Nonlinear membership functions $h_{(i)}(k), \forall\ i = 1, ..., 2$

Figure 14 depicts the basins of attraction and the corresponding estimates given by sets $\mathcal{S}_0$ using a simplified compensator with $C_c(h(k)) = C_c$, $D_c(h(k)) = D_c$ and $F_c(h(k)) = F_c$, as described in Remark 3.2. In these figures the dashed lines represent the boundary of the domain of validity. Firstly, it is observed that greater is the level of saturation ρ, the greater are these estimates. Furthermore, for any level of saturation $\rho \geq 1$, all the system states inside domain of validity can be steered to the origin, differently from the case without saturation shown in Example 2.3.

In Figure 15 is observed the state trajectories and control efforts considering three stabilizing initial conditions: $\xi(0) = [0.7\ 0]$ marked with □, $\xi(0) = [1.1\ 0]$ marked with X, both inside the level set $\mathcal{S}_0$ and $\xi(0) = [-1.28\ 0]$ marked with O, outside $\mathcal{S}_0$ but inside the domain of validity $\mathcal{X}$. Any trajectory initialized in $\mathcal{S}_0$ evolve inside it, even

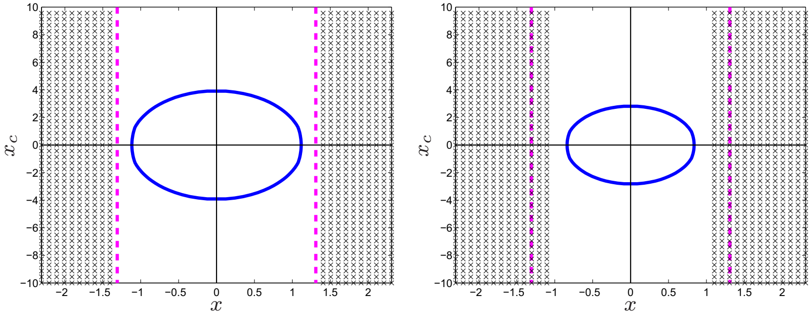

(a) $\rho = 1$ (b) $\rho = 0.75$

Figure 14 – Basin of attraction and S_0

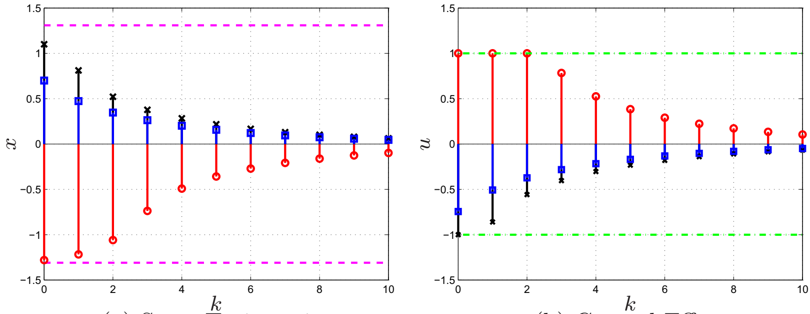

(a) State Trajectories (b) Control Effort

Figure 15 – State trajectories and control effort

with possible control saturation, as is the case for the second initial condition.

In the sequel, the proposed experiments correspond to the application of algorithm (3.30) to some of the plants represented by T-S fuzzy models described in Appendix B, aiming to elucidate the effectiveness of the N-fuzzy approach.

3.5.2 Example 2

Consider a modified version of the two dimensional nonlinear discrete-time system presented in Appendix B, section B.2, with state space representation as follows

$$
\begin{aligned}
x_{(1)}(k+1) &= -\frac{13}{20}x_{(1)}(k)+\frac{11}{20}x_{(2)}(k)+\frac{9}{40}x_{(1)}^2(k)+\frac{3}{40}x_{(1)}(k)x_{(2)}(k)+\varphi(k) \\
x_{(2)}(k+1) &= \frac{1}{5}x_{(1)}(k)+\frac{6}{5}x_{(2)}(k)+\frac{1}{5}x_{(1)}^2(k)+\frac{1}{20}x_{(1)}(k)x_{(2)}(k)+\frac{5}{4}u(k) \\
&\quad +\frac{1}{40}x_{(1)}(k)u(k) \\
y(k) &= x_{(1)}(k)
\end{aligned}
$$

where $\varphi(k) = \varphi(y(k)) = \dfrac{3}{10}y(k)(1+\sin(y(k))) \in S[0, 0.7]$ and the symmetrical limit of saturation is given by $\rho = 1.1$. The main modifications are related to disregard the disturbance and regulated output signals, and in the variable dependency of the sector nonlinearity $\varphi(k)$, that is required for their real-time computation and consequently for implementation purposes. An alternative to handle with unmeasurable states will be discussed later in Chapter 5.

Despite the above considerations, the equivalent N-fuzzy model is given in equation (B.3), with the domain of validity defined by $\mathcal{X} = \{x(k) \in \Re^2 : |x_{(1)}(k)| \leq 2 \text{ and } |x_{(2)}(k)| \leq 1.5\}$.

Firstly, in order to demonstrate the relationship between the performance parameter λ and the size of the corresponding contractive region, it is applied the algorithm (3.30) for the values $\lambda \in \{1, 0.9, 0.8\}$, where it is obtained, respectively, the values $\beta \in \{0.3617, 0.2869, 0.2153\}$. Notice that demanding a higher speed of convergence (lower value of λ), lower is the value of β and, in consequence, the size of the set S_0 in which the performance is guaranteed.

Figure 16 depicts the basin of attraction and the corresponding estimates given by S_R (stability region) considering $\lambda = 1$ and $\lambda = 0.9$. Based on real applications, the initial conditions of interest are of the type $\xi(0) = [x(0)', 0]'$. In this case, the region S_R (the set of admissible initial conditions) correspond to the intersection of S_0 with the plane formed by the states of the plant. Once the states of the controller x_c can assume non-zero values for $k > 0$, the projected trajectory over the subspace of the plant evolve in a domain called C_R (confinement region), i.e. $x(0) \in S_R \Rightarrow x(k) \in C_R \subseteq \mathcal{X}, \forall\ k > 0$ (see Appendix E, particularly Figure 46). The set C_R correspond to the orthogonal projection of S_0 with the plane formed by the states of the plant.

Also in Figure 16, the points marked with X correspond to destabilizing initial conditions and/or whose trajectories evolve outside the domain of validity $\mathcal{X}$ (leading to undesirable system behaviors). Note

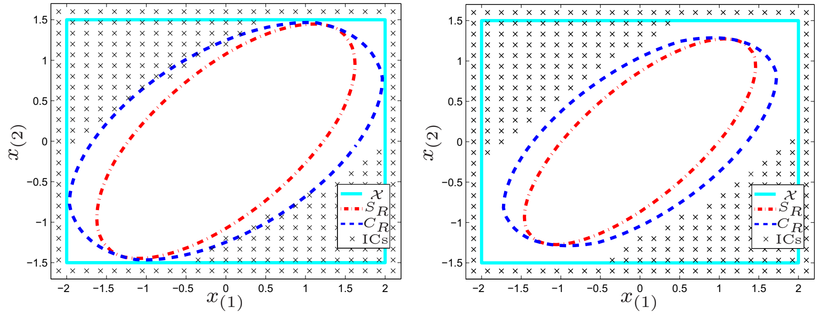

(a) with $\lambda = 1$ (b) with $\lambda = 0.9$

Figure 16 – Basin of attraction and associated sets

that such a condition can exist even inside $\mathcal{X}$, demonstrating again the importance of considering the local characteristics of the T-S fuzzy models. At last, comparing the sizes of S_R it is possible to verify the aforementioned trade-off between λ and β.

For the temporal simulation is considered the initial condition $\xi(0) = [x(0)', 0]'$, with $x(0) = \begin{bmatrix} 1.15 & 1 \end{bmatrix}'$. This initial condition belongs to the set of admissible initial conditions S_R of the controllers designed with $\lambda = 1$ and $\lambda = 0.9$. As expected, the best time-performance, relative to the lower contractive parameter λ, can be observed comparing the state trajectories in Figure 17, as well as by comparison the decrease of the Lyapunov function corresponding to these trajectories, as shown in Figure 18.

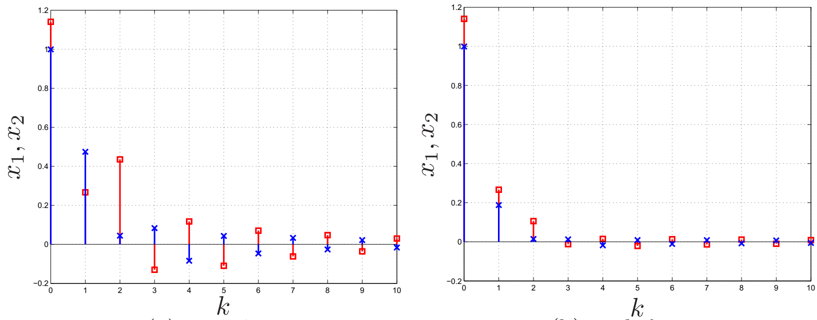

(a) with $\lambda = 1$ (b) with $\lambda = 0.9$

Figure 17 – State trajectories for example 1

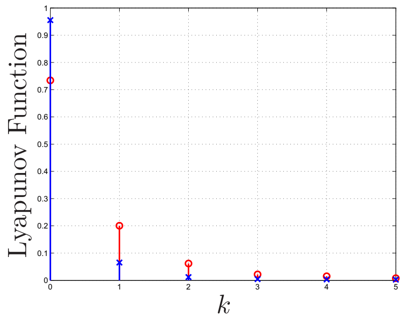

Figure 18 – Lyapunov Functions: "○" for $\lambda = 1$ and "×" for $\lambda = 0.9$

3.6 CONCLUDING REMARKS

In this chapter a convex design of a nonlinear parallel-distributed-compensator that, by dynamic output feedback, stabilizes a class of nonlinear discrete-time systems with saturated control inputs was presented. An important contribution is the consideration of the inherent local/regional validity of the fuzzy model, assuring that, with the proposed initial conditions, the closed-loop system will operate inside a specified domain of the state space (where the fuzzy model convexity is valid and/or the system operation is safe). The proposed controller contains a fuzzy anti-windup gain that helps mitigate the undesirable effects of saturation and considers some performance requirements, which are associated with the contractivity coefficient of the trajectories in the considered level set.

For now it is assumed the real time availability of the membership functions vector $h(k)$ for the controller. This fact implies that either $h(k)$ should be directly measurable, or it should be reconstituted by measurable signals/states, which is more common in practice. An alternative to handling unmeasurable states will be discussed later in Chapter 5. Another important detail is that the results obtained by using N-fuzzy modeling, despite the reduced number of rules, present a similar degree of conservatism in terms of the size of the stability and confinement regions, or even lower than the analogous results using the classical fuzzy approach.

4 CONTROL SYNTHESIS FOR NONLINEAR SYSTEMS SUBJECT TO ENERGY BOUNDED DISTURBANCES

In this chapter, it is addressed the local stabilization problem of nonlinear discrete-time systems subject to energy bounded disturbances by means of T-S fuzzy models. The proposed controller consists of a nonlinear state feedback which depends on the fuzzy membership function as well as the sector bounded nonlinearities, in the case of an N-fuzzy model. In this setup, LMI control design conditions are proposed to locally ensure the input-to-state stability in the ℓ_2-sense (ℓ_2-ISS) and a certain input-to-output performance (i.e., an upper bound for the system ℓ_2-gain) of the original nonlinear discrete-time system.

Additionally, the design conditions provide an estimate of the closed-loop reachable set (that is, a region inside the T-S domain of validity which bounds the state trajectories driven by the admissible class of ℓ_2 disturbances). Finally, three (convex) optimization problems are proposed to either minimize the estimate of the reachable set, improve the disturbance tolerance or minimize the ℓ_2-gain from the disturbance input to the regulated output; and numerical examples are considered to demonstrate the effectiveness of the proposed approach as a control design tool for nonlinear discrete-time systems subject to energy bounded disturbances. The results presented here are based on the works Klug, Castelan & Coutinho (2013), in which the ISS in the ℓ_2-sense was first investigated, and Klug, Castelan & Coutinho (2015b).

4.1 PROBLEM FORMULATION

Consider the class of nonlinear systems in (2.1) with the addition of a regulated output vector $z_k \in \mathcal{Z} \subset \Re^{n_z}$, represented by

$$\begin{array}{rcl} x(k+1) & = & f(x(k)) + \mathscr{V}(x(k))u(k) + \mathcal{T}(x(k))w(k) \\ z(k) & = & f_z(x(k)) + \mathscr{V}_z(x(k))u(k) + \mathcal{T}_z(x(k))w(k) \end{array} \tag{4.1}$$

where $x(k) \in \mathcal{X} \subset \Re^{n_x}$, $u(k) \in \mathcal{U} \subset \Re^{n_u}$ and $w_k \in \mathcal{W} \subset \Re^{n_w}$ are respectively the state, the control input and the exogenous disturbance vectors. The functions $f(\cdot) : \Re^{n_x} \longrightarrow \Re^{n_x}$, with $f(0) = 0$, $f_z(\cdot) : \Re^{n_x} \longrightarrow \Re^{n_z}$, with $f_z(0) = 0$, $\mathscr{V}(\cdot) : \Re^{n_x} \longrightarrow \Re^{n_x \times n_u}$, $\mathscr{V}_z(\cdot) : \Re^{n_x} \longrightarrow \Re^{n_z \times n_u}$, $\mathcal{T}(\cdot) : \Re^{n_x} \longrightarrow \Re^{n_x \times n_w}$ and $\mathcal{T}_z(\cdot) : \Re^{n_x} \longrightarrow \Re^{n_z \times n_w}$ are continuous and bounded for all $x(k) \in \mathcal{X}$. The additional signal $z(k)$ is required for the desired control purposes.

In order to design a state feedback control law $u_k = \kappa(x_k)$, the nonlinear system (4.1) will be represented by means of N-fuzzy model (using the procedure explained in section 2.2 with similar steps for the nonlinearities in the vector $z(k)$), described through the defuzzification method by center of gravity as

$$\begin{aligned} x(k+1) &= A(h(k))x(k)+B(h(k))u(k)+B_w(h(k))w(k)+G(h(k))\varphi(k)\\ z(k) &= C_z(h(k))x(k)+B_z(h(k))u(k)+B_{zw}(h(k))w(k)+G_z(h(k))\varphi(k) \end{aligned} \tag{4.2}$$

The disturbance input vector $w(k)$ is assumed to lie inside the following class of square summable sequences:

$$\mathcal{W} := \{w(k) : \|w(k)\|_{\ell_2}^2 \leq \delta^{-1}\}, \tag{4.3}$$

where δ is a positive scalar defining the size of $\mathcal{W}$ (i.e., the energy bound of $w(k)$). The set $\mathcal{W}$ will be often referred as the class of admissible disturbances.

Complementing the fuzzy model description (4.2), the vector of nonlinearities $\varphi(k) = \varphi(Lx(k)) \in \Re^{n_\varphi}$ verifies (at least locally) the sector condition (2.3), and the matrix structure is given by:

$$\begin{bmatrix} A(h(k)) & B(h(k)) & B_w(h(k)) & G(h(k)) \\ C_z(h(k)) & B_z(h(k)) & B_{zw}(h(k)) & G_z(h(k)) \end{bmatrix} = \sum_{i=1}^{n_r} h_{(i)}(k) \begin{bmatrix} A_i & B_i & B_{wi} & G_i \\ C_{zi} & B_{zi} & B_{zwi} & G_{zi} \end{bmatrix}.$$

At last, the T-S model domain of validity $\mathcal{X}$ is described by (2.17). It should be remembered that $x(k) \in \mathcal{X} \Rightarrow h(k) \in \Xi$, with Ξ as defined in (3.2), i.e. $\mathcal{X}$ is a region of the state space where the convexity property of set (3.2) holds true. Such domain of validity must be taken into account by any control synthesis or stability analysis condition that assumes description (4.2) instead of (4.1). In particular, loss of performance or even instability may occur when state trajectories evolve outside the domain of validity of the model (4.2). In this sense, one purpose is to handle the domain of validity of the T-S model into the controller synthesis stage to assure local closed-loop stability.

Assuming that the normalized membership functions $h(k)$ can be computed in real-time, a nonlinear controller can be proposed with the same fuzzy rules as the nonlinear T-S model in (4.2). In this case, the following nonlinear state feedback control law is proposed:

$$u(k) = \kappa(x_k) = K(h(k))x(k) + \Gamma(h(k))\varphi(k) \tag{4.4}$$

where $\left[\begin{array}{cc} K(h(k)) & \Gamma(h(k)) \end{array}\right] = \sum_{i=1}^{n_r} h_{(i)}(k) \left[\begin{array}{cc} K_i & \Gamma_i \end{array}\right]$, with $K_i \in \Re^{n_u \times n_x}$ and $\Gamma_i \in \Re^{n_u \times n_\varphi}$.

Taking (4.2) and (4.4) into account, the closed-loop T-S fuzzy model is as follows:

$$\begin{array}{rcl} x(k+1) & = & \mathcal{A}(h(k))x(k) + B_w(h(k))w(k) + \mathcal{G}(h(k))\varphi(k) \\ z(k) & = & \mathcal{C}(h(k))x(k) + B_{zw}(h(k))w(k) + \mathcal{F}(h(k))\varphi(k) \end{array} \tag{4.5}$$

with

$$\begin{array}{l} \mathcal{A}(h(k)) = A(h(k)) + B(h(k))K(h(k)), \\ \mathcal{G}(h(k)) = G(h(k)) + B(h(k))\Gamma(h(k)), \\ \mathcal{C}(h(k)) = C_z(h(k)) + B_z(h(k))K(h(k)) \text{ and} \\ \mathcal{F}(h(k)) = G_z(h(k)) + B_z(h(k))\Gamma(h(k)). \end{array}$$

The closed-loop matrices $\mathcal{A}(h(k))$, $\mathcal{G}(h(k))$, $\mathcal{C}(h(k))$ and $\mathcal{F}(h(k))$ can be generically rewritten, through summation properties, as

$$\mathscr{T}(h(k)) = \sum_{i=1}^{n_r} \sum_{j=i}^{n_r} (1 + \varsigma_{ij}) h_{(i)}(k) h_{(j)}(k) \frac{T_i + X_i Y_j + T_j + X_j Y_i}{2} \tag{4.6}$$

where the tuple $(\mathscr{T}, T, X, Y)$ represents either $(\mathcal{A}, A, B, K)$, $(\mathcal{G}, G, B, \Gamma)$, $(\mathcal{C}, C_z, B_z, K)$ or $(\mathcal{F}, G_z, B_z, \Gamma)$, and ς_{ij} is a binary variable such that (as previously defined in (3.8))

$$\varsigma_{ij} = \begin{cases} 1 & \text{if} \quad i \neq j, \\ 0 & \text{otherwise.} \end{cases} \tag{4.7}$$

Notice that the ℓ_2-ISS of system (4.5) for all $h(k) \in \Xi$ implies that the original nonlinear system in (4.1) with (4.4) is also ISS stable. This is satisfied if the trajectory $x(k)$ of (4.5) driven by $w(k) \in \mathcal{W}$ remains in $\mathcal{X}$ for all $k \geq 0$. In order to obtain LMI constraints guaranteeing the state trajectory boundness inside $\mathcal{X}$, the following problem will be addressed in this work.

Problem 4.1 *Determine the gain matrices K_i and Γ_i, for $i = 1, ..., n_r$, such that the trajectories of system (4.5) remain bounded in some region $\mathcal{D}$ containing the origin such that $\mathcal{D} \subset \mathcal{X}$ for any $w(k) \in \mathcal{W}$ and for all $h(k) \in \Xi$. In addition, determine a positive constant γ which bounds the induced ℓ_2-norm from $w(k)$ to $z(k)$.*

From the above control problem different optimization design criteria can be considered to compute the matrices K_i and Γ_i, as for example to minimize the ℓ_2-gain (by minimizing γ), to maximize the size of the class of admissible disturbances (by minimizing δ) or to minimize the size of a trajectory bounding set for a given class of admissible disturbances $\mathcal{W}$ (by considering that δ and γ are given). These optimization problems are better discussed later.

To end this section, some preliminary results which will be instrumental to derive the synthesis conditions are given below.

Let $V(x(k), h(k))$ be a fuzzy Lyapunov function (FLF)

$$\begin{array}{c} V(x(k), h(k)) : \Re^{n_x} \times \Xi \to \Re^{+} \ , \ V(0, h(k)) = 0 \\ \forall \ h(k) \in \Xi \end{array} \tag{4.8}$$

and the set $\mathcal{D}$ defined as follows

$$\mathcal{D} \triangleq \{x(k) \in \Re^{n_x} : V\left(x(k), h(k)\right) \leq \delta^{-1}, \forall \ h(k) \in \Xi\} \ , \tag{4.9}$$

where δ is the positive scalar defining the bound of $\mathcal{W}$ in (4.3).

In the following, it is defined the notion of input-to-state stability in the ℓ_2-sense for nonlinear discrete-time systems to be considered in this thesis.

Definition 4.2 *Consider the system (4.1), with* $x(0) = 0$*, and the level set* $\mathcal{D}$ *as defined in* (4.9) *for a given positive scalar* δ*. The unforced system in (4.1) is said to be* ℓ_2*-ISS*$_{\mathcal{D}}$ *(input-to-state stable with respect to* $\mathcal{D}$*), if for any* $w(k) \in \mathcal{W}$ *the system state* $x(k)$ *remains bounded in* $\mathcal{D}$ *for all* $k \geq 0$.

Observe that the above definition implies that $\mathcal{D}$ is a positively invariant set. Thus, $x(0) \in \mathcal{D}$ implies that

$$V(x(k), h(k)) \leq \delta^{-1} \ , \ \forall \ k \geq 0 \ , \ h(k) \in \Xi \ . \tag{4.10}$$

Lemma 4.3 *The unforced system (4.1), with* $x(0) = 0$*, is* ℓ_2*-ISS*$_{\mathcal{D}}$ *and there exists an upper bound* γ *on the* ℓ_2*-gain from* $w(k)$ *to* $z(k)$ *if the following holds for all* $x(k) \in \mathcal{D}$*,* $h(k) \in \Xi$ *and* $w(k) \in \mathcal{W}$*:*

$$\begin{aligned} \Delta V(k) \triangleq V\left(x(k+1), h(k+1)\right) - V\left(x(k), h(k)\right) \\ + \gamma^{-2} z^{'}(k) z(k) - w^{'}(k) w(k) < 0 \end{aligned} \tag{4.11}$$

Proof *Assume that (4.11) holds* $\forall \ x(k) \in \mathcal{D}, \ h(k) \in \Xi, \ w(k) \in \mathcal{W}$.

Then, for any $\bar{k} > 0$, leads to:

$$\begin{aligned} \sum_{k=0}^{\bar{k}-1} \Delta V(k) &= V\left(x(\bar{k}), h(\bar{k})\right) - V\left(x(0), h(0)\right) \\ &+\gamma^{-2} \sum_{k=0}^{\bar{k}-1} z(k)^{'} z(k) - \sum_{k=0}^{\bar{k}-1} w(k)^{'} w(k) < 0 \end{aligned} \tag{4.12}$$

Thus, in view of (4.3) and (4.8), the above implies:

i) *ℓ_2 input-to-state stability: note that $V(x(0), h(0)) = 0$, since $x(0) = 0$. Then, it has $V\left(x(\bar{k}), h(\bar{k})\right) \leq \|w(k)\|_2^2 \leq \delta^{-1}$, $\forall\, \bar{k} > 0$. That is, $\mathcal{D}$ is a positive invariant set.*

ii) *input-to-output performance: taking $\bar{k} \to \infty$, it follows that $\|z(k)\|_2 < \gamma\|w(k)\|_2$. That is, γ is an upper-bound on the system ℓ_2-gain.*

iii) *internal stability: let $\tilde{k}$ be a positive integer. If $w(k) = 0$ for all $k \geq \tilde{k}$, then the condition in (4.11) implies that $V(x(k+1), h(k+1)) - V(x(k), h(k)) < -\gamma^{-2} z(k)^{'} z(k) < 0$ guaranteeing that $x(k) \to 0$ as $k \to \infty$. In other words, $\mathcal{D}$ is a contractive positive invariant set whenever the disturbance $w(k)$ vanishes (see, e.g., (KLUG; CASTELAN; LEITE, 2011)).*

4.2 CONTROL DESIGN

For the purpose of synthesizing the controller (4.4) which ensures that the nonlinear system (4.1) is locally ℓ_2-ISS$_{\mathcal{D}}$ in closed-loop, it is considered the N-Fuzzy representation given in (4.5). To this end, let the following FLF:

$$V(x(k), h(k)) = x(k)^{'} Q^{-1}(h(k)) x(k), \quad Q(h(k)) = \sum_{i=1}^{n_r} h_{k(i)} Q_i \ , \tag{4.13}$$

with $Q_i = Q_i^{'} > 0 \in \Re^{n_x \times n_x}$, $i = 1, \ldots, n_r$, to be determined.

In light of the above, it is required to consider $\mathcal{D} \subset \mathcal{X}$ for all $h(k) \in \Xi$ in Lemma 4.3 to guarantee the convexity of the fuzzy model in (4.5). Furthermore, it can be shown that the level set $\mathcal{D}$ as defined in (4.9) with (4.13) will be the intersection of n_r ellipsoidal sets (HU; Z.; M., 2002; JUNGERS; CASTELAN, 2011), given by

$$\mathcal{D} \triangleq \bigcap_{i \in \{1, \ldots n_r\}} \mathcal{E}(Q_i^{-1}, \delta^{-1}) \tag{4.14}$$

where $\mathcal{E}(Q_i^{-1}, \delta^{-1}) = \left\{ x(k) \in \Re^{n_x} : x(k)' Q_i^{-1} x(k) \leq \delta^{-1} \right\}$ is the i-th ellipsoidal set.

In the sequel, sufficient design conditions based on LMIs to determine the control law (4.4) which locally stabilizes the nonlinear system (4.1) in the ℓ_2-ISS$_{\mathcal{D}}$ sense are presented.

Theorem 4.4 *Suppose there exist symmetric positive definite matrices $Q_i \in \Re^{n_x \times n_x}$, $i = 1, \ldots, n_r$; a diagonal positive definite matrix $\Delta \in \Re^{n_\varphi \times n_\varphi}$; matrices $Y_{1i} \in \Re^{n_u \times n_x}$, $Y_{2i} \in \Re^{n_u \times n_\varphi}$, $i = 1, \ldots, n_r$, and $U \in \Re^{n_x \times n_x}$; and positive scalars δ and γ satisfying the following LMIs:*

$$\begin{bmatrix} -Q_q & \Pi_{ij}^1 & \Pi_{ij}^3 & \dfrac{B_{wi} + B_{wj}}{2} & 0 \\ \star & \Pi_{ij}^2 & U' L' \Omega & 0 & \Pi_{ij}^4 \\ \star & \star & -2\Delta & 0 & \Pi_{ij}^5 \\ \star & \star & \star & -\gamma^2 I & \dfrac{B_{zwi}' + B_{zwj}'}{2} \\ \star & \star & \star & \star & -I \end{bmatrix} < 0 \tag{4.15}$$
$$\forall\ q, i = 1, \ldots, n_r \quad \textit{and} \quad j = i, \ldots, n_r$$

$$\begin{bmatrix} -Q_i & Q_i N_{\{\ell\}}' \\ \star & -\delta \phi_{\{\ell\}}^2 \end{bmatrix} \leq 0\ ,\ \forall\ i = 1, \ldots, n_r \quad \textit{and} \quad \ell = 1, \ldots, n_\phi\ , \tag{4.16}$$

where

$$\begin{aligned} \Pi_{ij}^1 &= 0.5\left(A_i U + B_i Y_{1j} + A_j U + B_j Y_{1i}\right), \\ \Pi_{ij}^2 &= 0.5\left(Q_i + Q_j\right) - U - U', \\ \Pi_{ij}^3 &= 0.5\left(G_i \Delta + B_i Y_{2j} + G_j \Delta + B_j Y_{2i}\right), \\ \Pi_{ij}^4 &= 0.5\left(U' C_{zi}' + Y_{1i}' B_{zj}' + U' C_{zj} + Y_{1j}' B_{zi}'\right), \\ \Pi_{ij}^5 &= 0.5\left(\Delta G_{zi}' + Y_{2i}' B_{zj}' + \Delta G_{zj}' + Y_{2j}' B_{zi}'\right). \end{aligned} \tag{4.17}$$

Let $K_i = Y_{1i} U^{-1}$ and $\Gamma_i = Y_{2i} \Delta^{-1}$, $i = 1, \ldots, n_r$. In addition, consider the nonlinear system (4.1), with (4.4), and its exact N-fuzzy representation in (4.5). Then, the following holds for zero initial conditions:

a) $x(k)$ remains bounded in $\mathcal{D}$ for any $w(k) \in \mathcal{W}$;

b) $\|z(k)\|_2 \leq \gamma \|w(k)\|_2$ for all $w(k) \in \mathcal{W}$;

c) $x(k) \to 0$ as $k \to \infty$ if there exists $\tilde{k} > 0$ such that $w(k) = 0$ for all $k \geq \tilde{k}$;

d) $\mathcal{D} \subseteq \mathcal{E}(Q_i^{-1}, \delta^{-1}) \subset \mathcal{X}$, *for* $i = 1, ..., n_r$.

Proof *Assume that (4.15) is verified for all* $q, i = 1, \ldots, n_r$ *and* $j = i, \ldots, n_r$. *Replace* Y_{1i} *and* Y_{2i} *respectively by* $K_i U$ *and* $\Gamma_i \Delta$. *Multiply the resulting inequalities successively by* $h_{(i)}(k)$, $h_{(j)}(k)$, $h_{(q)}(k+1)$, *and sum up on* $i, q = 1, \ldots, n_r$ *and* $j = i, \ldots, n_r$. *Thus, the inequality* $\mathcal{M}(h(k)) < 0$ *holds if* $h(k) \in \Xi$ *with*

$$\mathcal{M}(h) = \begin{bmatrix} -Q(h^+) & \mathcal{A}(h)U & \mathcal{G}(h)\Delta & B_w(h) & 0 \\ \star & U'Q^{-1}(h)U & U'L'\Omega & 0 & U'\mathcal{C}(h) \\ \star & \star & -2\Delta & 0 & \Delta\mathcal{F}(h) \\ \star & \star & \star & -\gamma^2 I & B_{zw}'(h) \\ \star & \star & \star & \star & -I \end{bmatrix}$$

and the shorthands $h = h(k)$ *and* $h^+ = h(k+1)$. *Note that the matrices* $Q(h)$, $B_w(h)$ *and* $B_{zw}(h)$ *can be written as* (SILVA et al., *2014*)

$$\begin{bmatrix} Q(h) \\ B_w(h) \\ B_{zw}(h) \end{bmatrix} = \sum_{i=1}^{n_r} \sum_{j=i}^{n_r} (1 + \varsigma_{ij}) h_{(i)}(k) h_{(j)}(k) \left(\frac{1}{2} \begin{bmatrix} Q_i + Q_j \\ B_{wi} + B_{wj} \\ B_{zwi} + B_{zwj} \end{bmatrix} \right),$$

and that $U'Q^{-1}(h)U \geq -Q(h) + U' + U$ *is verified since* U *is full rank from the* $(2,2)$ *block of the left-hand side of (4.15).*

Further, let the congruence transformation $\Pi\mathcal{M}(h)\Pi'$ *with*

$$\Pi = \begin{bmatrix} 0 & I & 0 & 0 & 0 \\ 0 & 0 & 0 & (U')^{-1} & 0 \\ 0 & 0 & \Delta^{-1} & 0 & 0 \\ I & 0 & 0 & 0 & 0 \\ 0 & 0 & 0 & 0 & I \end{bmatrix}.$$

Thus, applying the Schur's complement to $\Pi\mathcal{M}(h)\Pi' < 0$ *yields:*

$$\mathcal{M}_S(h) = \vartheta_1'(k) Q^{-1}(h^+) \vartheta_1(k) + \begin{bmatrix} \mathcal{C}'(h) \\ B_{zw}'(h) \\ \mathcal{F}'(h) \end{bmatrix} \begin{bmatrix} \mathcal{C}'(h) \\ B_{zw}'(h) \\ \mathcal{F}'(h) \end{bmatrix}'$$

$$- \begin{bmatrix} Q^{-1}(h) & 0 & -L'\Omega\Delta^{-1} \\ 0 & \gamma^2 I & 0 \\ -\Delta^{-1}\Omega L & 0 & 2\Delta^{-1} \end{bmatrix} < 0 \,. \quad (4.18)$$

with $\vartheta_1(k) = \begin{bmatrix} \mathcal{A}(h(k)) & B_w(h(k)) & \mathcal{G}(h(k)) \end{bmatrix}$.

Now, let $\vartheta_2(k) = \begin{bmatrix} x^{'}(k) & w^{'}(k) & \varphi^{'}(k) \end{bmatrix}^{'}$. *Then, in view of* (4.18), *one has that:*

$$\vartheta_2^{'}(k)\mathcal{M}_S(h(k))\vartheta_2(k) = \Delta V(k) - 2\varphi^{'}(k)\Delta^{-1}(\varphi(k) - \Omega L x(k)) < 0 \ , \tag{4.19}$$

if $h(k) \in \Xi$.

Hence, the condition (4.19) implies that $\Delta V(k) < 0$ *whenever* $h(k) \in \Xi$ *and the sector condition (2.3) is verified. Assuming that* $x(k)$ *does not leave* $\mathcal{X}$, *for all* $k \geq 0$, *it is inferred that condition (4.12) is also satisfied. In this way the properties a), b) and c) in Theorem 4.4 are guaranteed, and consequently i), ii) and iii) from Lemma 4.3.*

Now, it is required to show that $x(k) \in \mathcal{X}$, *for all* $k \geq 0$, *and consequently* $h(k) \in \Xi$. *To this end, assume that (4.16) is verified. Then, multiplying (4.16) by* $h_{(i)}(k)$ *and summing up on* $i = 1, \ldots, n_r$ *leads to:*

$$\Lambda = \begin{bmatrix} -Q(h(k)) & Q(h(k))N^{'}_{\{\ell\}} \\ \star & -\delta\phi^2_{\{\ell\}} \end{bmatrix} \leq 0.$$

Let $\mathcal{F} = \mathrm{diag}\{Q^{-1}(h(k)), 1\}$. *Hence, the congruence transformation* $\mathcal{F}^{'}\Lambda\mathcal{F} = \tilde{\Lambda}$ *yields*

$$\tilde{\Lambda} = \begin{bmatrix} -Q^{-1}(h(k)) & N^{'}_{\{\ell\}} \\ \star & -\delta\phi^2_{\{\ell\}} \end{bmatrix} \leq 0.$$

By applying the Schur's complement to $\tilde{\Lambda}$, *it is obtained:*

$$N^{'}_{\{\ell\}}(\delta\phi^2_{\{\ell\}})^{-1}N_{\{\ell\}} - Q^{-1}(h(k)) \leq 0.$$

Pre- and post-multiplying the above respectively by $x(k)^{'}$ *and* $x(k)$ *and considering the S-procedure leads to:*

$$x^{'}(k)N^{'}_{\{\ell\}}\phi^{-2}_{\{\ell\}}N_{\{\ell\}}x(k) \leq 1, \ \forall \ x(k) \in \mathcal{D} \ ,$$
$$\mathcal{D} = \{x : x^{'}(k)Q^{-1}(h(k))x(k) \leq \delta^{-1}\}$$

That is, $\mathcal{E}(Q_i^{-1}, \delta^{-1}) \subset \mathcal{X}$, $\forall i = 1, ..., n_r$. *Recalling from (4.14) that* $\mathcal{D} \subseteq \mathcal{E}(Q_i^{-1}, \delta^{-1})$, *it is possible to ensure the property d) and infer from Lemma 4.3 that* $x(k) \in \mathcal{D}$, *for all* $k \geq 0$, *which concludes the proof.*

Remark 4.5 *It is possible to apply Theorem 4.4 to systems represented by classical T-S fuzzy models (without the nonlinear term) by* *eliminating the third row and column block of the matrix on the left-hand side of (4.15).*

Remark 4.6 *It is interesting to note that the stabilization condition (4.15) has a reduced number of LMIs when compared to other techniques in literature. This is due to the use of the property (4.6) and the definition of the variable* ς_{ij} *in (4.7). See, for instance, Theorem* 6.6 *of (FENG, 2010), where the resulting LMIs are required to be verified* $\forall\ i, j, q = 1, ..., n_r$.

4.3 DESIGN ISSUES

Now, three extensions of Theorem 4.4 are proposed. The purpose is to demonstrate the potential of the described approach as a control design tool for nonlinear discrete-time systems subject to energy bounded disturbances.

4.3.1 Disturbance Tolerance

The disturbance tolerance criterion consists in maximizing a bound on the disturbance energy to which one can ensure that the system trajectories remain bounded (and inside the domain of validity). This can be accomplished by the following optimization problem.

$$\min_{Q_i, \Delta, Y_{1i}, Y_{2i}, U} \delta \quad \begin{cases} \text{subject to} \\ \text{LMIs (4.15) and (4.16).} \end{cases} \tag{4.20}$$

Notice that the minimization of δ implies in maximizing the set of admissible disturbances $\mathcal{W}$.

4.3.2 Disturbance Attenuation

For a given disturbance energy level δ^{-1}, the disturbance attenuation criterion consists in minimizing an upper bound on the ℓ_2-gain from $w(k)$ to $z(k)$ while guaranteeing that $x(k) \in \mathcal{X}$, which can be obtained from the solution of the following optimization problem:

$$\min_{Q_i, \Delta, Y_{1i}, Y_{2i}, U} \gamma \quad \begin{cases} \text{subject to} \\ \text{LMIs (4.15) and (4.16).} \end{cases} \tag{4.21}$$

4.3.3 Reachable Set Estimation

The reachable set estimation criterion consists in minimizing the set $\mathcal{D}$ (an estimate of the reachable set) for a specific disturbance energy level δ^{-1} and a guaranteed bound γ on the system ℓ_2-gain. This objective can be accomplished by considering the inclusion $\mathcal{E}(Q_i^{-1}, \delta^{-1}) \subset \beta\mathcal{X}$, $\forall i = 1, ..., n_r$, $\beta \in (0, 1]$, which is obtained by modifying the condition in (4.16) as follows:

$$\begin{bmatrix} -Q_i & Q_i N'_{\{\ell\}} \\ \star & -\beta^2 \delta \phi^2_{\{\ell\}} \end{bmatrix} \leq 0 \qquad (4.22)$$
$$\forall i = 1, ..., n_r \quad and \quad \ell = 1, ..., \eta$$

Then, the objective is to obtain the lowest value for β which will be useful in practice whenever the effects of the disturbances over the system trajectories are to be minimized. This criteria can be obtained by the following optimization problem:

$$\min_{Q_i, \Delta, Y_{1i}, Y_{2i}, U} \beta \quad \begin{cases} \text{subject to} \\ \text{LMIs (4.15), (4.22) and } 0 < \beta \leq 1 \ . \end{cases} \qquad (4.23)$$

4.4 EXPERIMENTS

Two numerical examples are presented in this section. The first one demonstrates some stability issues that can occur when the domain of validity is not considered. In this sense a nonlinear plant is modeled by the classical T-S form and the region $\mathcal{X}$, where the model convexity is guaranteed, is not taken into account in the design phase. In the second example, it is shown the effectiveness of the proposed technique considering the optimization problems described in the previous section.

4.4.1 Example 1

Consider the control problem of backing-up a truck-trailer as studied in Lo & Lin (2003). The state space representation of the system is described by (see Appendix B)

$$\begin{aligned}
x_{(1)}(k+1) &= x_{(1)}(k) - \frac{vT}{\mathcal{L}}\sin(x_{(1)}(k)) + \frac{vT}{l}u(k) \\
x_{(2)}(k+1) &= x_{(2)}(k) + \frac{vT}{\mathcal{L}}\sin(x_{(1)}(k)) + 0.2w(k) \\
x_{(3)}(k+1) &= x_{(3)}(k) + vT\cos(x_{(1)}(k))\sin(x_{(2)}(k) \\
&\quad + \frac{vT}{2\mathcal{L}}\sin(x_{(1)}(k))) + 0.1w(k) \\
z(k) &= 7x_{(1)}(k) - vTx_{(2)}(k) + 0.03x_{(3)}(k) - \frac{vT}{l}u(k)
\end{aligned}$$

where the variables definitions, constant values, and their equivalent fuzzy representation are presented in section B.3, equation (B.5), with $\mathcal{X} = \{x(k) \in \Re^2 : |x_{(1)}(k)| \leq \pi/3 \text{ and } |x_{(2)}(k)| \leq 170\pi/180\}$. In order to allow a comparison with other techniques was considered the classical modeling, resulting in eight linear local rules for the model. The objective is to demonstrate the problems that can occur in practice when the model validity domain is not considered (usually assumed in the literature).

In light of the above, and for comparison purposes, the following control approaches using classical T-S fuzzy models are taken into account:

- *case 1* - Theorem 6.6 of (FENG, 2010);
- *case 2* - Remark 4.5 without the inclusion constraint in (4.16).

By solving an optimization problem aiming the minimization of the upper bound on the ℓ_2-gain from $w(k)$ to $z(k)$, it is respectively obtained the upper-bounds $\gamma = 0.4171$ and $\gamma = 0.3430$ for the cases 1 and 2. Notice that the bound obtained in case 2 is less conservative than the one obtained in case 1.

Figure 19 shows the projections of the closed-loop system trajectories[1] on the plane $x_{(1)}, x_{(2)}$ and ℓ_2-gains using the results obtained in case 1, for the following three different disturbance signals with $\|w_1(k)\|_{\ell_2} = 7.8731$, $\|w_2(k)\|_{\ell_2} = 10.3923$ and $\|w_3(k)\|_{\ell_2} = 24$,

$$w_1(k) = \begin{cases} e^k, & 1 \leq k \leq 2 \\ 0, & k < 1, k > 2 \end{cases}, \quad w_2(k) = \begin{cases} -6, & 1 \leq k \leq 3 \\ 0, & k < 1, k > 3 \end{cases},$$

[1]The simulations were performed considering the closed-loop system composed of the designed fuzzy controller and the original nonlinear plant

$$w_3(k) = \begin{cases} 8, & 1 \leq k \leq 9 \\ 0, & k < 1, k > 9 \end{cases} .$$

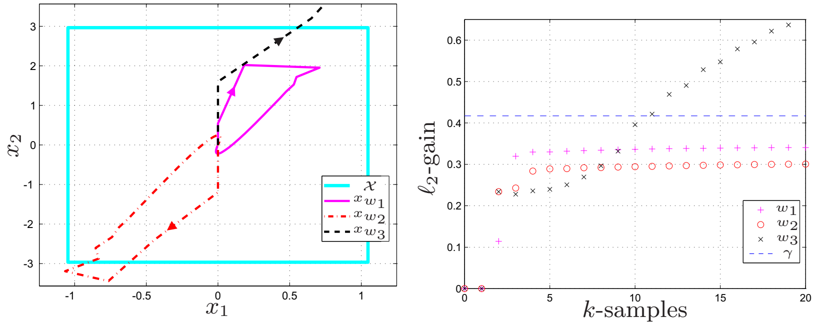

(a) Trajectories and $\mathcal{X}$ (b) ℓ_2-gain from $w(k)$ to $z(k)$

Figure 19 – Domain of validity, trajectories, and ℓ_2-gain

Figure 19(b) shows that the closed-loop state trajectory may either remain bounded or diverge to infinity. Precisely, the trajectories driven by $w_1(k)$ and $w_2(k)$ are bounded and by $w_3(k)$ goes to infinity. However, it is important to emphasize that although the trajectory imposed by $w_2(k)$ is bounded and verifies the required performance, it reaches an impracticable *jack-knife* condition for the system. The instability and *jack-knife* condition problems stem from the fact that the fuzzy model domain of validity $\mathcal{X}$ has not been considered in the design phase leading to undesirable system behaviors. Notice by applying optimization problem (4.21) that is possible to determine control laws which ensure that the state trajectory is confined to the domain of validity while guaranteeing upper-bounds on the ℓ_2-gain for the exogenous signals $w_1(k)$, $w_2(k)$ and $w_3(k)$.

4.4.2 Example 2

This experiment aims to demonstrate the potential of the described approach as a control design tool for nonlinear discrete-time systems subject to energy bounded disturbances. To this end, consider the two dimensional nonlinear system presented in Appendix B, section B.2. The state space representation of the system is given by:

$$
\begin{aligned}
x_{(1)}(k+1) = & -\frac{13}{20}x_{(1)}(k)+\frac{11}{20}x_{(2)}(k)+\frac{9}{40}x_{(1)}^2(k)+\frac{3}{40}x_{(1)}(k)x_{(2)}(k) \\
& +\frac{3}{10}x_{(2)}(k)(1+\sin(x_{(2)}(k))) \\
x_{(2)}(k+1) = & \ \frac{1}{5}x_{(1)}(k)+\frac{6}{5}x_{(2)}(k)+\frac{1}{5}x_{(1)}^2(k)+\frac{1}{20}x_{(1)}(k)x_{(2)}(k) \\
& +\frac{5}{4}u(k)+\frac{1}{40}x_{(1)}(k)u(k)+\frac{51}{100}w(k)+\frac{39}{400}x_{(1)}(k)w(k) \\
z(k) \quad = & \ x_{(1)}(k)+\frac{23}{20}u(k)+\frac{7}{40}x_{(1)}(k)u(k)
\end{aligned}
$$

The N-fuzzy model that represents the above system and the respective procedure for obtaining it are also presented in Appendix B, section B.2 (see (B.3) for the resulting equations of the model), with the domain of validity defined by $\mathcal{X} = \{x(k) \in \Re^2 : |x_{(1)}(k)| \leq 2 \text{ and } |x_{(2)}(k)| \leq 1.5\}$.

Firstly, applying the disturbance tolerance problem in (4.20) for a given set of ℓ_2-gain values, it is obtained the results shown in Table 1. Notice that smaller is the upper-bound γ on the system ℓ_2-gain, larger is the value of δ (i.e., the set of admissible disturbances is smaller).

Table 1 – Disturbance tolerance

γ	1.5	2	2.5	3
δ	0.4530	0.1860	0.1037	0.0671

On the other hand, considering that the bound on the admissible disturbances is known *a priori*, it is applied the disturbance attenuation optimization problem in (4.21). The results are described in Table 2 showing that larger values of δ will lead to smaller upper-bounds on the ℓ_2-gain.

Table 2 – Disturbance attenuation

δ	0.1	0.2	0.5	1
γ	2.5367	1.9487	1.4595	1.3273

These two experiments clearly illustrate that the disturbance attenuation properties of the original nonlinear system are state dependent contrasting with standard T-S fuzzy approaches which assume a constant ℓ_2-gain regardless the disturbance energy. To emphasize this point, Figures 20(a) and 20(b) show the estimates of the reachable set (given by $\mathcal{D}$) and the state trajectory evolution of the closed-loop system considering controllers derived from (4.20) and (4.21), respectively, for the pairs $\{\gamma\ ,\ \delta\} = \{2.5\ ,\ 0.1037\}$ and $\{\delta\ ,\ \gamma\} = \{0.1\ ,\ 2.5367\}$. The disturbance signals are respectively similar to the $w_2(k)$ and $w_1(k)$ signals considered in Example 1, but with a reduced amplitude to achieve the desired energy level, where x_{w_1} and x_{w_2} means state trajectories driven respectively by $w_1(k)$ and $w_2(k)$. Notice in both cases that: i) the state trajectories remains bounded in $\mathcal{X}$ for all samples; and ii) a certain duality between the optimization problems (4.20) and (4.21) since they led to similar estimates of the reachable set.

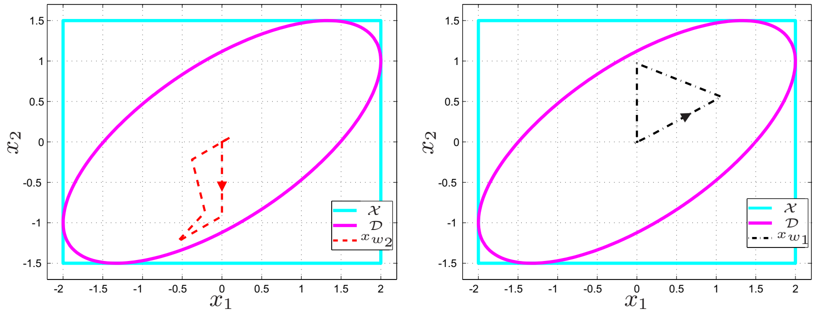

(a) Disturbance Tolerance (b) Disturbance Attenuation

Figure 20 – Regions and trajectories for the optimization algorithms

Finally, consider $\delta = 1$, $\gamma = 2$ and the reachable set estimation algorithm in (4.23). Thus, the following controller matrices are obtained:

$$K_1 = \begin{bmatrix} -0.4215 & -0.6371 \end{bmatrix},\ K_2 = \begin{bmatrix} -0.5453 & -0.7070 \end{bmatrix},$$

$$\Gamma_1 = 0.3949,\ \text{and}\ \Gamma_2 = 0.4186.$$

In Figure 21(a), it is observed the region estimated for this particular case with an optimal $\beta = 0.4313 \leq 1$. To evaluate the method conservativeness, the state trajectory driven by the following signal (which respects the energy bound)

$$w(k) = \begin{cases} 0.7, & 1 \leq k \leq 2 \\ 0, & \text{elsewhere} \end{cases}$$

is also plotted in Figure 21(a), demonstrating that the reachable set estimate is tight. For illustrative purposes, the time response of the state trajectories and the control effort are shown in Figures 21(b) and 22, respectively.

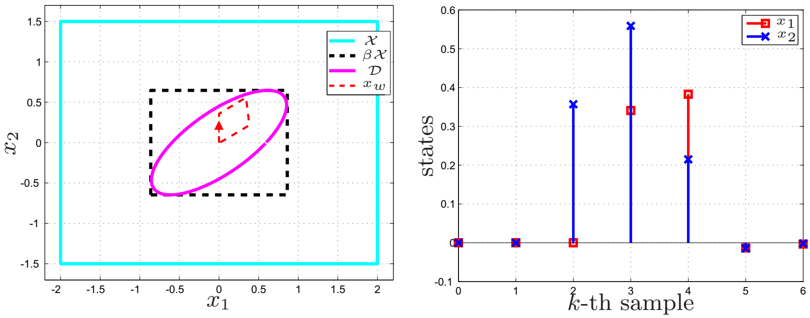

(a) Reachable Set Estimation (b) State trajectories

Figure 21 – Regions and trajectories

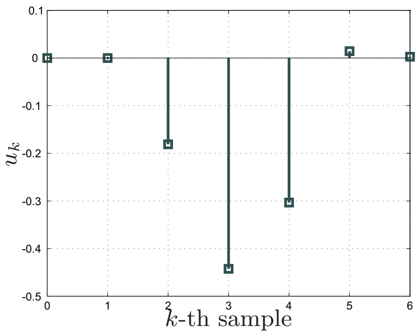

Figure 22 – Control effort

4.5 CONCLUDING REMARKS

A convex approach for the design of fuzzy controllers that locally stabilizes nonlinear discrete-time systems subject to energy bounded disturbances was addressed in this chapter. Considering fuzzy Lyapunov functions, three optimization problems in terms of LMI constraints were proposed to design a nonlinear state-feedback control law, which is a function of the membership fuzzy functions and cone sector nonlinearities. It turns out that the provided approach locally ensures the ℓ_2-ISS of the original nonlinear system while guaranteeing a certain input-to-output performance for a given class of disturbance signals. Also, the numerical examples stressed this ability of the proposed methodology to deal with the ℓ_2-control problems in a more realistic basis than other existing fuzzy techniques that do not consider the regional validity problematic. Additionally, it is worth mentioning that the considered problem can be extended to deal with the local ℓ_2-ISS stabilization problem in the presence of control saturation (TARBOURIECH et al., 2011a), using the framework described in the previous chapter.

5 CONTROL SYNTHESIS FOR NONLINEAR SYSTEMS SUBJECT TO AMPLITUDE BOUNDED DISTURBANCES

In this chapter the local stabilization problem of nonlinear discrete-time systems subject to amplitude bounded disturbances is addressed by means of T-S fuzzy models. Note that even though the dynamics of exogenous persistent signals are generally unknown, it is common to obtain an upper and a lower bound of the values that the signal can assume over time. It is also worth noting that in the presence of amplitude bounded disturbances, the asymptotic stability of the origin can not be guaranteed and in this case the concept of ultimate bounded (UB) stability is considered (i.e., the state trajectory is guaranteed to converge to a region in the vicinity of the system origin).

The proposed controllers are based on the state and dynamic output feedback, and the main contribution is related to the use of two ellipsoidal sets, $\mathcal{E}_E$ and $\mathcal{E}_I$, both contained in the region of validity of the fuzzy model, which have different shapes and are respectively associated with the set of admissible initial conditions and the concept of UB stability. In other words, the state trajectories starting in the set $\mathcal{E}_E$ will converge in finite-time to the internal set $\mathcal{E}_I$ and never leave it. In addition, the design conditions ensure that the state trajectory driven by admissible (amplitude bounded) disturbances remains inside the T-S domain of validity guaranteeing the closed-loop UB stability of the original nonlinear system. An optimization problem is proposed to maximize $\mathcal{E}_E$ and to minimize $\mathcal{E}_I$. The results presented here are based on the work Klug, Castelan & Coutinho (2015).

5.1 PROBLEM FORMULATION

Consider the class of nonlinear systems with state space representation affine in the input and disturbance signals defined in Chapter 2, which equation (2.1) is repeated here for sake of completeness:

$$\begin{aligned} x(k+1) &= f(x(k)) + \mathscr{V}(x(k))u(k) + \mathcal{T}(x(k))w(k) \\ y(k) &= Cx(k) \end{aligned}$$

where $x(k) \in \mathcal{X} \subset \Re^{n_x}$, $u(k) \in \mathcal{U} \subset \Re^{n_u}$, $y(k) \in \mathcal{Y} \subset \Re^{n_y}$ are respectively the state, the control input and the system output vectors. The functions $f(\cdot) : \Re^{n_x} \longrightarrow \Re^{n_x}$, with $f(0) = 0$, $\mathscr{V}(\cdot) : \Re^{n_x} \longrightarrow \Re^{n_x \times n_u}$

and $\mathcal{T}(\cdot):\Re^{n_x}\longrightarrow\Re^{n_x\times n_w}$ are continuous and bounded for all $x(k)\in\mathcal{X}$, and $C\in\Re^{n_y\times n_x}$ is a constant matrix. In this chapter, it is assumed with respect to (w.r.t.) system (2.1) that the disturbance input vector $w(k)$ lies inside the following set:

$$\mathcal{W}:=\{w(k)\in\Re^{n_w}:w^{'}(k)Rw(k)\leq\delta^{-1}\} \tag{5.1}$$

with $R=R^{'}>0$ and $\delta>0$. That is, the class of admissible disturbances consist on amplitude bounded signals (or any persistent signal, deterministic or stochastic, limited over time). For instance, if $R=\text{diag}\{r_1,r_2,...,r_{n_w}\}$, $r_i\in\Re$, then $\left|w_{(i)}(k)\right|\leq\sqrt{1/(\delta r_i)}$.

The objective is to design a control law $u(k)$ such that the closed-loop system is locally stable. To this end, the following definition of stability will be considered to deal with persistent disturbances (KHALIL, 2003).

Definition 5.1 (UB stability) *Consider system* (2.1) *with* $u(k)=0$. *The state trajectories* $x(k)$ *starting from a domain* $\mathcal{D}\subseteq\Re^{n_x}$ *are locally ultimately bounded, if there exist a compact convex set* $\mathcal{B}\subseteq\mathcal{D}$ *and a non-negative scalar* $\bar{k}=\bar{k}(x(0))$ *such that* $x(k)\in\mathcal{B}$ *for all* $k\geq\bar{k}$. *Moreover, if* $\mathcal{D}\equiv\Re^{n_x}$ *then the system is globally ultimately bounded.*

In view of the above definition, the set $\mathcal{B}$ will be referred as the ultimate bounded set (or simply UB set, which by definition is a positively invariant set). Similarly, the system whose state trajectories satisfy Definition 5.1 will be referred as locally (or globally) ultimate bounded stable (or simply UB stable).

The control design to be proposed is based on a FMB approach. Thus, the nonlinear system (2.1) is represented by means of a N-fuzzy model using the modeling procedure described in section 2.2. The resulting fuzzy model is given by the state space equation (2.5), also reproduced here as

$$\begin{array}{rcl} x(k+1) & = & A(h(k))x(k)+B(h(k))u(k)+B_w(h(k))w(k)+G(h(k))\varphi(k) \\ y(k) & = & Cx(k) \end{array} \tag{5.2}$$

Complementing the fuzzy model description (5.2), the vector of nonlinearities $\varphi(k)=\varphi(\pi(k))\in\Re^{n_\varphi}$, with $\pi(k)=Lx(k)$, verifies (at least locally) the sector condition (2.3), the T-S domain of validity $\mathcal{X}$ is conveniently defined by the polyhedral set (2.17), and the matrix structure is given by:

$$\left[\,A(h(k))\ B(h(k))\ B_w(h(k))\ G(h(k))\,\right]=\sum_{i=1}^{n_r}h_{(i)}(k)\left[\,A_i\ B_i\ B_{wi}\ G_i\,\right]$$

with $h_{(i)}(k)$ representing the membership function of the i^{th} local sub-model. Notice when assuming $h(k) \in \Xi$ that there exists a related region $\mathcal{X}$ of state space containing the origin such that $x(k) \in \mathcal{X} \Rightarrow h(k) \in \Xi$.

Now, to properly characterize the closed-loop stability in the presence of persistent disturbances, let $\mathcal{E}_E$ (external set) and $\mathcal{E}_I$ (internal set) be two distinct sets such that $0 \subset \mathcal{E}_I \subseteq \mathcal{E}_E \subset \mathcal{X}$. In particular, the sets $\mathcal{E}_E$ and $\mathcal{E}_I$ will be respectively associated to the region of admissible initial conditions and to the UB set (as explained in Definition 5.1). In other words, any initial condition starting in the external set $\mathcal{E}_E$ will converge to the internal set $\mathcal{E}_I$ in finite time. Moreover, the set $\mathcal{E}_I$ is positively invariant, that is, if a trajectory $x(k) \in \mathcal{E}_I$, for some $k \geq \bar{k}$ with $\bar{k}$ being a positive integer, then $x(k) \in \mathcal{E}_I$ for all $k \geq \bar{k}$ (TARBOURIECH et al., 2011b).

For illustrative purposes, Figure 23 shows a state trajectory (black solid line) starting in the external set $\mathcal{E}_E$ (magenta dashed line) and converging to the internal set $\mathcal{E}_I$ (green dot dashed line) which is positively invariant. Notice that the system trajectory evolves within the T-S domain of validity $\mathcal{X}$ (cyan solid line).

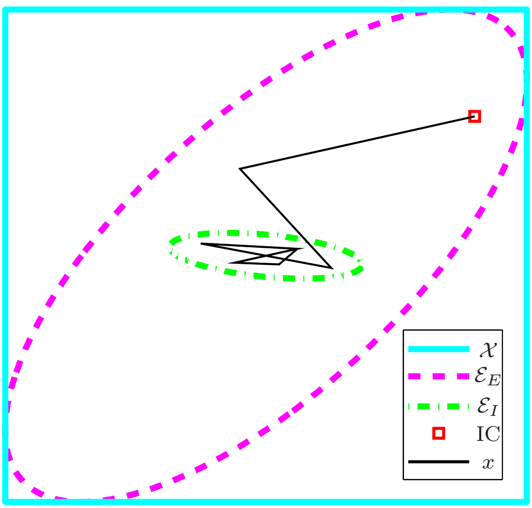

Figure 23 – Stability characterization for a persistent disturbance and a nonzero initial condition (IC).

In the sequel, two different problems of interest will be established. The first problem assumes that the normalized membership functions vector $h(k)$ is available online to implement a state feedback controller. The second one considers that only a part $\tilde{h}(k)$ of the membership functions vector $h(k)$ is available online to the controller which is employed for scheduling a dynamic output feedback controller.

5.1.1 Nonlinear State Feedback Design

Assume that the output matrix C is column full-rank[1]. Thus, $h(k)$ and $\varphi(k)$ can be made available online to the controller, see Klug et al. (2014), Klug, Castelan & Coutinho (2015a). In this case, the following control law will be considered:

$$u(k) = K(h(k))x(k) + \Gamma(h(k))\varphi(k) \tag{5.3}$$

where

$$\big[K(h(k))\ \Gamma(h(k))\big] = \sum_{i=1}^{n_r} h_{(i)}(k)\big[K_i\ \Gamma_i\big],\ \text{with } K_i \in \Re^{n_u \times n_x}, \Gamma_i \in \Re^{n_u \times n_\varphi}.$$

Then, similarly to the previous chapter, the closed-loop T-S fuzzy model can be described as follows:

$$x(k+1) = \mathcal{A}(h(k))x(k) + B_w(h(k))w(k) + \mathcal{G}(h(k))\varphi(k) \tag{5.4}$$

with

$$\begin{aligned}\mathcal{A}(h(k)) &= A(h(k)) + B(h(k))K(h(k)) \text{ and}\\ \mathcal{G}(h(k)) &= G(h(k)) + B(h(k))\Gamma(h(k))\end{aligned}$$

Note that $\mathcal{A}(h(k))$ and $\mathcal{G}(h(k))$ can be generically written in the following form through summation properties:

$$\mathscr{T}(h(k)) = \sum_{i=1}^{n_r}\sum_{j=i}^{n_r}(1+\varsigma_{ij})h_{(i)}(k)h_{(j)}(k)\frac{T_i + X_iY_j + T_j + X_jY_i}{2}$$

where the tuple $(\mathscr{T},T,X,Y)$ represents either $(\mathcal{A},A,B,K)$ or $(\mathcal{G},G,B,\Gamma)$, and ς_{ij} is binary a variable such that (as defined in (4.6) and (4.7))

[1] Hence, the state vector can be reconstructed from the measurements by means of $x(k) = (C'C)^{-1}C'y(k)$.

$$\varsigma_{ij} = \begin{cases} 1 & \text{if} \quad i \neq j, \\ 0 & \quad \text{otherwise.} \end{cases}$$

Hence, the state feedback design problem can be established as follows:

Problem 5.2 *Determine K_i and Γ_i, for $i = 1, ..., n_r$, and associated sets $\mathcal{E}_I$ and $\mathcal{E}_E$ such that for any initial condition $x(0) \in \mathcal{E}_E \subseteq \mathcal{X}$ and any disturbance $w(k) \in \mathcal{W}$ the state trajectory $x(k)$ of system (5.4) remains inside $\mathcal{E}_E$, converges to $\mathcal{E}_I$ in some finite time $\bar{k}$ and $x(k) \in \mathcal{E}_I$, $\forall\, k \geq \bar{k}$.*

5.1.2 Dynamic Output Feedback

Assume that the membership functions vector $h(k)$ are dependent on the measurable states, i.e., $h(k) = h(y(k))$. In this setup, consider the following nonlinear dynamic output feedback controller:

$$\begin{array}{rcl} x_c(k+1) & = & A_c(h(k))x_c(k) + B_c(h(k))u_c(k) \\ y_c(k) & = & C_c(h(k))x_c(k) + D_c(h(k))u_c(k) \end{array} \tag{5.5}$$

where $x_c(k) \in \Re^{n_x}$ is the controller state and the controller matrices are as follows

$$\begin{gathered} \left[\, A_c(h(k)) \;\; B_c(h(k)) \,\right] = \sum_{i=1}^{r} \sum_{j=i}^{r} (1+\varsigma_{ij}) h_{(i)}(k) h_{(j)}(k) \left[\frac{A_{cij}}{2} \;\; \frac{B_{cij}}{2} \right] \\ \left[\; C_c(h(k)) \quad D_c(h(k)) \;\right] = \sum_{i=1}^{r} h_{(i)}(k) \left[\; C_{ci} \quad D_{ci} \;\right]. \end{gathered} \tag{5.6}$$

Notice that the assumption $h(k) = h(y(k))$ is necessary to implement any output feedback controller based on the PDC strategy, in which the membership functions are shared between the fuzzy model and controller. Nevertheless, the N-fuzzy approach can be exploited to deal with unmeasurable nonlinearities (contrasting with the classical fuzzy modeling). More specifically, the vector $\varphi(k) = \varphi(\pi(k)) \in \Re^{n_\varphi}$, with $\pi(k) = Lx(k)$, can embed all nonlinearities which are functions of unmeasurable states (further details will be given in the section of experiments).

Thus, defining the augmented state vector $\xi(k) = \left[\, x^{'}(k) \; x_c^{'}(k) \,\right]^{'}$, the following closed-loop system is obtained:

$$\begin{aligned} \xi(k+1) = {} & [\mathbb{A}(h(k)) + \mathbb{B}(h(k))\mathbb{K}(h(k))]\, \xi(k) \\ & + \mathbb{G}(h(k))\varphi(\mathbb{L}\xi(k)) + \mathbb{B}_w(h(k))w(k) \end{aligned} \tag{5.7}$$

with $\mathbb{A}(\cdot), \mathbb{B}(\cdot), \mathbb{B}_w(\cdot), \mathbb{G}(\cdot), \mathbb{K}(\cdot)$ and $\mathbb{L}(\cdot)$ given by:

$$\mathbb{A}(h(k)) = \begin{bmatrix} A(h(k)) & 0 \\ B_c(h(k))C & A_c(h(k)) \end{bmatrix}, \ \mathbb{B}(h(k)) = \begin{bmatrix} B(h(k)) \\ 0 \end{bmatrix},$$

$$\mathbb{B}_w(h(k)) = \begin{bmatrix} B_w(h(k)) \\ 0 \end{bmatrix}, \ \mathbb{G}(h(k)) = \begin{bmatrix} G(h(k)) \\ 0 \end{bmatrix},$$

$$\mathbb{K}(h(k)) = \begin{bmatrix} D_c(h(k))C & C_c(h(k)) \end{bmatrix} \text{ and } \mathbb{L} = \begin{bmatrix} L & 0 \end{bmatrix}.$$

In light of the above, the problem of output feedback design can be formulated as follows:

Problem 5.3 *Determine the controller matrices A_{cij}, B_{cij}, C_{ci} and D_{ci}, for $i = 1, ..., n_r$, and associated sets $\mathcal{E}_I^{\{a\}}$ and $\mathcal{E}_E^{\{a\}}$ such that for any initial condition $\xi(0) \in \mathcal{E}_E^{\{a\}} \subseteq \mathcal{X}^{\{a\}}$ and any disturbance $w(k) \in \mathcal{W}$ the state trajectory $\xi(k)$ of system (5.7) remains inside $\mathcal{E}_E^{\{a\}}$, converges to the set $\mathcal{E}_I^{\{a\}}$ in some finite time $\bar{k}$ and $\xi(k) \in \mathcal{E}_I^{\{a\}}$, $\forall k \geq \bar{k}$.*

Remark 5.4 *It is often of interest when solving Problems 5.2 and 5.3 that the controller matrices are designed in order to maximize the external ellipsoidal set and to minimize the internal ellipsoidal set. Notice in the case of dynamic output feedback that it might be of interest to respectively minimize and maximize the orthogonal projections of $\mathcal{E}_I^{\{a\}}$ and $\mathcal{E}_E^{\{a\}}$ over the $x(k)$-plane.*

Remark 5.5 *The approach to be proposed can be applied to deal with some non-smooth nonlinearities such as dead zone, backlash and hysteresis, since they can be modeled by means of sector nonlinearities and amplitude bounded disturbances (DILDA; JUNGERS; CASTELAN, 2014).*

Before ending this section, it is introduced in the following a key result which will be instrumental to derive solutions to Problems 5.2 and 5.3. To this end, consider the following fuzzy Lyapunov-like functions (FLFs):

$$V_E(x(k), h(k)) : \mathcal{X} \times \Xi \to \Re^+, \ V_I(x(k), h(k)) : \mathcal{X} \times \Xi \to \Re^+, \\ V_{E,I}(0, h(k)) = 0, \forall \ h(k) \in \Xi, \quad (5.8)$$

and the following associated sets

$$\begin{aligned} \mathcal{E}_E &= \{x(k) \in \mathcal{X} : V_E(x(k), h(k)) \leq 1, \ \forall \ h(k) \in \Xi\}, \\ \mathcal{E}_I &= \{x(k) \in \mathcal{X} : V_I(x(k), h(k)) \leq 1, \ \forall \ h(k) \in \Xi\}. \end{aligned} \quad (5.9)$$

Then, the following lemma characterizes the stability conditions to ensure the UB stability of system (2.1).

Lemma 5.6 *Consider the system defined in (2.1), the sets defined in (5.9) such that $\mathcal{E}_I \subseteq \mathcal{E}_E \subseteq \mathcal{X}$, and the FLFs defined in* (5.8). *Suppose the following conditions are satisfied for all $w(k) \in \mathcal{W}$ and $h(k) \in \Xi$:*

$$\Delta V_E(x(k), h(k)) < 0, \ \forall\ x(k) \in \mathcal{E}_E \backslash \mathcal{E}_I \tag{5.10}$$

$$\Delta V_I(x(k), h(k)) + V_I(x(k), h(k)) \leq 1, \ \forall\ x(k) \in \mathcal{E}_I \tag{5.11}$$

with $\Delta V_{E,I}(x(k), h(k)) \triangleq V_{E,I}(x(k+1), h(k+1)) - V_{E,I}(x(k), h(k)) < 0.$

Then, the following holds:

i) *The system* (2.1) *is locally UB stable;*

ii) $\mathcal{E}_I$ *is an UB set;*

iii) *For any $x(0) \in \mathcal{E}_E$ and $w(k) \in \mathcal{W}$, there exists a $\bar{k} \in \mathbb{Z}^+$ such that the state trajectory $x(k) \in \mathcal{E}_I$, $\forall\ k \geq \bar{k}$.*

Proof *The condition (5.10) ensures that any state trajectory starting in $\mathcal{E}_E \backslash \mathcal{E}_I$ converges towards $\mathcal{E}_I$ in finite time (VIDYASAGAR, 2002). Furthermore, the condition (5.11) implies that if $x(k) \in \mathcal{E}_I$ then $x(k+1) \in \mathcal{E}_I$, that is, the set $\mathcal{E}_I$ is positive invariant. The rest of this proof follows straightforwardly from Definition 5.1.*

5.2 CONTROL DESIGN

In this section, LMI-based solutions are proposed for designing the control laws in (5.3) and (5.5) which locally ensures the UB stability of the nonlinear closed-loop system described by means of N-fuzzy models (5.4) and (5.7).

5.2.1 State Feedback Design

Consider that the FLFs in (5.8) are defined as follows:

$$V_E(x(k), h(k)) = x^{'}(k) Q^{-1}(h(k)) x(k),$$
$$V_I(x(k), h(k)) = x^{'}(k) W^{-1}(h(k)) x(k), \tag{5.12}$$

with the matrices $Q(\cdot)$ and $W(\cdot)$ being as follows:

$$Q(h(k)) = \sum_{i=1}^{n_r} h_{(i)}(k) Q_i \ , \ W(h(k)) = \sum_{i=1}^{n_r} h_{(i)}(k) W_i \ , \qquad (5.13)$$

where $Q_i, W_i \in \Re^{n_x \times n_x}$ are symmetric positive defined matrices to be determined for all $i = 1, \ldots, n_r$.

In light of the above, the sets $\mathcal{E}_E$ and $\mathcal{E}_I$ are defined as the intersection of n_r ellipsoidal sets (HU; Z.; M., 2002; JUNGERS; CASTELAN, 2011) formed by the matrices W_i^{-1} and Q_i^{-1} as detailed below

$$\mathcal{E}_E \triangleq \bigcap_{i \in \{1, \ldots n_r\}} \mathcal{E}(Q_i^{-1}) \ , \ \mathcal{E}_I \triangleq \bigcap_{i \in \{1, \ldots n_r\}} \mathcal{E}(W_i^{-1}) \ , \qquad (5.14)$$

where the $2n_r$ ellipsoidal sets $\mathcal{E}(Q_i^{-1})$ and $\mathcal{E}(W_i^{-1})$ are as follows

$$\mathcal{E}(Q_i^{-1}) = \left\{ x(k) \in \Re^{n_x} : x^{'}(k) Q_i^{-1} x(k) \leq 1 \right\} ,$$
$$\mathcal{E}(W_i^{-1}) = \left\{ x(k) \in \Re^{n_x} : x^{'}(k) W_i^{-1} x(k) \leq 1 \right\} .$$

Notice that additionally to the conditions of Lemma 5.6, the constraint $\mathcal{E}_E \subset \mathcal{X}$ has also to be considered to guarantee the convexity of the N-fuzzy model in (5.4).

In the sequel, sufficient design conditions based on LMI constraints are proposed to determine the control law in (5.3) which locally stabilizes the nonlinear system (2.1) subject to amplitude bounded disturbances.

Theorem 5.7 *Consider the system in* (2.1) *with* (5.1), *its fuzzy model in* (5.2), *and the control law in* (5.3). *Let* τ_1 *and* τ_3 *be two given positive scalars with* $\tau_3 \in (0, 1)$. *Suppose there exist symmetric positive definite matrices* $(Q_i, W_i) \in \Re^{n_x \times n_x}$, $i = 1, \ldots, n_r$; *a diagonal positive definite matrix* $\Delta \in \Re^{n_\varphi \times n_\varphi}$; *matrices* $Y_{1i} \in \Re^{n_u \times n_x}$, $Y_{2i} \in \Re^{n_u \times n_\varphi}$, $i = 1, \ldots, n_r$ *and* $U \in \Re^{n_x \times n_x}$; *and positive scalars* τ_2 *and* τ_4; *that satisfy* $Q_i \geq W_i$, $i = 1, \ldots, n_r$, *and the following LMIs:*

$$\begin{bmatrix} -Q_q & \Pi_{ij}^1 & \Pi_{ij}^3 & \dfrac{B_{wi} + B_{wj}}{2} & 0 \\ \star & \Pi_{ij}^2 & U^{'} L^{'} \Omega & 0 & U^{'} \tau_1 \\ \star & \star & -2\Delta & 0 & 0 \\ \star & \star & \star & -\tau_2 R & 0 \\ \star & \star & \star & \star & -\tau_1 \left(\dfrac{W_i + W_j}{2} \right) \end{bmatrix} < 0$$
$$\forall \ q, i = 1, \ldots, n_r \ \textit{and} \ j = i, \ldots, n_r \qquad (5.15)$$

$$\begin{bmatrix} -W_q & \Pi^1_{ij} & \Pi^3_{ij} & \dfrac{B_{wi}+B_{wj}}{2} \\ \star & \tau_3\left(\dfrac{W_i+W_j}{2} - U - U^{'}\right) & U^{'}L^{'}\Omega & 0 \\ \star & \star & -2\Delta & 0 \\ \star & \star & \star & -\tau_4 R \end{bmatrix} \leq 0$$

$$\forall\ q, i = 1, \ldots, n_r \ \ and\ j = i, \ldots, n_r \tag{5.16}$$

$$\delta^{-1}\tau_2 - \tau_1 < 0 \tag{5.17}$$

$$\tau_3 + \tau_4\delta^{-1} - 1 \leq 0 \tag{5.18}$$

$$-\phi^2_{\{\ell\}} + N_{\{\ell\}}Q_i N^{'}_{\{\ell\}} \leq 0, \quad \forall\ i = 1, \ldots, n_r \ \ and\ \ell = 1, \ldots, n_\phi \tag{5.19}$$

where

$$\begin{aligned} \Pi^1_{ij} &= 0.5\left(A_i U + B_i Y_{1j} + A_j U + B_j Y_{1i}\right), \\ \Pi^2_{ij} &= 0.5\left(Q_i + Q_j\right) - U - U^{'}, \\ \Pi^3_{ij} &= 0.5\left(G_i\Delta + B_i Y_{2j} + G_j\Delta + B_j Y_{2i}\right). \end{aligned}$$

Let $K_i = Y_{1i}U^{-1}$ *and* $\Gamma_i = Y_{2i}\Delta^{-1}$ *for* $i = 1, \ldots, n_r$. *Then, the following holds:*

i) The closed-loop system consisting of (2.1) *and* (5.3) *is locally UB stable;*

ii) $\mathcal{E}_I$ *as defined in* (5.14) *is an UB set;*

iii) For any $w(k) \in \mathcal{W}$ *and* $x(0) \in \mathcal{E}_E$*, with* $\mathcal{E}_E$ *as defined in* (5.14)*, there exists a* $\bar{k} \in \mathbb{Z}^+$ *such that* $x(k) \in \mathcal{E}_I$, $\forall\ k \geq \bar{k}$.

Proof *The condition* $Q_i \geq W_i$ *implies that* $\mathcal{E}_I \subseteq \mathcal{E}_E$. *Now, assume that (5.15) and (5.16) are verified for all* $q, i = 1, \ldots, n_r$ *and* $j = i, \ldots, n_r$. *Replace* Y_{1i} *and* Y_{2i} *respectively by* $K_i U$ *and* $\Gamma_i\Delta$. *Multiply the resulting inequalities successively by* $h_{(i)}(k)$, $h_{(j)}(k)$, $h_{(q)}(k+1)$, *and sum up on* $i, q = 1, \ldots, n_r$ *and* $j = i, \ldots, n_r$. *Thus, the inequalities* $\mathcal{M}_1(h(k)) < 0$ *and* $\mathcal{M}_2(h(k)) < 0$ *holds if* $h(k) \in \Xi$ *with*

$$\mathcal{M}_1(h) = \begin{bmatrix} -Q(h^+) & \mathcal{A}(h)U & \mathcal{G}(h)\Delta & B_w(h) & 0 \\ \star & -U^{'}Q^{-1}(h)U & U^{'}L^{'}\Omega & 0 & U^{'}\tau_1 \\ \star & \star & -2\Delta & 0 & 0 \\ \star & \star & \star & -\tau_2 R & 0 \\ \star & \star & \star & \star & -\tau_1 W(h) \end{bmatrix},$$

$$\mathcal{M}_2(h) = \begin{bmatrix} -W(h^+) & \mathcal{A}(h)U & \mathcal{G}(h)\Delta & B_w(h) \\ \star & -\tau 3U^{'}W(h)U & U^{'}L^{'}\Omega & 0 \\ \star & \star & -2\Delta & 0 \\ \star & \star & \star & -\tau_4 R \end{bmatrix},$$

and the shorthands $h = h(k)$ *and* $h^+ = h(k+1)$. *Note that the matrices* $Q(h)$, $W(h)$ *and* $B_w(h)$ *can be written as* (SILVA et al., 2014)

$$\begin{bmatrix} Q(h) \\ W(h) \\ B_w(h) \end{bmatrix} = \sum_{i=1}^{n_r}\sum_{j=i}^{n_r}(1+\varsigma_{ij})h_{(i)}(k)h_{(j)}(k)\left(\frac{1}{2}\begin{bmatrix} Q_i + Q_j \\ W_i + W_j \\ B_{wi} + B_{wj} \end{bmatrix}\right),$$

and that $-U'Q^{-1}(h)U \leq Q(h) - U' - U$ *is verified since* U *is full rank from the* $(2,2)$ *block of the left-hand side of (5.15) and (5.16).*

Further, consider the congruence transformations $\Pi\mathcal{M}_1(h)\Pi^{'}$ *and* $\Pi\mathcal{M}_2(h)\Pi^{'}$ *with* $\Pi = \text{diag}\{I, (U^{'})^{-1}, \Delta, I, I\}$. *In the sequel, applying the Schur's complement (twice for* $\Pi\mathcal{M}_1(h)\Pi^{'}$*) yields:*

$$\mathcal{M}_{S1}(h) = \vartheta_1^{'}(k)Q^{-1}(h^+)\vartheta_1(k) + \begin{bmatrix} -Q^{-1}(h) + \tau_1 W^{-1}(h) & L^{'}\Omega\Delta^{-1} & 0 \\ \star & -2\Delta^{-1} & 0 \\ \star & \star & -\tau_2 R \end{bmatrix} < 0 \quad (5.20)$$

$$\mathcal{M}_{S2}(h) = \vartheta_1^{'}(k)W^{-1}(h^+)\vartheta_1(k) + \begin{bmatrix} -\tau_3 W^{-1}(h) & L^{'}\Omega\Delta^{-1} & 0 \\ \star & -2\Delta^{-1} & 0 \\ \star & \star & -\tau_4 R \end{bmatrix} < 0 \quad (5.21)$$

with $\vartheta_1(k) = \begin{bmatrix} \mathcal{A}(h(k)) & \mathcal{G}(h(k)) & B_w(h(k)) \end{bmatrix}$. *Now, let* $\vartheta_2(k) = \begin{bmatrix} x^{'}(k) & w^{'}(k) & \varphi^{'}(k) \end{bmatrix}^{'}$. *Then, in view of (5.20) and (5.21), it is obtained the following:*

$$\vartheta_2^{'}(k)\mathcal{M}_{S1}(h(k))\vartheta_2(k) = \Delta V_{\mathcal{E}_E}(x(k), h(k)) - \tau_1(1 - x^{'}(k)W^{-1}(h(k))x(k)) - 2\varphi^{'}(k)\Delta^{-1}(\varphi(k) - \Omega L x(k)) < 0 \quad (5.22)$$

$$\vartheta_2^{'}(k)\mathcal{M}_{S1}(h(k))\vartheta_2(k) = \Delta V_{\mathcal{E}_I}(x(k), h(k)) + V_{\mathcal{E}_I}(x(k), h(k)) - \tau_3(x^{'}(k)W^{-1}(h(k))x(k) - 1) - 2\varphi^{'}(k)\Delta^{-1}(\varphi(k) - \Omega L x(k)) < 1 \ , \quad (5.23)$$

Hence, by considering the S*-procedure, the condition (5.22) with (5.17) implies that condition (5.10) from Lemma 5.6 is satisfied whenever: i)* $h(k) \in \Xi$*; ii) the sector condition (2.3) is verified; and iii)* *assuming that $x(k)$ does not leave $\mathcal{X}$, for all $k \geq 0$. The same procedure can be extended to (5.23) with (5.18) resulting in the verification of (5.11).*

Now, is required to show that $x(k) \in \mathcal{X}$, for all $k \geq 0$, and consequently $h(k) \in \Xi$. To this end, assume that (5.19) is verified. Then, multiplying (5.19) by $h_{(i)}(k)$ and summing up on $i = 1, \ldots, n_r$ leads to:

$$-\phi^2_{\{\ell\}} + N_{\{\ell\}} Q(h(k)) N^{'}_{\{\ell\}} \leq 0,$$

which is equivalent to (see Klug, Castelan & Coutinho (2015a))

$$N^{'}_{\{\ell\}} (\phi^2_{\{\ell\}})^{-1} N_{\{\ell\}} - Q^{-1}(h(k)) \leq 0.$$

Pre- and post-multiplying the above respectively by $x^{'}(k)$ and $x(k)$ and considering the S-procedure leads to:

$$x^{'}(k) N^{'}_{\{\ell\}} \phi^{-2}_{\{\ell\}} N_{\{\ell\}} x(k) \leq 1, \ \forall \ x(k) \in \mathcal{E}_E$$

That is, $\mathcal{E}(Q_i^{-1}) \subset \mathcal{X}$, $\forall i = 1, ..., n_r$. Therefore it is ensured that $x(k)$ does not leave $\mathcal{X}$, for all $k \geq 0$, which concludes the proof.

Notice that the conditions of Theorem 5.7 are LMI constraints if the positive scalars τ_1 and τ_3 are given *a priori*. To obtain a less conservative result, a griding technique can be applied to determine these parameters taking into account that $\tau_3 \in]0, 1[$ due to the scalar inequality in (5.18). To avoid a possible large computational effort, it is possible to constraint the sets $\mathcal{E}_E$ and $\mathcal{E}_I$ to have the same shape (i.e., the set $\mathcal{E}_E$ is a scaled version of $\mathcal{E}_I$). As a result, the only parameter to be searched is τ_1 in a bounded space. Thus, the sets $\mathcal{E}_E$ and $\mathcal{E}_I$ are redefined as follows:

$$\mathcal{E}_E \triangleq \bigcap_{i \in \{1, \ldots n_r\}} \mathcal{E}\left(Q_i^{-1}, c^{-1}\right) , \ \mathcal{E}_I \triangleq \bigcap_{i \in \{1, \ldots n_r\}} \mathcal{E}\left(Q_i^{-1}, 1\right) , \tag{5.24}$$

where the n_r ellipsoidal sets $\mathcal{E}\left(Q_i^{-1}, c^{-1}\right)$ are as follows:

$$\mathcal{E}\left(Q_i^{-1}, c^{-1}\right) = \left\{ x(k) \in \Re^n : x^{'}(k) Q_i^{-1} x(k) \leq c^{-1} \ , \ c^{-1} \geq 1 \right\} \tag{5.25}$$

for $i = 1, \ldots, n_r$ and with c being a parameter defining the size of $\mathcal{E}_E$.

Therefore, the stabilization conditions proposed in Theorem 5.7 are simplified to the following result.

Corollary 5.8 *Consider the system in* (2.1) *with* (5.1), *its fuzzy model in* (5.2), *and the control law in* (5.3). *Let* τ_1 *be a given positive scalar such that* $0 < \tau_1 < 1$. *Suppose there exist symmetric positive definite matrices* $Q_i \in \Re^{n_x \times n_x}$, $i = 1, \ldots, n_r$; *a diagonal positive definite matrix* $\Delta \in \Re^{n_\varphi \times n_\varphi}$; *matrices* $Y_{1i} \in \Re^{n_u \times n_x}$, $Y_{2i} \in \Re^{n_u \times n_\varphi}$, $i = 1, \ldots, n_r$, *and* $U \in \Re^{n_x \times n_x}$; *and positive scalars* τ_2 *and* c *with* $0 < c \leq 1$; *that satisfy the following LMIs:*

$$\begin{bmatrix} -Q_q & \dfrac{A_iU + B_iY_{1j} + A_jU + B_jY_{1i}}{2} & \Pi_{ij}^3 & \dfrac{B_{wi} + B_{wj}}{2} \\ \star & (1-\tau_1)\left(\dfrac{Q_i + Q_j}{2} - U - U'\right) & U'L'\Omega & 0 \\ \star & \star & -2\Delta & 0 \\ \star & \star & \star & -\tau_2 R \end{bmatrix} < 0$$

$$\forall\ q, i = 1, \ldots, n_r \text{ and } j = i, \ldots, n_r \tag{5.26}$$

$$\tau_2 - \delta\tau_1 < 0 \tag{5.27}$$

$$-c\phi_{\{\ell\}}^2 + N_{\{\ell\}} Q_i N_{\{\ell\}}^{'} \leq 0, \quad \forall\ i = 1, \ldots, n_r \text{ and } \ell = 1, \ldots, n_\phi \tag{5.28}$$

Let $K_i = Y_{1i}U^{-1}$ *and* $\Gamma_i = Y_{2i}\Delta^{-1}$ *for* $i = 1, \ldots, n_r$. *Then, the following holds:*

i) The closed-loop system consisting of (2.1) *and* (5.3) *is locally UB stable;*

ii) $\mathcal{E}_I$ *as defined in* (5.24) *with* (5.25) *is an UB set;*

iii) For any $w(k) \in \mathcal{W}$ *and* $x(0) \in \mathcal{E}_E$, *with* $\mathcal{E}_E$ *as defined in* (5.24) *with* (5.25), *there exists a* $\bar{k} \in \mathbb{Z}^+$ *such that* $x(k) \in \mathcal{E}_I$, $\forall\ k \geq \bar{k}$.

Proof *This proof follows similar steps to those employed in Theorem 5.7 and thus will be omitted.*

Observe that Corollary 5.8 assumes the same shape for the external and internal sets. Hence, a single LMI condition ensures that (5.10) and (5.11) from Lemma 5.6 are satisfied. Also, it should be noted that the (2, 2) block of (5.26) arises from the term $-(1-\tau_1)Q^{-1}(h(k))$ and thus $0 < \tau_1 < 1$. Moreover, Corollary 5.8 can be applied to obtain an estimate of τ_1 for the solution of Theorem 5.7 likely yielding a less conservative result.

Remark 5.9 *Either Theorem 5.7 or Corollary 5.8 can be applied to nonlinear systems represented by classical T-S fuzzy models (i.e., with* $\varphi(k) \equiv 0$*) by eliminating the third row and column blocks of the matrix on the left-hand side of (5.15) and (5.16), or (5.26), respectively.*

5.2.2 Dynamic Output Feedback

Let the following FLF's:

$$\mathbb{V}_I(\xi(k), h(k)) = \xi^{'}(k)\mathbb{W}^{-1}(h(k))\xi(k),$$
$$\mathbb{V}_E(\xi(k), h(k)) = \xi^{'}(k)\mathbb{Q}^{-1}(h(k))\xi(k), \quad (5.29)$$

with

$$\mathbb{W}(h(k)) = \sum_{i=1}^{n_r} h_{(i)}(k)\mathbb{W}_i \ , \ \mathbb{Q}(h(k)) = \sum_{i=1}^{n_r} h_{(i)}(k)\mathbb{Q}_i \ , \quad (5.30)$$

and $\mathbb{W}_i, \mathbb{Q}_i \in \Re^{2n_x \times 2n_x}$ are symmetric matrices to be determined for $i = 1, \ldots, n_r$.

Accordingly, the internal and external sets characterizing the UB stability are redefined as follows:

$$\mathcal{E}_I^{\{a\}} \triangleq \bigcap_{i \in \{1, \ldots n_r\}} \mathcal{E}(\mathbb{W}_i^{-1}) \ , \ \mathcal{E}_E^{\{a\}} \triangleq \bigcap_{i \in \{1, \ldots n_r\}} \mathcal{E}(\mathbb{Q}_i^{-1}) \ , \quad (5.31)$$

with $\mathcal{E}(\mathbb{W}_i^{-1})$ and $\mathcal{E}(\mathbb{Q}_i^{-1})$ being ellipsoidal sets as defined below:

$$\begin{aligned} \mathcal{E}(\mathbb{W}_i^{-1}) &= \left\{ \xi(k) \in \Re^{2n_x} : \xi^{'}(k)\mathbb{W}_i^{-1}\xi(k) \leq 1 \right\}, \\ \mathcal{E}(\mathbb{Q}_i^{-1}) &= \left\{ \xi(k) \in \Re^{2n_x} : \xi^{'}(k)\mathbb{Q}_i^{-1}\xi(k) \leq 1 \right\}. \end{aligned} \quad (5.32)$$

Also, the T-S domain of validity is redefined in terms of the augmented space (equal to the definition (3.10) in Chapter 3):

$$\mathcal{X}^{\{a\}} = \{\xi(k) \in \Re^{2n_x} : |\mathbb{N}\xi(k)| \preceq \phi\}, \quad (5.33)$$

where $\mathbb{N} = [\, N \quad 0_{n_\phi \times n_x} \,]$.

Similarly to the procedure performed in Chapter 3, section 3.3, consider n_x-dimensional real square matrices X, Y, P and Z such that the following matrices are nonsingular:

$$\mathbb{U} = \begin{bmatrix} X & \bullet \\ Z & \bullet \end{bmatrix}, \ \mathbb{U}^{-1} = \begin{bmatrix} Y & \bullet \\ P & \bullet \end{bmatrix}, \ \Theta = \begin{bmatrix} Y & I_n \\ P & 0 \end{bmatrix} , \quad (5.34)$$

with $\bullet$ denoting any real matrix with compatible dimensions. In view of the above definitions, note that:

$$\mathbb{U}\Theta = \begin{bmatrix} I_n & X \\ 0 & Z \end{bmatrix} .$$

Hence, the parametrization $\Theta'\mathbb{U}\Theta$ yields:

$$\hat{\mathbb{U}} = \Theta'\mathbb{U}\Theta = \begin{bmatrix} Y' & T' \\ I_n & X \end{bmatrix} , \; T' = Y'X + P'Z \; . \tag{5.35}$$

Furthermore, partitioning the matrices $\mathbb{Q}_i$ and $\mathbb{W}_i$ as follows:

$$\mathbb{Q}_i = \begin{bmatrix} Q_{11i} & Q_{12i} \\ \star & Q_{22i} \end{bmatrix} , \; \mathbb{W}_i = \begin{bmatrix} W_{11i} & W_{12i} \\ \star & W_{22i} \end{bmatrix}$$

leads to :

$$\hat{\mathbb{Q}}_i = \Theta'\mathbb{Q}_i\Theta = \begin{bmatrix} \begin{matrix} Y'Q_{11i}Y + P'Q'_{12i}Y + \\ Y'Q_{12i}P + P'Q_{22i}P \end{matrix} & \begin{matrix} Y'Q_{11i} + \\ P'Q'_{12i} \end{matrix} \\ \star & Q_{11i} \end{bmatrix} = \begin{bmatrix} \hat{Q}_{11i} & \hat{Q}_{12i} \\ \star & \hat{Q}_{22_i} \end{bmatrix} .$$

$$\hat{\mathbb{W}}_i = \Theta'\mathbb{W}_i\Theta = \begin{bmatrix} \begin{matrix} Y'W_{11i}Y + P'W'_{12i}Y + \\ Y'W_{12i}P + P'W_{22i}P \end{matrix} & \begin{matrix} Y'W_{11i} + \\ P'W'_{12i} \end{matrix} \\ \star & W_{11i} \end{bmatrix} = \begin{bmatrix} \hat{W}_{11i} & \hat{W}_{12i} \\ \star & \hat{W}_{22_i} \end{bmatrix} .$$

Then, the following result is proposed to determine the matrices of the dynamic output feedback controller (5.5).

Theorem 5.10 *Consider the nonlinear system in* (2.1)*, its N-fuzzy representation in* (5.2) *with* $h(k) = h(y(k))$*, and the controller defined in* (5.5)*. Let the positive scalars* τ_1 *and* $\tau_3 \in (0,1)$*, and a diagonal positive definite matrix* $\Delta \in \Re^{n_\varphi \times n_\varphi}$*. Suppose there exist symmetric positive definite matrices* $\hat{\mathbb{Q}}_i, \hat{\mathbb{W}}_i \in \Re^{2n_x \times 2n_x}$*,* $i = 1, \ldots, n_r$*; matrices* X*,* Y*,* T*,* $\hat{A}_{ij}$*,* $\hat{B}_{ij}$*,* $\hat{C}_i$*,* $\hat{D}_i$ *of appropriate dimensions; and positive scalars* τ_2 *and* τ_4*; that satisfy* $\hat{\mathbb{Q}}_i \geq \hat{\mathbb{W}}_i$ *and the following LMIs:*

$$\left[\begin{array}{c|c|c|c|c} -\hat{\mathbb{Q}}_q & \Pi^1_{ij} & \Pi^2_{ij} & \Pi^3_{ij} & 0 \\ \hline \star & \dfrac{\hat{\mathbb{Q}}_i + \hat{\mathbb{Q}}_j}{2} - \hat{\mathbb{U}} - \hat{\mathbb{U}}' & \begin{matrix} L'\Omega \\ X'L'\Omega \end{matrix} & 0 & \tau_1 \hat{\mathbb{U}}' \\ \hline \star & \star & \begin{matrix} -2\Delta \\ 0 \end{matrix} & \begin{matrix} 0 \\ -\tau_2 R \end{matrix} & 0 \\ \hline \star & \star & \star & \star & -\tau_1\left(\dfrac{\hat{\mathbb{W}}_i + \hat{\mathbb{W}}_j}{2}\right) \end{array}\right] < 0$$

$$\forall \; q, i = 1, ..., n_r \; \textit{and} \; j = i, ..., n_r \tag{5.36}$$

$$-\tau_1 + \tau_2\delta^{-1} < 0 \tag{5.37}$$

$$\left[\begin{array}{c:c:c:c} -\hat{\mathbb{W}}_q & \Pi^1_{ij} & \Pi^2_{ij} & \Pi^3_{ij} \\ \hdashline \star & \tau_3\left(\dfrac{\hat{\mathbb{W}}_i + \hat{\mathbb{W}}_j}{2} - \hat{\mathbb{U}} - \hat{\mathbb{U}}'\right) & \begin{array}{c} L'\Omega \\ X'L'\Omega \end{array} & 0 \\ \hdashline \star & \star & \begin{array}{c} -2\Delta \\ 0 \end{array} & \begin{array}{c} 0 \\ -\tau_4 R \end{array} \end{array}\right] \leq 0$$

$$\forall\ q, i = 1, ..., n_r \ \ and\ j = i, ..., n_r \tag{5.38}$$

$$\tau_3 + \tau_4\delta^{-1} - 1 \leq 0 \tag{5.39}$$

$$\left[\begin{array}{c:c} -\hat{\mathbb{Q}}_i + \hat{\mathbb{U}} + \hat{\mathbb{U}}' & \begin{array}{c} N'_{\{\ell\}} \\ (NX)'_{\{\ell\}} \end{array} \\ \hdashline \star & \phi^2_{\{\ell\}} \end{array}\right] > 0,$$

$$\forall\ i = 1, ..., n_r \ \ and\ \ell = 1, ..., n_\phi \tag{5.40}$$

where $\hat{\mathbb{U}}$ *is as in* (5.35) *and*

$$\Pi^1_{ij} = \begin{bmatrix} \dfrac{Y'(A_i + A_j) + \hat{B}_{ij}C}{2} & \dfrac{\hat{A}_{ij}}{2} \\ \dfrac{A_i + A_j + (B_i\hat{D}_j + B_j\hat{D}_i)C}{2} & \dfrac{(A_i + A_j)X + B_i\hat{C}_j + B_j\hat{C}_i}{2} \end{bmatrix},$$

$$\Pi^2_{ij} = \begin{bmatrix} Y'\left(\dfrac{G_i + G_j}{2}\right)\Delta \\ \left(\dfrac{G_i + G_j}{2}\right)\Delta \end{bmatrix},$$

$$\Pi^3_{ij} = \begin{bmatrix} \dfrac{B_{wi} + B_{wj}}{2} \\ 0 \end{bmatrix}.$$

Let P *be any nonsingular matrix and define the following matrices:*

$$\begin{aligned} Z &= (P')^{-1}(T' - Y'X),\ \ D_{ci} = \hat{D}_i \\ C_{ci} &= (\hat{C}_i - D_{ci}CX)Z^{-1}, \\ B_{cij} &= (P')^{-1}\left[\hat{B}_{ij} - Y'(B_iD_{cj} + B_jD_{ci})\right], \\ A_{cij} &= (P')^{-1}\left[\hat{A}_{ij} - Y'(A_i + A_j)X - \hat{B}_{ij}CX - Y'(B_iC_{cj} + B_jC_{ci})Z\right]Z^{-1}, \end{aligned} \tag{5.41}$$

with $i, j = 1, \ldots, n_r$. Then, the following holds:

i) The closed-loop system consisting of (2.1) and (5.5) is locally UB stable;

ii) $\mathcal{E}_I^{\{a\}}$ as defined in (5.31) with (5.32) is an UB set;

iii) For any $w(k) \in \mathcal{W}$ and $x(0) \in \mathcal{E}_E^{\{a\}}$, with $\mathcal{E}_E^{\{a\}}$ as defined in (5.31) with (5.32), there exists a $\bar{k} \in \mathbb{Z}^+$ such that $x(k) \in \mathcal{E}_I^{\{a\}}$, $\forall\ k \geq \bar{k}$.

Proof *Suppose there exists a solution to (5.36)-(5.40) for all $q, i = 1, \ldots, n_r$, $j = i, \ldots, n_r$ and $l = 1, \ldots, n_\phi$. Then, from the $(2,2)$ block of (5.36), it follows that $\hat{\mathbb{U}} > 0$. Hence, in view of (5.35), the matrices X, Y and $(T' - Y'X)$ are nonsingular. As a result, for any nonsingular P, the matrices defined in (5.41) are well-defined.*

Next, consider the matrix inequalities in (5.36) and (5.38), and replace the matrices $\hat{A}_{ij}$, $\hat{B}_{ij}$, $\hat{C}_i$ and $\hat{D}_i$ by their following equivalent representations:

$$
\begin{aligned}
\hat{C}_i &= D_{ci}CX + C_{ci}Z, \\
\hat{D}_i &= D_{ci}, \\
\hat{B}_{ij} &= Y^{'}(B_iD_{cj} + B_jD_{ci}) + W^{'}B_{cij}, \\
\hat{A}_{ij} &= Y^{'}(A_i + A_j)X + \hat{B}_{ij}CX + Y^{'}(B_iC_{cj} + B_jC_{ci})Z + W^{'}A_{cij}Z.
\end{aligned}
$$

Now, apply the congruence transformations $\mathrm{diag}\{(\Theta')^{-1}, (\Theta')^{-1}, I, I, (\Theta')^{-1}\}$ *and* $\mathrm{diag}\{(\Theta')^{-1}, (\Theta')^{-1}, I, I\}$*, respectively. Multiplying the resulting matrix inequalities successively by $h_{(i)}(k)$, $h_{(j)}(k)$, $h_{(q)}(k+1)$ and summing up on $i, q = 1, \ldots, n_r$ and $j = i, \ldots, n_r$, the following hold for all $h(k) \in \Xi$:*

$$
\mathbb{M}_1(h) = \begin{bmatrix}
-\mathbb{Q}(h^+) & \mathbb{A}_f(h)\mathbb{U} & \mathbb{G}(h)\Delta & \mathbb{B}_w(h) & 0 \\
\star & -\mathbb{U}^{'}\mathbb{Q}(h)\mathbb{U} & \mathbb{U}^{'}\mathbb{L}^{'}\Omega & 0 & \tau_1\mathbb{U}^{'} \\
\star & \star & -2\Delta & 0 & 0 \\
\star & \star & \star & -\tau_2 R & 0 \\
\star & \star & \star & \star & \tau_1\mathbb{W}(h)
\end{bmatrix} < 0\ ,
$$

$$
\mathbb{M}_2(h) = \begin{bmatrix}
-\mathbb{W}(h^+) & \mathbb{A}_f(h)\mathbb{U} & \mathbb{G}(h)\Delta & \mathbb{B}_w(h) \\
\star & -\tau_3\mathbb{U}^{'}\mathbb{W}(h)\mathbb{U} & \mathbb{U}^{'}\mathbb{L}^{'}\Omega & 0 \\
\star & \star & -2\Delta & 0 \\
\star & \star & \star & -\tau_4 R
\end{bmatrix} \leq 0,
$$

with $\mathbb{A}_f(h) = \mathbb{A}(h) + \mathbb{B}(h)\mathbb{K}(h)$ *and the shorthands* $h = h(k)$ *and* $h^+ = h(k+1)$.

The rest of this proof follows from the proof of Theorem 4.4.

5.3 DESIGN ISSUES

In this section the controllers design based on the previous results is proposed through optimization problems, which aims: i) to obtain the smallest UB set $\mathcal{E}_I$; or ii) to obtain the set of initial conditions $\mathcal{E}_E$ that cover as much as possible the domain of validity $\mathcal{X}$; and iii) to consider the two previous objectives into a multiobjective problem.

5.3.1 State and Sector Nonlinearities Feedback Design

5.3.1.1 Minimization of $\mathcal{E}_I$

In this case the objective consists in minimizing the UB set $\mathcal{E}_I$. For this purpose the set $\mathcal{E}_I$ will be included in the sphere with radius equal to $\sqrt{\gamma}$, which will be minimized. Then, $\mathcal{E}_I \subseteq \mathcal{E}\left(\frac{1}{\gamma}I_{n_x}\right) \Leftrightarrow x^{'}(k)\frac{1}{\gamma}I_{n_x}x(k) \leq 1 \;\forall\; x^{'}(k)W^{-1}(h(k))x(k) \leq 1$, which can be equivalently represented by (DILDA; JUNGERS; CASTELAN, 2014):

$$\begin{bmatrix} \gamma I_{n_x} & W_i \\ \star & Wi \end{bmatrix} \geq 0 \qquad \forall\; i = 1, ..., n_r \tag{5.42}$$

Thus, the following convex optimization problem is proposed:

$$\begin{gathered} \min_{Q_i, W_i, \Delta, Y_{1i}, Y_{2i}, U, \tau_2, \tau_4} \gamma \\ \text{subject to} \\ \text{LMIs (5.15), (5.16), (5.17) , (5.18), (5.19) and (5.42).} \end{gathered} \tag{5.43}$$

5.3.1.2 Maximization of $\mathcal{E}_E$

Ideally, the set of initial conditions should be coincident with the domain of validity $\mathcal{X}$. However, to ensure that the system trajectories do not evolve outside this domain (where T-S model convexity cannot be guaranteed), the set $\mathcal{E}_E$ represents the admissible region of initial conditions. In this way, the objective is to maximize the set $\mathcal{E}_E \subseteq \mathcal{X}$. For this purpose, it is considered that $\mathcal{X}$ can be described by

$$\mathcal{X} = Co\{v_\sigma \in \Re^{n_x}, \quad \sigma = 1, ..., n_\sigma\}$$

where the set of vectors $\{v_\sigma \in \Re^{n_x}\}$ contain the information necessary to characterize the shape of $\mathcal{X}$. Then, the objective consists in maximizing the factor β such that the inclusion $\beta\mathcal{X} \subseteq \mathcal{E}_E$ is verified. Considering $\mu = 1/\beta^2$, this inclusion is equivalent to

$$\begin{gathered} \begin{bmatrix} \mu & v_\sigma^{'} \\ \star & Q_i \end{bmatrix} \geq 0 \\ \forall\ i = 1, ..., n_r \ \text{ and } \ \sigma = 1, ..., n_\sigma \end{gathered} \tag{5.44}$$

In this case, the following convex optimization problem is proposed:

$$\begin{gathered} \min_{Q_i, W_i, \Delta, Y_{1i}, Y_{2i}, U, \tau_2, \tau_4} \mu \\ \text{subject to} \\ \text{LMIs (5.15), (5.17), (5.16), (5.18), (5.19) and (5.44).} \end{gathered} \tag{5.45}$$

5.3.1.3 Multiobjective Problem

It is possible to formulate a multiobjective optimization problem for considering the previous objectives at the cost of losing convexity. A nonconvex optimization is hard to be solved and approximate convex solutions might be applied to this end. In this way, the following approximate multiobjective optimization problem is proposed:

$$\begin{gathered} \min_{Q_i, W_i, \Delta, Y_{1i}, Y_{2i}, U, \tau_2, \tau_4} \lambda\gamma + (1-\lambda)\mu \\ \text{subject to} \\ \text{LMIs (5.15), (5.17), (5.16), (5.18), (5.19), (5.42) and (5.44).} \end{gathered} \tag{5.46}$$

Observe that the design parameter $\lambda \in [0, 1]$ is responsible for weighting each objective.

Remark 5.11 *Notice that in any of the above optimization problems, it is required to perform a search in space $\tau_1 \times \tau_3 \in]0, 1[$, to select the values that yields the best optimized objective, as will be illustrated in the experiments section.*

5.3.2 Dynamic Output Feedback Design

For sake of conciseness, the optimization problems of dynamic output feedback design will be briefly presented as direct extensions of those described for the state feedback design.

5.3.2.1 Minimization of $\mathcal{E}_I^{\{a\}}$

For practical purposes, it is chosen to minimize the set $\mathcal{E}_I^{\{a\}}$ only in the directions associated with the states of the plant. This can be accomplished by the following optimization algorithm, in which the supplementary constraint accounts for $\mathcal{E}_I \subseteq \mathcal{E}\left(\frac{1}{\gamma}\begin{bmatrix} I_n & 0 \\ 0 & 0 \end{bmatrix}\right)$.

$$\begin{gathered} \min_{\hat{\mathbb{Q}}_i, \hat{\mathbb{W}}_i, X, Y, T, \hat{A}_{ij}, \hat{B}_{ij}, \hat{C}_i, \hat{D}_i, \tau_2, \tau_4} \gamma \\ \text{subject to} \\ \text{LMIs (5.36), (5.37), (5.38), (5.39), (5.40) and} \\ \left[\begin{array}{c|c} \gamma I_{n_x} & \begin{bmatrix} I_{n_x} & X \end{bmatrix} \\ \hline \star & -\hat{\mathbb{W}}_i + \hat{\mathbb{U}} + \hat{\mathbb{U}}' \end{array}\right] \geq 0. \\ \forall\ i = 1, ..., n_r \end{gathered} \tag{5.47}$$

5.3.2.2 Maximization of $\mathcal{E}_E^{\{a\}}$

As in the previous case, and aiming to maximize the set of initial conditions in the directions associated with the states of the plant, the following optimization algorithm is proposed

$$\begin{gathered} \min_{\hat{\mathbb{Q}}_i, \hat{\mathbb{W}}_i, X, Y, T, \hat{A}_{ij}, \hat{B}_{ij}, \hat{C}_i, \hat{D}_i, \tau_2, \tau_4} \mu \\ \text{subject to} \\ \text{LMIs (5.36), (5.37), (5.38), (5.39), (5.40) and} \\ \left[\begin{array}{c|c} \mu & \begin{bmatrix} v_\sigma' Y & v_\sigma' \end{bmatrix} \\ \hline \star & \hat{\mathbb{Q}}_i \end{array}\right] \geq 0. \\ \forall\ i = 1, ..., n_r \ \text{ and } \ \sigma = 1, ..., n_\sigma \end{gathered} \tag{5.48}$$

5.3.2.3 Multiobjetive Problem

The approximate multiobjective optimization problem blends (5.47) and (5.48) in the same way as in (5.46), with the weighting parameter $\lambda \in [0,1]$. As a result, the following convex optimization problem is proposed:

$$
\begin{gathered}
\min_{\hat{\mathbb{Q}}_i, \hat{\mathbb{W}}_i, X, Y, T, \hat{A}_{ij}, \hat{B}_{ij}, \hat{C}_i, \hat{D}_i, \tau_2, \tau_4} \lambda\gamma + (1-\lambda)\mu \\
\text{subject to} \\
\text{LMIs (5.36), (5.37), (5.38), (5.39), (5.40),} \\
\left[\begin{array}{c:c} \gamma I_{n_x} & \left[\begin{array}{cc} I_{n_x} & X \end{array}\right] \\ \hdashline \star & -\hat{\mathbb{W}}_i + \hat{\mathbb{U}} + \hat{\mathbb{U}}' \end{array}\right] \geq 0 \quad \text{and} \quad \left[\begin{array}{c:c} \mu & \left[\begin{array}{cc} v_\sigma' Y & v_\sigma' \end{array}\right] \\ \hdashline \star & \hat{\mathbb{Q}}_i \end{array}\right] \geq 0. \\
\forall\ i=1,\dots,n_r \qquad\qquad \forall\ i=1,\dots,n_r \ \text{ and } \ \sigma=1,\dots,n_\sigma
\end{gathered}
\tag{5.49}
$$

5.4 EXPERIMENTS

Consider the two dimensional nonlinear system presented in Appendix B, section B.4. The state space representation of the system is given by:

$$
\begin{aligned}
x_{(1)}(k+1) = {} & \frac{3}{10}x_{(1)}(k) - \frac{1}{2}x_{(2)}(k) - \frac{1}{10}x_{(1)}^2(k) + \frac{1}{4}x_{(1)}(k)x_{(2)}(k) \\
& + \frac{3}{10}x_{(2)}(k)(1+\sin(x_{(2)}(k))) + \frac{7}{10}u(k) + \frac{1}{20}x_{(1)}(k)u(k) \\
& - \frac{1}{2}w_{(1)}(k) - \frac{1}{4}x_{(1)}(k)w_{(1)}(k) - \frac{11}{20}w_{(2)}(k) + \frac{7}{40}x_{(1)}(k)w_{(2)}(k) \\
x_{(2)}(k+1) = {} & \frac{1}{20}x_{(1)}(k) - \frac{3}{10}x_{(2)}(k) + \frac{9}{40}x_{(1)}^2(k) - \frac{1}{10}x_{(1)}(k)x_{(2)}(k) \\
& - \frac{1}{20}u(k) + \frac{1}{40}x_{(1)}(k)u(k) + \frac{9}{10}w_{(1)}(k) + \frac{9}{20}x_{(1)}(k)w_{(1)}(k) \\
& + \frac{1}{20}w_{(2)}(k) + \frac{19}{40}x_{(1)}(k)w_{(2)}(k)
\end{aligned}
\tag{5.50}
$$

The above nonlinear system will be used to demonstrate the potential of the described approach as a control design tool for nonlinear discrete-time systems subject to persistent disturbances. To this end, it is considered that the states are constrained in the domain defined by $|x_{(1)}(k)| \leq 2$ and $|x_{(2)}(k)| \leq 1.5$, and that disturbance vector lies inside the set $\mathcal{W}$, in (5.1), defined by $\delta = 20$ and $R = \text{diag}\{13.88, 20\}$. Figure 24 shows a particular disturbance vector $w_k \in \mathcal{W}$ used in the simulations.

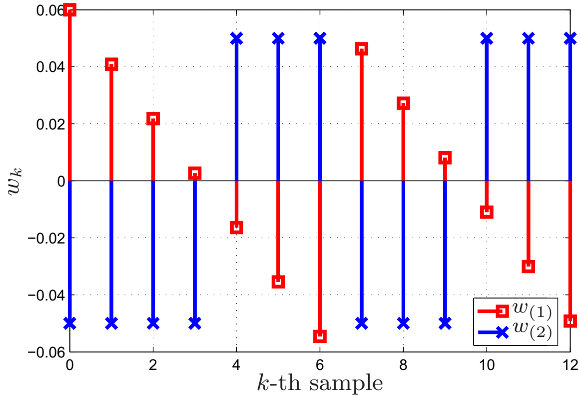

Figure 24 – Disturbance signal for numerical example

i) Classical T-S Modeling: For this case the considered nonlinear system is represented by the classical T-S fuzzy model given in (B.8), composed by four linear local rules.

In the sequel, observing the particularies in Remark 5.9, it is possible to apply the optimization problem (5.46) to compute a state feedback control law $u(k) = K(h(k))x(k)$, with $K(h(k)) = \sum_{i=1}^{r} h_{(i)}(k)K_i$. By choosing the weighting parameter $\lambda = 0.5$, and by gridding the space $\tau_1 \times \tau_3 \in]0,1[$ with steps of 0.1, the best solution was found for the pair $\{\tau_1, \tau_3\} = \{0.1, 0.9\}$ with the respective lowest value of $\gamma = 0.9949$ and highest value of $\beta = 0.6799$. In other words, this specific case combines the smallest ellipsoidal set $\mathcal{E}_I$ (the UB set) and the greatest ellipsoidal set $\mathcal{E}_E$ (initial conditions set) retrieved from the multiobjective algorithm (5.46) and the gridding search strategy. The corresponding gain matrices are:

$$K_1 = \begin{bmatrix} -0.8255 & 1.4385 \end{bmatrix}, \quad K_2 = \begin{bmatrix} -0.8605 & 0.5587 \end{bmatrix},$$
$$K_3 = \begin{bmatrix} -0.1097 & -0.0704 \end{bmatrix}, \quad K_4 = \begin{bmatrix} -0.1097 & -0.8187 \end{bmatrix}.$$

In Figure 25, it is observed the two regions and some closed-loop trajectories obtained for the specific allowed disturbance in Figure 24. It can be noticed that for every initial condition (represented by a red square) in $\mathcal{E}_E$ (represented by a dashed line in magenta) the corresponding trajectory, as desired, evolve inside of $\mathcal{X}$ (represented by a continuous line in cyan) and, in a finite time, converge to the positively invariant UB set $\mathcal{E}_I$ (represented by a dashed dotted line in green).

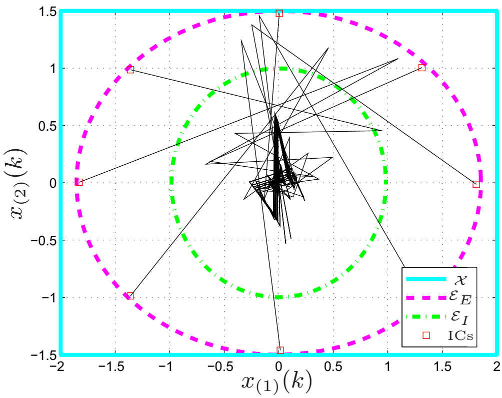

Figure 25 – Ellipsoidal sets and trajectories for example i)

ii) N-Fuzzy Modeling: For this case the considered nonlinear systems is represented by the N-fuzzy model given in (B.10), composed by two nonlinear local rules. As can be noted, the number of rules for representing the nonlinear system was reduced by 50%, without compromissing the exactness of the model.

In the sequel, it is possible to apply the multiobjective optimization problem (5.46) to compute a nonlinear state feedback control law as in (5.3). Choosing the weighting parameter $\lambda = 0.5$, and by gridding the space $\tau_1 \times \tau_3 \in]0, 1[$ with steps of 0.1, the best solution was found, as the previous case, for the pair $\{\tau_1, \tau_3\} = \{0.1, 0.9\}$, with the respective lowest value of $\gamma = 0.9992$ and highest value of $\beta = 0.6795$. It should be highlighted that the solution time to apply the optimization problem was reduced from 2.993s to 1.258s, as a result of lower numerical complexity provided by the N-fuzzy model. The corresponding gain matrices are:

$$K_1 = \begin{bmatrix} -0.9021 & 1.4173 \end{bmatrix}, \quad K_2 = \begin{bmatrix} -0.4850 & -0.6688 \end{bmatrix},$$
$$\Gamma_1 = -1.6381, \qquad \Gamma_2 = -1.2500.$$

Similarly to the state feedback case for classical fuzzy models, it is possible to observe in Figure 26 the two regions and some closed-loop trajectories obtained for the specific allowed disturbance in Figure 24. As in the previous case, it can be noticed that for every initial condition in $\mathcal{E}_E$, the corresponding trajectory, as desired, evolve inside of $\mathcal{X}$ and, in a finite time, converge to the positively invariant UB set $\mathcal{E}_I$. For the specific initial condition $x(0) = [-1.341 \ \ -1]'$, the closed-loop state trajectory is shown in Figure 27.

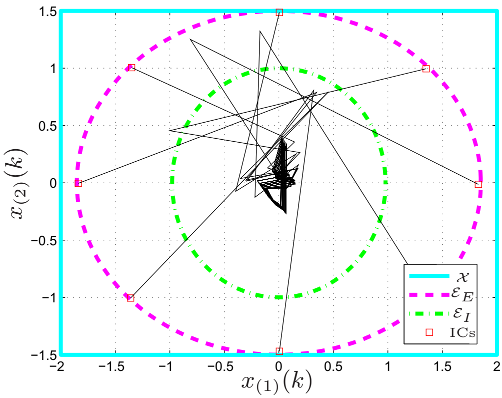

Figure 26 – Ellipsoidal sets and trajectories for example ii)

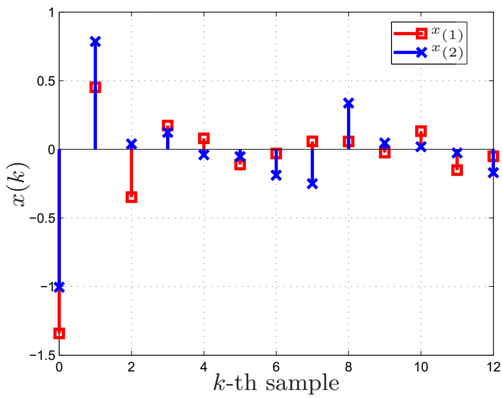

Figure 27 – State trajectories for example ii)

At last, by comparing the associated values of γ and β, and by comparing Figures 25 and 26, it can be seen that there is no significant qualitative difference between the two solution.

iii) Output Feedback: In previous numerical experiments, the state variables $x_{(1)}(k)$ and $x_{(2)}(k)$ were assumed to be measurable, allowing the implementation of fuzzy control laws that depend of $h(k) = h(x_{(1)}(k), x_{(2)}(k))$ when designed from the classical T-S model, or of $h(k) = h(x_{(1)}(k))$ and $\varphi(k) = \varphi(x_{(2)}(k))$ when designed from the N-fuzzy model.

Next, to show how the proposed dynamic output feedback strategy can be useful in practice, it is also considered the N-fuzzy model in (B.10), but additionally defining the output equation by $y(k) = [1\ 0]\, x(k)$, i.e., the only available signal to compute the control law is the state $x_{(1)}(k)$. Such additional constraint makes the use of the classical T-S model not adequate to design and use a fuzzy dynamic output feedback controller which gains would be dependent of $h(k) = h(x_{(1)}(k), x_{(2)}(k))$. However, because the nonlinearity $\varphi(x_{(2)}(k)) = 0.3x_{(2)}(k)(1 + \sin(x_{(2)}(k)))$ is sector bounded, even being dependent of the unmeasurable state $x_{(2)}(k)$, the dynamic output feedback controller in (5.5)-(5.6) can be designed from the N-fuzzy model (B.10), because in this case $h(k) = h(y(k))$, and also be used in practice.

Thus, by applying the multiobjective optimization problem (5.49), with $\lambda = 0.5$ and gridding the space $\tau_1 \times \tau_3 \in]0, 1[$ and the positive diagonal matrix Δ, we obtain the lowest value of $\gamma = 1.8345$ and the highest value of $\beta = 0.6228$, for the triple $\{\tau_1, \tau_3, \Delta\} = \{0.1, 0.8, 2\}$.

Figure 28 shows the regions obtained for the above-mentioned problem and some closed-loop trajectories considering the disturbance signals described in Figure 24. The regions $\mathcal{E}_E$ and $\mathcal{E}_I$ are respectively the intersection of $\mathcal{E}_E^{\{a\}}$ with the plane formed by the states of the plant and the orthogonal projection of $\mathcal{E}_I^{\{a\}}$ onto the same subspace (see Appendix E). It should be noted that despite appearing a certain conservatism in the size of the set $\mathcal{E}_I$, the simulation considers only a distinct sequence of the disturbance signal $w(k)$. In this way, other disturbance sequences $w(k)$ could lead the trajectories to evolve closer to the border of UB set.

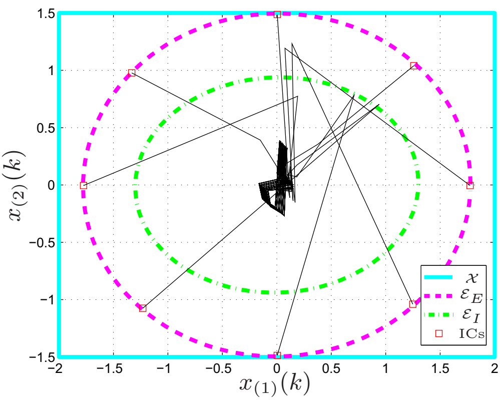

Figure 28 – Ellipsoidal sets and trajectories for example iii)

In Figure 29, it is shown the state trajectories for the initial condition $x(0) = [1.77\ \ 0]^{'}$ and $x_c(0) = [0\ \ 0]^{'}$. Notice that the overall performance is similar to that achieved with the state and sector nonlinearity feedback.

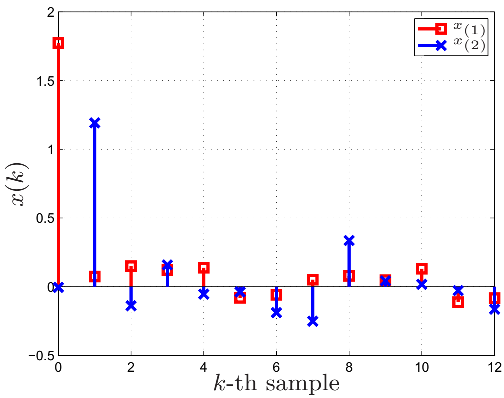

Figure 29 – State trajectories for example iii)

5.5 CONCLUDING REMARKS

In this chapter a convex approach for the design of fuzzy controllers that locally stabilizes nonlinear discrete-time systems subject to amplitude bounded disturbances was presented. Considering fuzzy Lyapunov functions, optimization problems in terms of LMI constraints were proposed to design a nonlinear state-feedback control law, which is a function of the membership fuzzy functions and cone sector nonlinearities, and to design a dynamic output feedback control law. An interesting characteristic is that the dynamic output case admits the existence of nonlinearities with unmeasured states in the original system, as opposed to the classical literature strategies and the approach lately proposed in Chapter 3. Additionally, two ellipsoidal sets, $\mathcal{E}_E$ and $\mathcal{E}_I$, are taken into account, associated respectively to the admissible region of initial conditions and the concept of ultimate bounded . Both the theoretical developments and the design strategies consider that the convexity of the fuzzy models holds in a given domain of validity.

6 INTERACTIVE SOFTWARE AND HARDWARE IMPLEMENTATION

Chapters 2, 3, 4 and 5 provide theoretical tools for modeling and control of nonlinear systems via T-S fuzzy approach. In this chapter, aiming to assist students, researches and engineers in the control design of nonlinear systems using FMB techniques, the following results are proposed:

i) an interactive software for modeling and control of nonlinear systems, and

ii) a Hardware-in-the-Loop (HIL) implementation is applied to evaluate the digital implementation of T-S fuzzy controllers.

The proposed interactive software is a *Matlab*-based toolbox freely available for the scientific community which provides a user-friendly interactive environment for modeling and control of nonlinear systems considering FMB approaches. The fuzzy toolbox is summarized in the reference Klug, Castelan & Coutinho (2015a).

The second result of this chapter regards practical aspects of a digital implementation of T-S fuzzy controllers. More specifically, a virtual plant runs over an *Matlab/Simulink* environment and a digital controller is built over a FPGA (Field Programmable Gate Array) development board which communicates with the virtual plant using a Ethernet network. These results are summarized in the reference Klug et al. (2014).

This chapter is organized as follows: in Section 6.1, the details of the interactive software operation, as well as its modules and possible configurations are discussed. Section 6.2 deals with the hardware implementation, specifying the programming platform to be used and the HIL structure, and resulting in a comparative example. Finally, the conclusions of this chapter are presented in Section 6.3.

6.1 INTERACTIVE SOFTWARE FOR MODELING AND CONTROL DESIGN

The mathematical modeling of dynamical systems is an important research field in automatic control (GUZMAN et al., 2008). An analytical model is essential for running simulations and designing model-based control systems, despite, in many cases, not representing every aspect of reality. Nevertheless, obtaining at least an approximate representation is a good step for deriving a controller that generally performs better than those obtained with non-formal methods purely based on empirical knowledge of the process to be controlled. In addition, if the plant model accurately describes the system dynamics (e.g., through an exact modeling approach), then the closed-loop stability of the original system can be guaranteed, at least in a local context.

In light of the above, and considering that the dynamics of practical control systems are inherently nonlinear, an application was initially developed in order to automate the process of obtaining an equivalent representation of a given nonlinear system. The interactivity was the major premise, so that any change in parameters could be readily visualized, facilitating the understanding and data interpretation by the user. Currently, this application is published as a *Matlab* app, accessible from the web site www.mathworks.com/discovery/matlab-apps.html for releases *R2012b* or newer.

In order to provide an internationalization of the use of the modeling application, three languages are available (Portuguese, English and French), wherein the user can toggle between them through the appropriate menu. Figure 30 shows the number of downloads since the launch of the app in November 2014.

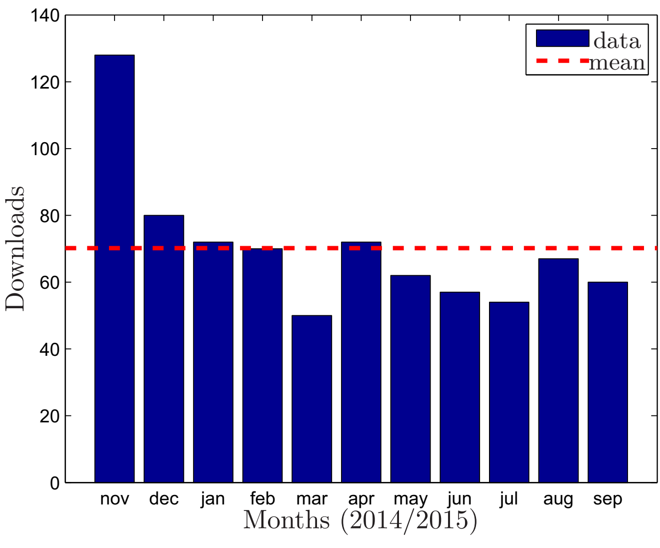

Figure 30 – Number of downloads

It can be noted that after an elevated number of downloads in the first month, that number remained near the average thereafter. This demand, coupled with the comments received during the lecture entitled “Control of Nonlinear Systems Using T-S Fuzzy Models: Theory and Implementation”, offered in the Brazilian Conference on Automatic Control - CBA 2014, led to the development of another application. This time the objective was the control design of fuzzy controllers.

For the control application, the basic idea is to automatically import the fuzzy model originating from the modeling application, and obtain the gains of a particular controller that satisfy the closed-loop performance requirements, after defining parameters and optimization criteria. Among the available library of control laws are the controllers developed during the author’s doctoral studies. Further details on the modeling and control applications are presented in the following subsections.

6.1.1 Modeling Application

This application uses the theoretical fuzzy T-S modeling basis presented in Chapter 2, based on the works Teixeira & Zak (1999), Tanaka & Wang (2001), Feng (2010) and Klug & Castelan (2011). The programming code uses symbolic math and string handling, among other packages/toolboxes of the *Matlab* environment. The starting window, shown in Figure 31, allows the user to select the type of modeling technique and the desired language.

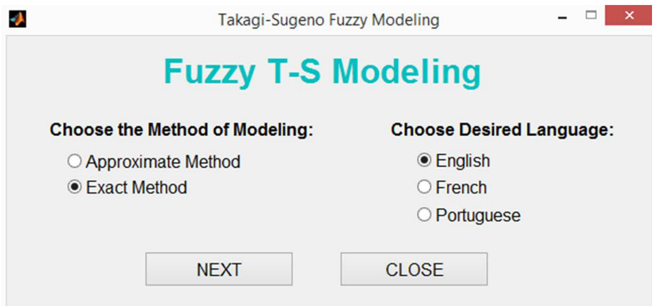

Figure 31 – Initial window

Once the first configurations are defined in the starting window, the application is divided into two distinct modules, approximate and exact modeling, whose features are described below.

6.1.1.1 Approximate Modeling Module

In this module the approximate T-S fuzzy modeling approach presented in Appendix A is used. Basically, the procedure is performed by choosing a finite number of Operation Points (OPs) which will be associated with local linear submodels. These local submodels approximately represent the behavior of the nonlinear plant in the neighborhood of the associated OPs, whose quantities and position are based on the physical knowledge of the system dynamics and the desired approximation error.

Thus, the approximate T-S fuzzy model is obtained by the interconnection of local submodels, provided by the use of membership functions. These functions usually have a particular shape, such as triangular, trapezoidal, Gaussian or bell-shaped, and should respect the convex sum property.

The main window of this module is illustrated in Figure 32 with the following subdivisions (a menu and five panels):

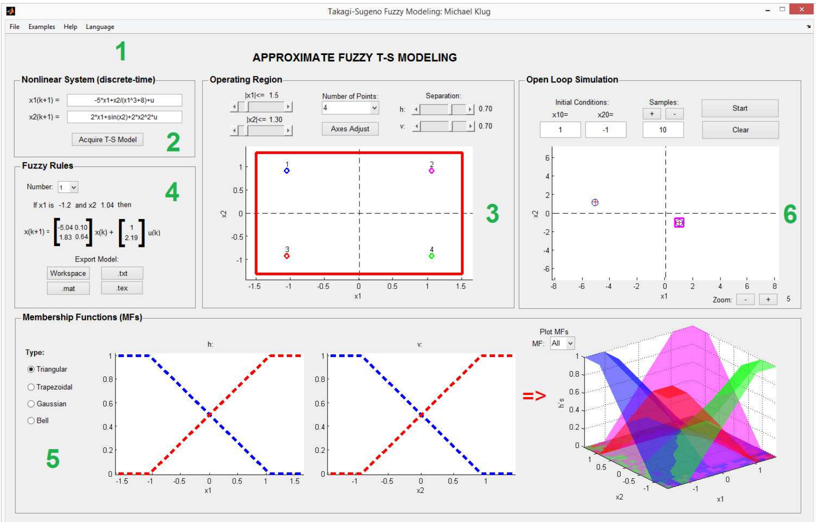

Figure 32 – Approximate modeling module window

1. *Menu:* the user can access pre-defined examples, save and open a nonlinear system data, as well as change the language of the program.

2. *Nonlinear System Panel:* the user enters the analytical equations of the nonlinear system, using, by default, pre-declared states x_1 and x_2.

3. *Region of Operation Panel:* the user can configure the region of interest (via slide bars) and the desired number of operation points.

4. *Fuzzy Rules Panel:* the user can visualize the fuzzy rules.

5. *Membership Functions Panel:* it allows the user to change and visualize the shape of the membership functions (not all types are pre-programmed).

6. *Open Loop Simulation:* it allows the user to execute a comparative simulation with the original nonlinear plant and the respective T-S fuzzy model.

The user interface was made to be intuitive. Once the nonlinear system is inserted and the operation region configured (quantity and positioning of the OPs), the approximate fuzzy model is obtained by pressing the "Acquire T-S Model" button. In this way, the application computes the optimal local submodels and presents them in the "Fuzzy Rules Panel", also allowing the user to export the final result in various formats, including .txt, .tex and .mat (required to use the control software) .

Finally, once the nonlinear system is modeled, the user can run an open loop simulation setting up the desired initial condition and the number of samples. This simulation allows a comparative analysis of the trajectories emanating from the initial condition, represented by a square, of the original system with the fuzzy model, represented respectively by the "+" and "∘" symbols.

In order to provide an evidence of how much each subsystem contributes to the global fuzzy T-S model, each membership function is represented with the same color as the associated operation point. This fact allows the user to observe which regions of the state space where there is dominance from a particular membership function, and therefore where each local submodel has a larger weight on the representation.

It is also important to emphasize that, as part of the desired software interactivity, following any changes in the settings/parameters that generates the fuzzy model (such as the quantity and positioning of the OPs), all graphics are immediately rendered considering this new conjuncture. This is an important feature for the control designer, facilitating a suitable choice in the trade-off between the number of fuzzy rules and the numerical and implementation complexity, also associated with the accuracy of the representation.

6.1.1.2 Exact Modeling Module

In this part, the application allows to handle T-S fuzzy models that accurately represent the original nonlinear system in a specific domain of the state space. Notice that this module requires some knowledge of the user with the exact fuzzy modeling technique and it has more step configurations than the previous module. User-made choices will determine whether the resulting model will have classical or N-fuzzy structure.

The main window is observed in Figure 33. There is one menu and four panels which are identical to the ones described previously: panels 2, 5, 6 and 7. These panels are in accordance with the previous panels 2, 4, 5 and 6. The following two panels have specific functions:

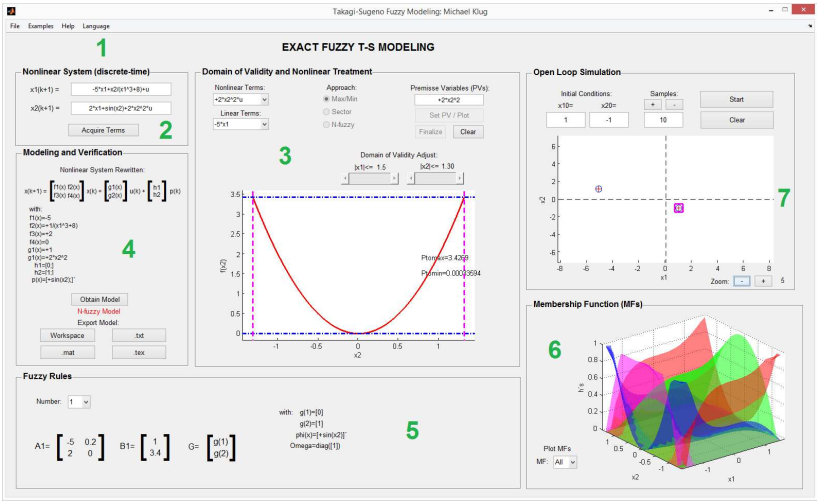

Figure 33 – Exact modeling module window

3. *Validity Domain and Nonlinear Treatment Panel:* the user sets the desired domain of validity, where the model convexity is guaranteed, via slide bars. Then, fuzzification is performed separately

for each nonlinearity, by choosing the desired approach (max/min, sector or n-fuzzy) each time.

4. *Modeling and Verification Panel:* once the system is inserted and the nonlinear treatment configured, the application rewrites the original equations in a particular form which should be verified by the user.

The procedure for obtaining the exact T-S fuzzy model is based on the individual treatment of nonlinearities of the system. After the nonlinear system is inserted, the user must press the button "Acquire Terms". In this way, the program will separate the linear terms (which do not require treatment) from the nonlinear terms (requiring treatment). Next, for each nonlinearity, the user has to choose the desired method of treatment (max/min, sector or n-fuzzy) and define the premise variable, which is preset with a default value.

It is worth mentioning that for the max/min method a state variable must be isolated when choosing the premise variable. For instance, if the nonlinearity is x_1^3, the premise variable must be defined as x_1^2; if the nonlinearity is x_1x_2, the premise variable can be defined either by x_1 or x_2. Once the premise variable is defined, the user should press the button "Set PV / Plot", verify the graph and press the button "Next". This procedure is repeated for all remaining nonlinearities. At last, after pressing the button "Finish", the user should verify if the rewritten equation of the system is correct in panel 4, and obtain the exact model by pressing the button "Obtain Model". In this way, the final result can be visualized and exported in various formats, as in the approximate modeling module.

Also similarly to the previous case, the user can run an open loop simulation comparing the trajectories emanating from a given initial condition for the original nonlinear system and its respective fuzzy model. In this case, as long as all procedures are correctly performed, the dynamics of the model will match the dynamics of the original nonlinear system, and there will not be any observable differences between the two curves. The weight of each local submodel can be seen through the membership functions, graphically represented in the panel 6.

6.1.2 Control Application

After the release of the modeling application, and considering the feedback received through the lecture given (and the article published) at the XX-CBA 2014, a second *Matlab*-based application aiming the fuzzy controller design was developed. Thus, the two apps become an interesting tool to study the control of nonlinear systems via T-S fuzzy models. This is one of the contributions of this work, since very few similar works are found in the literature which systematizes the nonlinear control design in light of results found in the scope of Linear-Time Invariant (LTI) systems.

To use this application, it is necessary to have previously obtained the T-S fuzzy model with the modeling software (if necessary, the model can be manually inserted, using permitted notation and symbols). The program is able to load .mat files (a *Matlab* format) and compute the controller gains based on a selected control law and a few performance requirements and optimization settings. The user must have installed the *Yalmip* Interface, and solvers *Sedumi* and *SPDT3*.

Until now, the following fuzzy controllers are available: state feedback, state and sector nonlinearity feedback, and dynamic output feedback, depending on how the system is represented (classical or N-fuzzy). These controllers are based on the work described in the preceding chapters and in the articles Klug & Castelan (2011), Klug & Castelan (2012) and Klug et al. (2014).

Figure 34 shows the user's interface window. The use of the menu is similar to the modeling application, allowing the user to load pre-defined examples and change the language, among other features. The following panels have specific functions:

2. *Fuzzy Model Loading Panel:* the user has to import the fuzzy model obtained with the modeling app or insert it manually using a .mat file.

3. *Controller Settings Panel:* the user defines the desired control law and the optimization objectives to be used.

4. *Solver Settings Panel:* it allows the user to choose the solver and its properties/settings.

5. *Statistics Panel:* it allows the user to visualize the data returned by the solver in the solution of the optimization problem.

6. *Simulation and Controller Gains Panel:* it displays the controller gains and enables the execution of a closed-loop simulation.

The use of the app is simple. Once the fuzzy model data is loaded, the application identifies the type of model and the number of rules, only enabling the relevant controllers, depending on how the

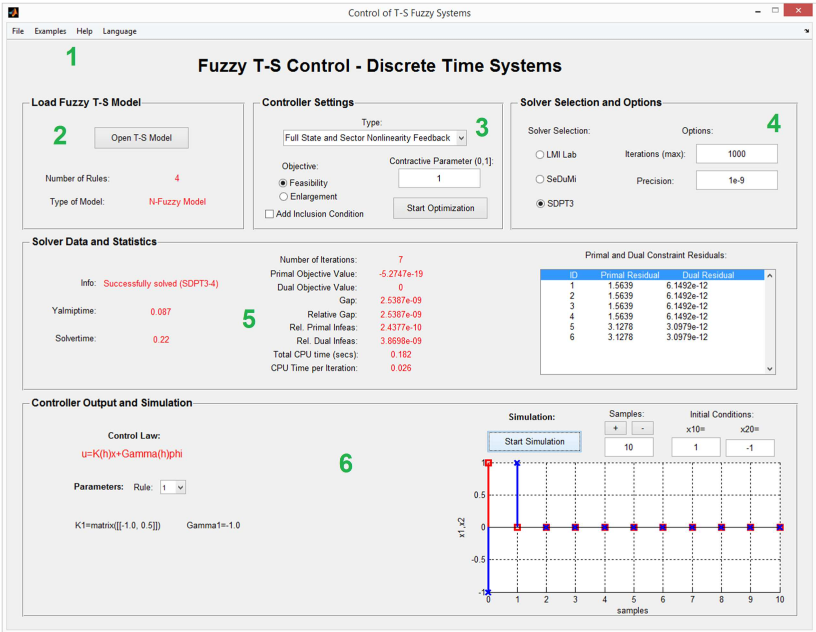

Figure 34 – Control design program window

system is represented (classical or N-fuzzy). Then, the user must select the desired controller and objectives for optimization, which are limited to feasibility or enlargement of the stability region (using a unit ball or shape approach). Additionally, an inclusion condition can be inserted to ensure that closed-loop trajectories emanating from the computed level set do not leave the local domain of validity. Finally, the user must select the LMI-solver and associated properties in the panel 4, and then call the optimization problem by pressing the “Start Optimization” button. At the end of this process, whose time depends on the numerical complexity of the control algorithm, and also on the number of rules, the controller gains are displayed in panel 6.

Furthermore, as in the modeling app, the user can run simulations from the generated data. In this case, a closed-loop simulation considering the obtained controller and the loaded T-S fuzzy model can be simply configured by setting the desired initial condition and the number of samples. Then, by pressing the button “Start Simulation”, the user can verify that stability and performance requirements have been satisfied.

6.2 HIL IMPLEMENTATION

In this section some aspects related to the practical implementation of T-S fuzzy controllers on real platforms are considered. For this purpose, HIL simulations were performed comparing a controller developed in this thesis, and other found in literature. In this sense, the study of the computational burden to the digital implementation of nonlinear control systems is evaluated using the classical and N-fuzzy approaches.

The HIL simulation is a technique for the development and test of complex systems, typically used at the project level to design and tune a controller. It is common to simulate the dynamics of the plant in real-time, either because the physical prototype is not available or because real experiments of the project involve unnecessary costs in certain phases (development time and investment). The HIL framework is characterized by the combined use of real and simulated components/parts, where e.g. the hardware is the controller, and the software is a virtual simulation of the real system.

The platform chosen to embed the control law is the FPGA development board $DE2-115$, manufactured by Altera and illustrated in Figure 35. This board is equipped with the Cyclone EP4CE115F29C7, 114480 logic elements and 266 multipliers. The FPGAs are emerging as appropriate platforms for the implementation of control systems because, for instance, they offer advantages such as high performance and concurrent computing, since the hardware is optimized to run a specific application (GUPTA; KHARE; SINGH, 2010; LOPES; FAVARIM; CARATI, 2012). Moreover, this type of device is more efficient in terms of power and performance compared to General Purpose Processors (GPPs, such as microcontrollers and digital signal processors), and it has a shorter design validation cycle and lower costs compared to Application Specific Integrated Circuits (ASICs). Although the performance improvement in the execution of high-demanding applications is prominent, there are some obstacles still making difficult further dissemination of the use of FPGAs, such as: the learning of new programming languages (Hardware Description Languages - HDLs), and the paradigm that allows the execution of several tasks in parallel.

In this context, the proposed setup consists on a *Matlab/Simulink* application based and the *HDL Coder/Verifier* toolbox to generate code for the embedded device and also to perform verification tests, saving time and avoiding the introduction of coding errors.

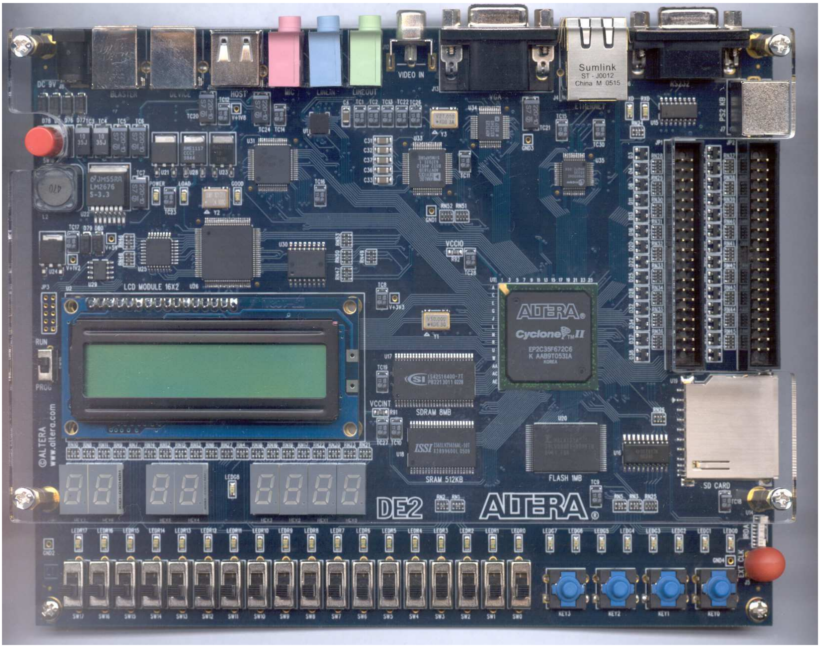

Figure 35 – FPGA development board DE2 – 115

In Figure 36, a comparison of the percentages of time spent for the development of a functional design in HDL using manual and automatic coding is presented (BEEK; SHARMA, 2011).

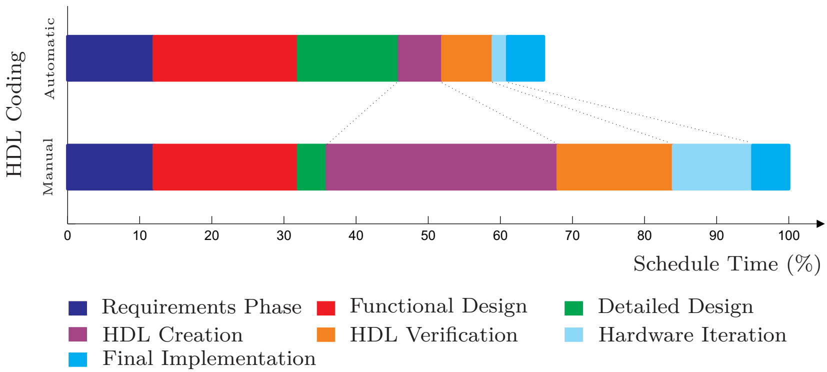

Figure 36 – FPGA prototyping workflow

Notice that the use of code generation tools allows for a significant reduction in the overall development time. Also, as automatic HDL code generation is a faster process than hand-coding, the cycle time for the development of a product is shorter, and thus it is the time-to-market (i.e. the time from design/analysis to its availability for purchase). Nowadays, this is an essential characteristic in developing a product because of market competitiveness (MEYER-BASE et al., 2006). Additionally, engineers can better use this time saved to produce higher quality algorithms in the detailed design phase, resulting in a higher quality FPGA prototype.

6.2.1 FPGA-in-the-loop Structure

The HIL implementation is performed with the physical plant emulated on the computer through a *Simulink* diagram, and the controller embedded on the development board DE2 – 115. This structure is shown in Figure 37, also referred to as the FPGA-in-the-loop.

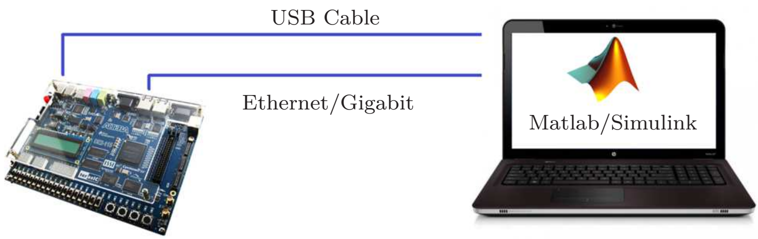

Figure 37 – FPGA-in-the-loop structure

It can be observed that the development board is connected to a computer, which must have a Gigabit network card, through a crossover cable. This connection is responsible for real-time communication between the real controller and the virtual plant. A second connection is made via a USB cable, which performs the loading of FPGA configuration files, also known as *bitstreams*. These files contain the necessary information to reconfigure the hardware which is required for the desired application.

All simulations were performed using a computer with an Intel Core i7-3612QM processor and 8GB of RAM, running Windows 8 and

Matlab 2013a. To deal with the LMIs, the parser YALPMIP and the solver SDPT3 were used.

6.2.2 Requirements and Development Stages

To accomplish with the HIL implementation, resources at hardware level, such as the computer and the development board, are required, as shown in the FPGA-in-the-loop structure, as well as resources at software level, including *Matlab/Simulink* with certain toolboxes and Quartus II, manufactured by the Altera Corporation. The two programs exchange information to generate the configuration *bitstream* for the FPGA.

Once all hardware and software requirements are fulfilled, steps briefly described below are performed (detailed settings and coding process will not be shown):

i) Controller design using *Simulink* blocks compatible with the toolbox *HDL Coder*

   At this development phase the control designer should pay attention to use only blocks that have HDL code generation compatibility. There are over 170 blocks available, including basic arithmetic operations, logical operations, and complex functions such as the Fast Fourier Transform (FFT) and digital filter. However, there are functions that are not natively supported, such as some trigonometric and transcendental functions. In this case solutions such as the use of Look-Up Tables (LUTs) and/or symmetry properties can be used.

ii) Floating-point to fixed-point algorithm conversion

   Engineers typically test new ideas and develop initial algorithms using floating-point data types. However, hardware implementation in FPGAs and ASICs usually requires fixed-point data representation. This representation generally has some advantages with respect to the circuit size, power consumption, memory usage, speed and cost. Thus, the standard floating-point *Matlab* algorithm must be converted to fixed-point. This can be achieved manually, redefining the data type of each variable/signal, or optimally using the toolbox *Fixed-Point Designer*, where the bit widths are optimized for a more efficient hardware generation.

iii) VHDL Coding

Once the controller algorithm is correctly set to run in fixed-point, the control designer have to generate the HDL code to be embedded in the FPGA development board. For this purpose the *HDL coder* toolbox is employed, which can generate codes compatible with *Simulink* diagrams using the hardware description languages Verilog and VHDL (or VHSIC hardware description language, from Very High Speed Integrated Circuits). In this work the second language was used, which is currently the most popular.

iv) Preparing FPGA-in-the-loop simulation

In this step, the configurations for the proper communication between the virtual plant and the real controller are performed. A *Simulink* diagram should be built containing the dynamics of the plant, which will exchange data over the Ethernet network with the controller embedded in the development board DE2 − 115. Thus, for a correct communication between *Simulink* and development board, the Internet Protocol (IP) settings must be correctly configured. To assist in this process, the *HDL WorkAdvisor* inside the *HDL Coder* toolbox can be used.

v) Loading FPGA and simulation

Finally, the code generated in the previous steps shall be loaded into the FPGA by using an USB cable. Then, with the FPGA configured by the *bitstream* file, it is possible to execute the HIL simulation and analyze the collected data. Several reports are generated, allowing comparisons in terms of time consumption, number of operations, number of logic elements, among others, which are explored in the example described in the following section.

6.2.3 Complexity of Implementation

The complexity analysis of the control systems digital implementation is of great importance to determine the ideal programmable platform in which is embedded the control law, ensuring there exists enough processing power to perform all the required computations in the stipulated time. In this perspective, together with the growing demand for high-performance devices with reduced size and low-energy consumption, the objective is to demonstrate that the use of N-fuzzy models has significant advantages, when compared to the classical fuzzy techniques.

It is worth noting that the fuzzy rule reduction provided by the use of N-fuzzy models yields a smaller numerical complexity of the control algorithms. This property has already been demonstrated in Appendix D, and it can also be checked considering the time required to solve the optimization problems of the preceding chapters. This is an important attribute because it prevents the computational burden from increasing to a point where solvers may fail even in solving simple problems. However, it should be clarified that, commonly, the computational system that solves the optimization algorithm is not the same as that performing the control action. In addition, the process for obtaining the controller gains runs offline, and it is not necessary to recalculate at each sampling time. Thus, although there are obvious advantages related to feasibility and the time to solve the control algorithms, the numerical complexity analysis has no direct influence over the real implementation (platform to be chosen).

For comparing the complexity of implementation between controllers developed for classical and N-fuzzy models, the following dynamic output feedback control laws are considered:

- Controller 1: Theorem 8.10 of Feng (2010)
- Controller 2: Theorem 1 of Klug, Castelan & Silva (2012)

The conditions established in the above articles have been adapted to obtain a fair comparative criterion. Hence, the conditions regarding the domain of validity, saturation treatment, among others, were not taken into account. In other words, only those related to the stabilization problem were used.

6.2.3.1 Nonlinear System

Consider the unidimensional nonlinear system represented by:

$$x(k+1) = x^3(k) + sin(x(k)) + (0,2 + x^2(k))u(k). \qquad (6.1)$$

It is assumed, for instance, due to physical reasons, that the system state is restricted to the region represented by $x(k) \in [-\pi/3, \pi/3]$. Therefore, it is possible to locally encompass the nonlinearity $\sin(x_k)$ into a limited sector, i.e., $\varphi(k) = sin(x(k)) \in S[\Omega_1, \Omega_2]$, with $\Omega_1 = 3\sqrt{3}/2\pi$ and $\Omega_2 = 1$. Also, the premise variable $\nu_k = x^2(k)$ is defined, and then $\nu(k) \in [d_1, d_2]$, with $d_1 = 0$ and $d_2 = \pi^2/9$ being the limits of $\nu(k)$. Thus, system (6.1) can be described by the following N-fuzzy model with two nonlinear local rules:

$$x(k+1) = \sum_{i=1}^{2} \alpha_{(i)}(k)\left[d_i x(k) + (0,2 + d_i)u(k)\right] + \varphi(k), \tag{6.2}$$

with $\alpha_{(1)}(k) = \dfrac{d_2 - \nu(k)}{d_2 - d_1}$ and $\alpha_{(2)}(k) = \dfrac{\nu(k) - d_1}{d_2 - d_1}$.

Otherwise, the nonlinearity $\varphi(k)$ might be rewritten as follows:

$$\varphi(k) = \sin(x(k)) = \left(\sum_{j=1}^{2} \epsilon_{(j)}(k)\Omega_j\right) x(k), \tag{6.3}$$

with $\epsilon_{(j)}(k)$, $j = 1, 2$, being any function validating (6.3) and satisfying the properties $\epsilon_{(1)} + \epsilon_{(2)} = 1$ and $\epsilon_{(j)} \geq 0,\ j = 1, 2.$ For instance, one can choose[1]

$$\epsilon_{(1)} = \begin{cases} \dfrac{\sin(x) - \Omega_1 x}{x(\Omega_2 - \Omega_1)}, & x \neq 0 \\ 1, & x = 0 \end{cases} \quad \text{and } \epsilon_{(2)} = \begin{cases} \dfrac{\Omega_2 x - \sin(x)}{x(\Omega_2 - \Omega_1)}, & x \neq 0 \\ 0, & x = 0 \end{cases}$$

Hence, the following classic T-S fuzzy model with four linear local rules is obtained:

$$\begin{aligned} x(k+1) &= \sum_{i=1}^{2}\sum_{j=1}^{2} \alpha_{(i)}(k)\epsilon_{(j)}(k)\left\{(d_i + \Omega_j)x(k) + (0.2 + d_i)u(k)\right\} \\ &= \sum_{i=1}^{4} h_{(i)}(k)\left\{A_i x(k) + B_i u(k)\right\} \end{aligned} \tag{6.4}$$

where $A_i = d_i + \Omega_j,\ B_i = 0.2 + d_i$ and $h_{(i)}(k) = \alpha_{(i)}(k)\epsilon_{(j)}(k)$, for $i = j + 2(i-1)$ and $i, j = 1, 2$.

6.2.3.2 Results

Four different cases are defined to analyze the complexity of implementation, taking into account the type of fuzzy modeling used to represent the system to be controlled and the structure of the dynamic compensator (previously presented in section 6.2.3):

---

[1] For convenience, the time dependence is omitted.

- Case 1: Classical T-S fuzzy model with Controller 1;
- Case 2: Classical T-S fuzzy model with Controller 2;
- Case 3: N-fuzzy model with Controller 2 considering $\varphi(k)$ computed;
- Case 4: N-fuzzy model with Controller 2 considering $\varphi(k)$ measured;

All of the above cases were implemented in HIL structure using the nonlinear plant described in (6.1) and the procedures explained in section 6.2.2. Thus, through the reports generated by *Matlab* and by the FPGA software Quartus II, it is possible to compare the four proposed cases using as performance criteria: i) the number of operations, ii) the compiler time to generate the bitstream, and iii) the occupied hardware area, which are described in the sequel.

In Table 3, the number of operations required to compute the control laws can be observed. Notice the smaller number of operations for the cases which use the N-fuzzy modeling, likely contributing to a reduction on the implementation complexity.

Table 3 – Number of operations

	Classical		N-fuzzy	
Operation	Case 1	Case 2	Case 3	Case 4
Multiplication	58	57	30	28
Addition / Subtraction	50	50	28	21
Multiplexing	23	23	14	6

It is also important to mention that a smaller number of operations has direct influence on the runtime of the control loop, regardless the platform used (FPGAs, microprocessors, DSPs). This factor is evidenced by the reports generated by the Quartus II FPGA compiler, as well as experimentally by measurements performed with the use of an oscilloscope (where it was shown that the controller in case 4 takes about half the time to be computed in comparison with case 1). Based on this data, it can be seen that the N-fuzzy approach is more suitable for systems demanding high sampling rates.

The computational efficiency when controlling nonlinear systems using N-fuzzy models can also be verified by the time required to compile/build the code for the FPGA, given in Table 4. A 46% reduction in the total time can be noted from case 1 to case 4.

Table 4 – Compilation time (in minutes)

	Classical		N-fuzzy	
Phase	Case 1	Case 2	Case 3	Case 4
Analysis / Synthesis	01’40”	01’30”	01’01”	01’59”
Filter	04’34”	04’33”	02’55”	02’16”
Assembler	00’07”	00’06”	00’07”	00’06”
TimeQuest	00’15”	00’15”	00’11”	00’11”
Total	**06’36”**	**06’24”**	**04’14”**	**03’32”**

In Table 5, the number of logic elements used to implement the control law and communication in the FPGA development board[2] can be verified. A reduction of $35,39\%$ and $37,42\%$, in case 1 and cases 3 and 4 is observed, respectively. Thus, considering the number of logic elements available in the development board $\mathrm{DE2}-115$, it would be possible to introduce 8 compensators in parallel in the hardware, of the type described in case 1, whereas for case 4, it would be possible to introduce 13 compensators.

Table 5 – Hardware occupation

	Classical		N-fuzzy	
	Case 1	Case 2	Case 3	Case 4
Logical Elements	13139	12056	8488	8222
Combinational Functions	12576	11450	7947	7620
9-bits Multipliers	324	252	127	116

In Figure 38, the temporal evolution of the system state to the initial condition $x_0 = 0,5$ and $x_{c,0} = 0$, for the cases 1 (classical model) and 4 (N-fuzzy model) can be seen. Notice that stabilization is achieved in both cases, with a faster trajectory convergence for the case 4, although no specific condition was included for this purpose.

The difference between the HIL simulation, performed with the controller implemented on the FPGA development board, and the simulation implemented entirely on the computer, is shown in Figure 39. This is a quantization error, derived from the conversion of control algorithm from floating-point to fixed point. Therefore, a suitable choice

[2]For comparison purposes, all the optimization criteria were equally selected between the simulations

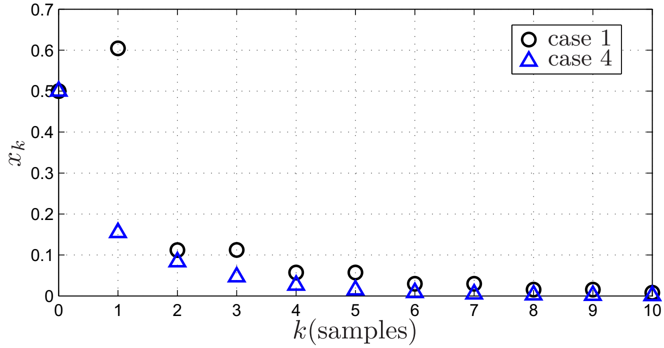

Figure 38 – State trajectory $x(k)$

of the bit widths is important to avoid overflows, which may affect the performance of the closed loop system.

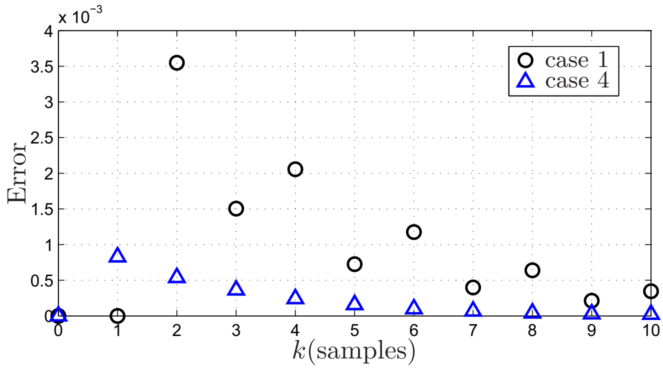

Figure 39 – Quantization error

6.3 CONCLUDING REMARKS

In this chapter, general tools concerning the analysis and design of nonlinear control systems using T-S fuzzy models were presented. Two software programs were developed in order to assist researchers and engineers to design, in a few steps, a reasonable controller for a known nonlinear system. It also allows users to quickly obtain results for comparison with their own techniques. From another point of view, the software interactivity enhances the learning process by exploiting the advantages of immediately seeing the effects of changes, which can never be shown in static pictures. Three languages are available, as well as other interesting features, such as different types of modeling, predefined examples, possibility to open/save and export data in various formats, as well as the execution of open and closed-loop simulations. Presently, the first app has been published as a *Matlab* app, also running from an executable file, provided the user has the Matlab Compiler Runtime (MCR) installed. In a future release it will be launched it as a standalone application, independent of external libraries and/or other toolboxes.

Regarding the practical implementation of fuzzy controllers, HIL simulations were performed considering the physical plant running virtually in a *Matlab/Simulink* environment using a desktop computer, and the control law embedded in a FPGA development board. Thus, a higher numerical and implementation efficiency when using N-fuzzy models was demonstrated, with a significant reduction in the computational burden required to obtain the controller gains, in the time taken to generate the internal architecture of the FPGA, in the number of operations to compute the control law, and in the area of the FPGA circuit. This proves that the use of the N-fuzzy model is more adequate for critical applications in terms of sampling rate, and/or low-powered programming platforms, without compromising the overall performance of the control system.

7 CONCLUSION

In this thesis, novel approaches to control design, applied to nonlinear discrete-time systems by means of T-S fuzzy models have been presented. For fuzzy modeling, an alternative method was proposed based on the use of nonlinear local rules, instead of the classical ones, providing the following benefits: i) it can reduce the number of rules when compared to the classical T-S representation, leading to a lower numerical complexity while maintaining the model exactness; and ii) it allows the design and practical implementation of dynamic output feedback controllers in the presence of unmeasurable nonlinearities. Furthermore, the proposed results consider inherent issues in the control problem, such as the regional validity of the T-S fuzzy models, physical constraints of actuators, and the presence of external signals usually found in real systems. Examples were provided throughout the document, in order to illustrate the proposed techniques.

At first, in Chapter 2, the features and mathematical machinery of T-S fuzzy models were presented. The procedure to obtain an N-fuzzy model for a class of nonlinear systems was described in detail. It is important to remark that the local characteristic of T-S modeling is often not considered in most literature FMB results, which may lead to poor performance or even instability of the closed-loop system. Also, rule reduction, provided by the use of nonlinear local submodels, and its implication in the numerical complexity, were demonstrated, preventing the computational burden from increasing to a point where solvers may fail to solve even simple problems.

Next, in Chapter 3, the synthesis of a fuzzy dynamic output feedback controller was discussed, taking into account the saturation of the actuator and the regional validity of the fuzzy model. An anti-windup gain was considered as an attempt to mitigate the undesired effects of saturation, as well as the use of a performance index based on the λ-contractivity of the level set, associated with the Lyapunov function, in order to ensure a certain rate of temporal convergence of the closed-loop system trajectories.

In Chapters 4 and 5, the control of nonlinear systems subject to external disturbances, bounded in energy and amplitude, respectively, was considered. In the first case, LMI-based conditions and three convex optimization problems were proposed to locally ensure the input-to-state stability in the ℓ_2-sense and a certain input-to-output performance through an upper bound for the system ℓ_2-gain. Otherwise, in the presence of amplitude bounded disturbances, it is not possible to ensure the asymptotic stability of the origin, and in this case the concept of ultimate bounded (UB) stability was considered. Two ellipsoidal sets having different shapes, associated to the set of admissible initial conditions and to the concept of UB stability, were taken into account to handle the control problem. Moreover, the proposed dynamic controller admits the presence of unmeasurable nonlinearities, which is not possible for the classical PDC dynamic controllers.

Later, in Chapter 6, practical aspects of the real implementation of fuzzy controllers were considered. Hardware-in-the-loop simulations were performed, enabling the complexity analysis of the digital implementation of classical and N-fuzzy controllers. Also, an interactive tool aiming to assist students and researchers in the nonlinear control design using fuzzy strategies was presented.

7.1 CONTRIBUTIONS OF THE THESIS

Prior to this document, the contributions of the research throughout this PhD include the following journal articles:

- **Local Stabilization of Nonlinear Discrete-Time Systems Subject to Amplitude Bounded Disturbances**. Klug, M., Castelan, E. B. and Coutinho, D. *in submission process.*

- **T-S Fuzzy Approach to the Local Stabilization of Nonlinear Discrete-Time Systems Subject to Energy-Bounded Disturbances**. Klug, M., Castelan, E. B. and Coutinho, D. *Journal of Control, Automation and Electrical Systems - IJCAES 2015.*

- **Fuzzy Dynamic Output Feedback Control Through Nonlinear Takagi-Sugeno Models**. Klug, M., Castelan, E. B., Leite, V. J. S. and Silva, L. F. P. *Fuzzy Sets and Systems - FSS 2014.*

- **Local Stabilization of Time-Delay Nonlinear Discrete-Time Systems Using Takagi-Sugeno Models and Convex Optimization**. Silva, L. F. P., Leite, V. J. S., Castelan, E. B. and Klug, M. *Mathematical Problems in Engineering - 2014.*

- **Compensadores Dinâmicos para Sistemas Discretos no Tempo com Parâmetros Variantes e Aplicação a um Sis-**

tema Fuzzy Takagi-Sugeno. Klug, M. and Castelan, E. B. *Revista SBA: Controle & Automação - 2012*.

The following papers, published in conference proceedings, were also a part of this research:

- **Interactive Software for Modeling and Control of Nonlinear Systems: A T-S Fuzzy Approach**. Klug, M., Castelan, E. B. and Coutinho, D. *XII Simpósio Brasileiro de Automação Inteligente - SBAI 2015*.

- **Compensadores Dinâmicos para Sistemas Não Lineares Utilizando Modelos Fuzzy T-S: Estudo Comparativo e Implementação HIL**. Klug, M., Castelan, E. B., Coutinho, D. and Silva, L. F. P. *XX Congresso Brasileiro de Automática - CBA 2014*.

- **Local Stabilization of Nonlinear Discrete-Time Systems with Uncertain Time-Delay Using T-S Models**. Silva, L. F. P., Leite, V. J. S., Castelan, E. B., Feng, G. and Klug, M. *XX Congresso Brasileiro de Automática - CBA 2014*.

- **Control of Nonlinear Discrete-Time Systems Subject to ℓ_2-Bounded Disturbances Using Local Nonlinear Fuzzy T-S Models**. Klug, M., Castelan, E. B. and Coutinho, D. *IEEE 52nd Annual Conference on Decision and Control - CDC 2013*.

- **Controle Seguro de Sistemas Não Lineares Utilizando Modelos Híbridos Fuzzy L'ure com Saturação dos Atuadores**. Klug, M., Castelan, E. B. and Silva, L. F. P. *XIX Congresso Brasileiro de Automática - CBA 2012*.

- **Síntese Convexa de Controladores Fuzzy para Sistemas Takagi-Sugeno Discretos no Tempo com Atraso e Limitação nos Estados**. Silva, L. F. P., Leite, V. J. S., Castelan, E. B. and Klug, M. *XIX Congresso Brasileiro de Automática - CBA 2012*.

- **A Dynamic Compensator for Parameter Varying Systems Subject to Actuator Limitations Applied to a T-S Fuzzy System**. Klug, M., Castelan, E. B. and Leite, V. J. S. *Proc. of 18th IFAC World Congress - IFAC 2011*.

- **Redução de Regras e Compensação Robusta para Sistemas Takagi-Sugeno com Utilização de Modelos Não**

Lineares Locais. Klug, M. and Castelan, E. B. *X Simpósio Brasileiro de Automação Inteligente - SBAI 2011.*

Further, all acquired expertise also provided the doctoral student with the opportunity to give a lecture entitled “Control of Nonlinear Systems Using T-S Fuzzy Models: Theory and Implementation”, offered in CBA 2014, as well as invitations to review articles in the following journals: Automatica, Journal of the Franklin Institute, Mathematical Problems in Engineering, IET Control Theory & Applications, International Journal of Adaptative Control and Signal Processing and Neurocomputing; and conferences: IFAC 2011, CBA 2012 and 2014, SBAI 2011 and 2015, and ISIE 2015.

7.2 PERSPECTIVES

Among some possible extensions to the work presented in this thesis, the following research directions can be mentioned:

- Extend the proposed approaches to the application in nonlinear continuous-time systems;
- Investigate the use of N-fuzzy models with non-PDC strategies, suitable for static and dynamic output feedback controllers;
- Consider other typical actuator nonlinearities, such as dead-zone, backlash, hysteresis and relay;
- Analyze the effects of discretization when considering hybrid systems;
- Improve the control algorithms in order to obtain less conservative results regarding the guaranteed domain of stability;
- Apply the concepts and strategies developed to real systems.

REFERENCES

ALATA, M.; DEMIRLI, K.; BULGAK, A. Interpolation behavior of T-S fuzzy controllers. In: *IEEE International Symposium on Intelligent Control*. Cambridge, MA, USA: [s.n.], 1999. p. 359–364.

ANDREA, C. Q.; PINTO, J. O. P.; ASSUNÇÃO, E.; TEIXEIRA, M. C. M. Controle ótimo H_∞ de sistemas não lineares com modelos fuzzy Takagi-Sugeno. *Revista Controle & Automação*, v. 19, n. 3, p. 256–269, 2008.

ARCAK, M.; LARSEN, M.; KOKOTOVIC, P. Circle and Popov criteria as tools for nonlinear feedback designs. *Automatica*, v. 39, p. 643–650, 2003.

ASEMANI, M. H.; MAJD, V. J. A robust H_∞ observer-based controller design for uncertain T–S fuzzy systems with unknown premise variables via LMI. *Fuzzy Sets and Systems*, v. 212, n. 1, p. 21–40, 2013.

BEEK, S.; SHARMA, S. Best practices for FPGA prototyping of Matlab and Simulink algotithms. *Journal of Electronic Engineering*, 2011.

BOYD, S.; GHAOUI, L. E.; FERON, E.; BALAKRISHNAN, V. *Linear Matrix Inequalities in System and Control Theory*. Philadelphia, USA: Society for Industrial and Applied Mathematics, 1994.

CASTELAN, E. B.; LEITE, V. J. S.; MIRANDA, M. F.; MORAES, V. M. Synthesis of Output Feedback Controllers for a Class of Nonlinear Parameter-Varying Discrete-Time Systems Subject to Actuators Limitations. In: *American Control Conference (ACC), 2010*. Baltimore, USA: [s.n.], 2010. p. 4235–4240.

CASTELAN, E. B.; TARBOURIECH, S.; QUEINNEC, I. Control design for a class of nonlinear continuous-time systems. *Automatica*, v. 44, n. 8, p. 2034–2039, 2008.

CHADLI, M.; GUERRA, T. M. LMI Solution for Robust Static Output Feedback Control of Takagi-Sugeno Fuzzy Models. *IEEE Transactions on Fuzzy Systems*, v. 20, n. 6, p. 1160–1165, 2012.

CHANG, X. Robust nonfragile H_∞ filter of fuzzy systems with linear fractional parametric uncertainties. *IEEE Transactions on Fuzzy Systems*, v. 20, n. 6, p. 1001–1011, 2012.

CHANG, X.; YANG, G. Nonfragile H_∞ filter desing for T-S fuzzy systems in standard form. *IEEE Transactions on Industrial Electronics*, v. 61, n. 7, p. 3448–3458, 2014.

DARUICHI, E. R. M. *Modelagem e Controle de Sistemas Fuzzy Takagi-Sugeno*. Tese (Doutorado) — Universidade Estadual Paulista (UNESP) - Faculdade de Engenharia de Ilha Solteira, 2003.

DILDA, V.; JUNGERS, M.; CASTELAN, E. B. Uniform ultimate boundedness analysis and synthesis for linear systems with dead-zone in the actuators. *International Journal of Robust and Nonlinear Control*, doi:10.1002/rnc.3223, 2014.

DONG, J.; WANG, Y.; YANG, G. Control synthesis of continuous-time T-S fuzzy systems with local nonlinear models. *Systems, Man, and Cybernetics, Part B: Cybernetics, IEEE Transactions on*, v. 39, n. 5, p. 1245–1258, October 2009.

DONG, J.; WANG, Y.; YANG, G. Output feedback fuzzy controller design with local nonlinear feedback laws for discrete-time nonlinear systems. *Systems, Man, and Cybernetics, Part B: Cybernetics, IEEE Transactions on*, v. 40, n. 6, p. 1447–1459, December 2010.

DONG, J.; YANG, G. Dynamic output feedback control synthesis for continuous-time T-S fuzzy systems via a switched fuzzy control scheme. *Systems, Man, and Cybernetics, Part B: Cybernetics, IEEE Transactions on*, v. 38, n. 4, p. 1166–1175, August 2008.

FARIA, F. A.; SILVA, G. N.; OLIVEIRA, V. A. Reducing the conservatism of LMI-based stabilization conditions for T-S fuzzy systems using fuzzy Lyapunov functions. *International Journal of Systems Science*, v. 44, n. 10, p. 1956–1969, 2013.

FENG, G. A survey on analysis and design of model-based fuzzy control systems. *Fuzzy Systems, IEEE Transactions on*, v. 14, n. 5, p. 676–697, October 2006.

FENG, G. *Analysis and Synthesis of Fuzzy Control Systems: A Model-Based Approach*. [S.l.]: CRC Press, 2010.

FENG, G.; MA, J. Quadratic stabilization of uncertain discrete-time fuzzy dynamics systems. *IEEE Transaction on Circuits and Systems - I: Fundamental Theory and Applications*, v. 48, n. 11, p. 1337–1344, 2001.

FIGUEREDO, L. F. C.; ISHIHARA, J. Y.; BORGES, G. A.; BAUCHSPIESS, A. Robust H_∞ output tracking control for a class of nonlinear systems with time-varying delays. *Circuits, Systems and Signal Processing*, v. 33, p. 1451–1471, 2014.

GAHINET, P.; NEMIROVSKI, A.; LAUB, A. J.; CHILALI, M. *LMI Control Toolbox for use with Matlab - User Guide*. Natick, MA: The MathWorks Inc, 1995.

GAO, Q.; ZENG, X. J.; FENG, G.; WANG, Y. Universal Fuzzy Models and Universal Fuzzy Controllers Based on Generalized T-S Fuzzy Models. In: *IEEE World Congress on Computational Intelligence, Brisbane, Australia*. [S.l.: s.n.], 2012.

GOLABI, A.; BEHESHTI, M.; ASEMANI, M. H. H_∞ robust fuzzy dynamic observer-based controller for uncertain Takagi-Sugeno fuzzy systems. *IET Control Theory and Applications*, v. 6, n. 10, p. 1434–1444, 2012.

Gomes da Silva Jr., J. M.; TARBOURIECH, S. Anti-windup design with guaranteed regions of stability: an LMI-based approach. *Automatic Control, IEEE Transactions on*, v. 50, n. 1, p. 106–111, January 2005.

GUERRA, T. M.; BERNAL, M.; GUELTON, K.; LABIOD, S. Non-Quadratic Local Stabilization for Continuous-Time Takagi-Sugeno Models. *Fuzzy Sets and Systems*, v. 201, n. 16, p. 40–54, 2012.

GUERRA, T. M.; KERKENI, H.; LAUBER, J.; VERMEIREN, L. An efficient Lyapunov function for discrete T-S models: Observer design. *IEEE Transactions on Fuzzy Systems*, v. 20, n. 1, p. 187–192, 2012.

GUERRA, T.-M.; KRUSZEWSKI, A.; LAUBER, J. Discrete Tagaki-Sugeno models for control: Where are we? *Annual Reviews in Control*, v. 33, n. 1, p. 37–47, 2009.

GUERRA, T. M.; VERMEIREN, L. LMI-based relaxed nonquadratic stabilization conditions for nonlinear systems in the Takagi-Sugeno's form. *Automatica*, v. 40, n. 5, p. 823–829, 2004.

GUPTA, V.; KHARE, K.; SINGH, R. P. Efficient Design and FPGA Implementation of Digital Controller Using Xilinx SysGen. *International Journal of Electronics Engineering*, v. 2, n. 1, p. 99–102, 2010.

GUZMAN, J. L.; ASTRON, K. J.; DORMIDO, S.; HAGGLUND, T.; PIGUET, Y.; BERENGUEL, M. Interactive learning module: Basic modelling and identification concepts. In: *Proceedings of the 17th IFAC World Congress*. [S.l.: s.n.], 2008. p. 14606–14611.

HU, T.; Z., L. Composite quadratic Lyapunov functions for contrained control systems. *Automatic Control, IEEE Transactions on*, v. 48, n. 3, p. 440–450, March 2003.

HU, T.; Z., L.; M., C. B. An analysis and design method for linear systems subject to actuator saturation and disturbance. *Automatica*, v. 38, n. 2, p. 351–359, 2002.

HUANG, S.; HE, X.; ZHANG, N. New results on H_∞ filter design for nonlinear systems with time delay via T-S fuzzy models. *IEEE Transactions on Fuzzy Systems*, v. 19, n. 1, p. 193–199, 2011.

JUNGERS, M.; CASTELAN, E. Gain-sheduled control design for a class of discrete-time nonlinear systems with saturating actuators. *Systems & Control Letters*, v. 60, n. 3, p. 169–173, 2011.

KHALIL, H. K. *Nonlinear Systems*. Third. [S.l.]: Prentice Hall, 2003.

KLUG, M.; CASTELAN, E.; COUTINHO, D. Local stabilization of nonlinear discrete-time systems subject to amplitude bounded disturbances. *Submitted to the International Journal of Systems Science*, 2015.

KLUG, M.; CASTELAN, E.; SILVA, L. F. P. Controle seguro de sistemas não lineares utilizando modelos híbridos Fuzzy L'ure com saturação nos atuadores. In: *Proc. of XIX CBA*. [S.l.: s.n.], 2012. p. 2620–2626.

KLUG, M.; CASTELAN, E. B. Redução de regras e compensação robusta para sistemas Takagi-Sugeno com utilização de modelos não lineares locais. In: *Proc. of X SBAI*. [S.l.: s.n.], 2011.

KLUG, M.; CASTELAN, E. B. Compensadores dinâmicos para sistemas discretos no tempo com parâmetros variantes e aplicação a um sistema fuzzy Takagi-Sugeno. *Revista Controle & Automação*, v. 23, n. 5, p. 517–529, 2012.

KLUG, M.; CASTELAN, E. B.; COUTINHO, D. Control of nonlinear discrete-time systems subject to ℓ_2-bounded disturbances using local nonlinear fuzzy T-S models. In: *52nd IEEE Conference on Decision and Control*. [S.l.: s.n.], 2013.

KLUG, M.; CASTELAN, E. B.; COUTINHO, D. Interactive Software for Modeling and Control of Nonlinear Systems: A T-S Fuzzy Approach. In: *Proc. of XII SBAI*. [S.l.: s.n.], 2015.

KLUG, M.; CASTELAN, E. B.; COUTINHO, D. A T-S fuzzy approach to the local stabilization of nonlinear discrete-time systems subject to energy-bounded disturbances. *Journal of Control, Automation and Electrical Systems*, v. 26, n. 3, p. 191–200, 2015.

KLUG, M.; CASTELAN, E. B.; COUTINHO, D.; SILVA, L. F. P. Compensadores Dinâmicos para Sistemas Não Lineares Utilizando Modelos Fuzzy T-S: Estudo Comparativo e Implementação HIL. In: *Proc. of XX CBA*. [S.l.: s.n.], 2014.

KLUG, M.; CASTELAN, E. B.; LEITE, V. J. S. A dynamic compensator for parameter varying systems subject to actuator limitations applied to a T-S fuzzy system. In: *Proc. of 18th IFAC World Congress*. Milan, Italy: [s.n.], 2011. p. 14495–14500.

KLUG, M.; CASTELAN, E. B.; LEITE, V. J. S.; SILVA, L. F. P. Fuzzy dynamic output feedback control through nonlinear Takagi-Sugeno models. *Fuzzy Sets and Systems*, v. 263, p. 92–111, 2014.

KOSKO, B. *Fuzzy Engineering*. [S.l.]: Prentice Hall, 1997.

LAM, H. K. LMI-based stability analysis for fuzzy-model-based control systems using artificial T-S fuzzy model. *IEEE Transactions on Fuzzy Systems*, v. 19, n. 3, p. 505–513, 2011.

LEE, D. H.; JOO, Y. H.; TAK, M. H. Local H_∞ Control and Invariant Set Analysis for Continuous-Time T–S Fuzzy Systems with Magnitude- and Energy-Bounded Disturbances. In: *Proc. of IEEE International Conference on Fuzzy Systems*. Beijing, China: [s.n.], 2014. p. 1990–1997.

LEEKWIJCK W. V. AMD KERRE, E. Defuzzification: Criteria and classification. *Fuzzy Sets and Systems*, v. 108, n. 2, p. 159–178, 1999.

LEITE, V. J. S.; MONTAGNER, V. F.; OLIVEIRA, P. J.; OLIVEIRA, R. C. L. F.; RAMOS, D. C. W.; PERES, P. L. D. Estabilidade robusta de sistemas lineares através de desigualdades matriciais lineares. *Revista Controle & Automação*, SciELO Brasil, v. 15, p. 24–40, 2004.

LöFBERG, J. YALMIP: A toolbox for modeling and optimization in MATLAB. In: *Proceedings of the CACSD Conference*. Taipei, Taiwan: [s.n.], 2004.

LI, F.; SHI, P.; WU, L.; ZHANG, X. Fuzzy-Model-Based $\mathcal{D}$-Stability and Nonfragile Control for Discrete-Time Descriptor Systems With Multiple Delays. *IEEE Transactions on Fuzzy Systems*, v. 22, n. 4, 2014.

LIBERZON, M. R. Essays on the absolute stability theory. *Automation and Remote Control*, v. 67, n. 10, p. 1610–1644, 2006.

LO, J. C.; LIN, M. L. Robust H_∞ nonlinear control via fuzzy static output feedback. *IEEE Transactions on Circuits and Systems I: Fundamental Theory and Applications*, v. 50, n. 11, p. 1494–1502, 2003.

LOPES, A. B.; FAVARIM, F.; CARATI, E. G. Estruturas Paralelas Baseadas em FPGA para Implementação de Compensadores Seletivos de Harmônicas. In: *Proc. of XX CBAI*. [S.l.: s.n.], 2012. p. 3329–3336.

MAMDANI, E. Application of fuzzy algotithms for control of simple dynamic plant. In: *IEEE Control & Science*. [S.l.: s.n.], 1974. v. 121, n. 12, p. 1585–1588.

MAMDANI, E. Application of Fuzzy Logic to Approximate Reasoning Using Linguistic Synthesis. *IEEE Transactions on Computers*, v. 26, n. 12, p. 1182–1191, 1977.

MAMDANI, E. H.; ASSILIAN, S. An experiment in linguistic synthesis with a fuzzy logic controller. *Int. J. Man-machine Studies*, v. 7, p. 1–13, 1975.

MEYER-BASE, U.; VERA, A.; MEYER-BASE, A.; PATTICHIS, M.; PERRY, R. Discrete Wavelet Transform FPGA Design Using Matlab/Simulink. In: *Proc. of International Society for Optics and Photonics*. [S.l.: s.n.], 2006. v. 6247.

MONTAGNER, V. F.; OLIVEIRA, R. C.; PERES, P. L. D. Relaxações convexas de convergência garantida para o projeto de controladores para sistemas nebulosos de Takagi Sugeno. *Revista Controle & Automação*, v. 21, n. 1, p. 82–95, 2010.

MOZELLI, L. A.; PALHARES, R. M. Less conservative H_∞ fuzzy control for discrete-time Takagi-Sugeno systems. *Mathematical Problems in Engineering*, 2011.

MOZELLI, L. A.; PALHARES, R. M. Stability analysis of linear time-varying systems: improving conditions by adding more information about parameter variation. *Systems & Control Letters*, v. 60, n. 5, p. 338–343, 2011.

NGUYEN, A.; DEQUIDT, A.; DAMBRINE, M. Anti-windup based dynamic output feedback controller design with performance consideration for constrained Takagi-Sugeno systems. *Engineering Applications of Artificial Intelligence*, v. 40, p. 76–83, 2015.

OLIVEIRA, M. Z.; SILVA JUNIOR, J. M. G.; COUTINHO, D.; TARBOURIECH, S. Anti-windup Design for a Class of Multivariable Nonlinear Control Systems: an LMI-based Approach. In: *50th IEEE Conference on Decision and Control, 2011. CDC*. [S.l.: s.n.], 2011. p. 4797–4802.

QIU, J.; FENG, G.; GAO, H. Static-output-feedback H_∞ control of continous-time T-S fuzzy affine systems via piecewise Lyapunov functions. *IEEE Transactions on Fuzzy Systems*, v. 21, n. 2, p. 245–261, 2013.

SCHERER, C.; GAHINET, P.; CHILALI, M. Multiobjective output-feedback control via LMI optimization. *Automatic Control, IEEE Transactions on*, v. 42, n. 7, p. 896–911, July 1997.

SILVA, L. F. P.; LEITE, V. J. S.; CASTELAN, E. B.; KLUG, M. Local Stabilization of Time-Delay Nonlinear Discrete-Time Systems Using Takagi-Sugeno Models and Convex Optimization. *Mathematical Problems in Engineering*, v. 2014, n. 10 pages, 2014.

STURM, J. Using SeDuMi 1.02, a MATLAB toolbox for optimization over symmetric cones. *Optimization Methods and Software*, v. 11-12, p. 625–653, 1999.

SU, X.; SHI, P.; WU, L.; SONG, Y. A novel approach to filter design for T-S fuzzzy discrete-time systems with time-varying delay. *IEEE Transactions on Fuzzy Systems*, v. 20, n. 6, p. 1114–1129, 2012.

TAKAGI, T.; SUGENO, M. Fuzzy identification of systems and its applications to modeling and control. *IEEE Transactions on Systems, Man and Cybernetics*, SMC-15, n. 1, p. 116–132, 1985.

TANAKA, K.; TANAKA, M.; OHTAKE, H.; WANG, H. O. Polynomial fuzzy observer designs: A sum-of-squares approach. *IEEE Transactions on Systems, Man, and Cybernetics*, v. 42, n. 5, p. 1330–1342, 2012.

TANAKA, K.; TANAKA, M.; OHTAKE, H.; WANG, H. O. Shared nonlinear control in wireless-based remote stabilization: A theoretical approach. *IEEE/ASME Transactions on Mechatronics*, v. 17, n. 3, p. 443–453, 2012.

TANAKA, K.; WANG, H. O. *Fuzzy Control Systems Design and Analysis: A Linear Matrix Inequality Approach*. New York, USA: John Wiley & Sons, 2001.

TANIGUCHI, T.; TANAKA, K.; OHTAKE, H.; WANG, H. O. Model construction, rule reduction, and robust compensation for generalized form of Takagi-Sugeno fuzzy systems. *IEEE Transactions on Fuzzy Systems*, v. 9, n. 4, p. 525–538, August 2001.

TARBOURIECH, S.; GARCIA, G.; Gomes da Silva Jr., J. M.; QUEINNEC, I. *Stability and Stabilization of Linear Systems with Saturating Actuators*. [S.l.]: Springer-Verlag London, 2011.

TARBOURIECH, S.; QUEINNEC, I.; ALAMO, T.; FIACCHINI, M.; CAMACHO, T. Ultimate bounded stability and stabilization of linear systems interconnected with generalized saturated functions. *Automatica*, v. 47, n. 1, p. 1473–1481, 2011.

TARBOURIECH, S.; VALMÓRBIDA, G.; GARCIA, G.; BIANNIC, J.-M. Stability and performance analysis for linear systems with actuator and sensor saturations subject to unmodeled dynamics. In: *Proceedings of the* 2008 *American Control Conference*. Seattle, WA, USA: [s.n.], 2008. p. 401–406.

TEIXEIRA, M. C. M.; ZAK, H. Stabilizing controller design for uncertains nonlinear systems using fuzzy models. *IEEE Transactions on Fuzzy Systems*, v. 7, n. 2, p. 133–142, 1999.

TOGNETTI, E. S.; OLIVEIRA, R. C. L. F.; PERES, P. L. D. Selective H_2 and H_∞ stabilization of Takagi-Sugeno fuzzy systems. *IEEE Transactions on Fuzzy Systems*, v. 19, n. 5, p. 890–900, 2011.

TOGNETTI, E. S.; OLIVEIRA, R. C. L. F.; PERES, P. L. D. Reduced-order dynamic output feedback control of continuou-time T-S fuzzy systems. *Fuzzy Sets and Systems*, v. 207, p. 27–44, 2012.

TOGNETTI, E. S.; OLIVEIRA, R. C. L. F.; PERES, P. L. D. LMI Relaxations for H_∞ and H_2 Static Output Feedback of Takagi-Sugeno Continuous-Time Fuzzy Systems. *Journal of Control, Automation and Electrical Systems*, v. 24, p. 33–45, 2013.

TOGNETTI, E. S.; OLIVEIRA, V. A. Fuzzy pole placement based on piecewise Lyapunov functions. *International Journal of Robust and Nonlinear Control*, v. 20, p. 571–578, 2009.

TOH, K. C.; TUTUNCU, R. H.; TODD, M. J. On the implementation of SDPT3 (version 3.1) - a MATLAB software package for Semidefinite-Quadratic-Linear Programming. In: *IEEE International Symposium on CACSD*. [S.l.: s.n.], 2004. p. 290–296.

VIDYASAGAR, M. *Nonlinear Systems Analysis*. Second. [S.l.]: SIAM: Society for Industrial and Applied Mathematics, 2002.

WANG, L. K.; LIU, X. D. Local analysis of continuous-time Takagi–Sugeno fuzzy system with disturbances bounded by magnitude or energy: A Lagrange multiplier method. *Information Sciences*, v. 248, n. 1, p. 89–102, 2013.

WANG, L. K.; PENG, J. L.; LIU, X. D.; ZHANG, H. G. An approach to observer design of continuous-time Takagi–Sugeno fuzzy model with bounded disturbances. *Information Sciences*, v. 324, n. 1, p. 108–125, 2015.

WU, L.; SU, X.; SHI, P.; QIU, J. A new approach to stability analysis and stabilization of discrete-time T-S fuzzy time-varying delay systems. *IEEE Transactions on Systems Man and Cybernetics*, v. 41, n. 1, p. 273–286, 2011.

YANG, Z.; YANG, Y. New delay-dependent stability analysis and synthesis of T-S fuzzy systems with time-varying delay. *International Journal of Robust and Nonlinear Control*, v. 20, p. 313–322, 2012.

YONEYAMA, J. Non-fragile output feedback control design of uncertain Takagi-Sugeno fuzzy systems. In: *53rd IEEE Conference on Decision and Control*. [S.l.: s.n.], 2014. p. 6764–6769.

ZADEH, L. Fuzzy sets. *Information and Control*, v. 8, p. 338–353, 1965.

ZHANG, K.; JIANG, B.; STAROSWIECKI, M. Dynamic output feedbacl fault tolerant controller design for Takagi-Sugeno fuzzy systems with actuators faults. *IEEE Transactions on Fuzzy Systems*, v. 18, n. 1, p. 194–201, 2010.

ZHU, B.; LIU, A.; GU, Y.; ZHANG, Q. Finite-time H_∞ performance analysis for a kind of T-S fuzzy descriptor system with time-Delayelay. In: *27th CCDC*. [S.l.: s.n.], 2015. p. 210–215.

APPENDIX A – Approximate Modeling

A.1 APPROXIMATE T-S FUZZY MODELS

In this appendix, it is presented an approximate modeling method that can be used to obtain a more compact fuzzy representation (with reduced number of rules) at the cost of losing the accuracy of the model. This approach will be described here considering a nonlinear continuous-time system, as originally proposed in the reference Teixeira & Zak (1999), and that can be easily adapted to the discrete-time case.

Let the nonlinear plant given by:

$$\dot{\boldsymbol{x}} = \boldsymbol{f}(\boldsymbol{x}) + \boldsymbol{\mathcal{V}}(\boldsymbol{x})\boldsymbol{u}, \quad \boldsymbol{f}(\boldsymbol{x}) = \left[\begin{array}{ccc} \boldsymbol{f}_{(1)}(\boldsymbol{x}) & \cdots & \boldsymbol{f}_{(n_x)}(\boldsymbol{x}) \end{array}\right]'. \tag{A.1}$$

It is desired to obtain a fuzzy model that approximates the original nonlinear system in a particular region of the state space. To this end, the control designer must define $\boldsymbol{n_r}$ Operation Points (OPs) which will be associated with local submodels. The amount and spatial positioning of these points are based on the physical knowledge of the system dynamics. The objective is that each submodel represents approximately the behavior of the nonlinear plant in the neighborhood of the associated OP.

For the cases where the OP is also an equilibrium point of the system, it is possible to obtain the local submodel using Taylor series. An additional requirement is that the equilibrium occurs for the pair $\{\boldsymbol{x_{eq}}, \boldsymbol{u_{eq}}\} = \{\boldsymbol{0}, \boldsymbol{0}\}$, avoiding a affine term in the submodel equations. For the other cases an alternative approach will be performed, as follows.

Consider $\boldsymbol{x_0}$ an OP that do not correspond to an equilibrium point of the nonlinear system. Thus, the following problem for obtain the submodel is considered:

$$\begin{cases} \boldsymbol{f}(\boldsymbol{x}) + \boldsymbol{\mathcal{V}}(\boldsymbol{x})\boldsymbol{u} \approx \boldsymbol{A}\boldsymbol{x} + \boldsymbol{B}\boldsymbol{u} \text{ for all } \boldsymbol{u},\, \boldsymbol{x} \approx \boldsymbol{x_0} \\ \boldsymbol{f}(\boldsymbol{x_0}) + \boldsymbol{\mathcal{V}}(\boldsymbol{x_0})\boldsymbol{u} = \boldsymbol{A}\boldsymbol{x_0} + \boldsymbol{B}\boldsymbol{u} \text{ for all } \boldsymbol{u},\, \boldsymbol{x} = \boldsymbol{x_0} \end{cases}$$

i.e. the linear local submodel should represent approximately the dynamic behavior of the plant (A.1) for $\boldsymbol{x} \approx \boldsymbol{x_0}$, and exactly for $\boldsymbol{x} = \boldsymbol{x_0}$. The optimal solution for this problem is described in Teixeira & Zak (1999), and can be represented by:

$$\begin{cases} \boldsymbol{B} = \boldsymbol{\mathcal{V}}(\boldsymbol{x_0}) \\ \boldsymbol{A} = \left[\begin{array}{ccc} \boldsymbol{a}_{(1)} & \cdots & \boldsymbol{a}_{(n_x)} \end{array}\right]', \\ \boldsymbol{a}_{(i)} = \nabla \boldsymbol{f}_{(i)}(\boldsymbol{x_0}) + \dfrac{\boldsymbol{f}_{(i)}(\boldsymbol{x_0}) - \boldsymbol{x_0^T} \nabla \boldsymbol{f}_{(i)}(\boldsymbol{x_0})}{\|\boldsymbol{x_0}\|_2^2} \boldsymbol{x_0} \end{cases}, \quad \boldsymbol{x_0} \neq \boldsymbol{0} \tag{A.2}$$

where $\boldsymbol{\nabla f_{(i)}(x)} = \left[\begin{array}{ccc} \boldsymbol{\partial f_{(i)}(x)/\partial x_{(1)}} & \cdots & \boldsymbol{\partial f_{(i)}(x)/\partial x_{(n_x)}} \end{array} \right]'$ and $\boldsymbol{\|x_0\|^2 = x_0' x_0}$. So, the T-S fuzzy model is given by

$$\boldsymbol{\dot{x} = \sum_{i=1}^{n_r} h_{(i)} \left\{ A_i x + B_i u \right\}}$$

with $\boldsymbol{h_{(i)}}, \forall\ \boldsymbol{i = 1, ..n_r}$ being membership functions chosen by the control designer generally with one of the following shapes: triangular, trapezoidal, gaussian or bell, as show in Figure 40.

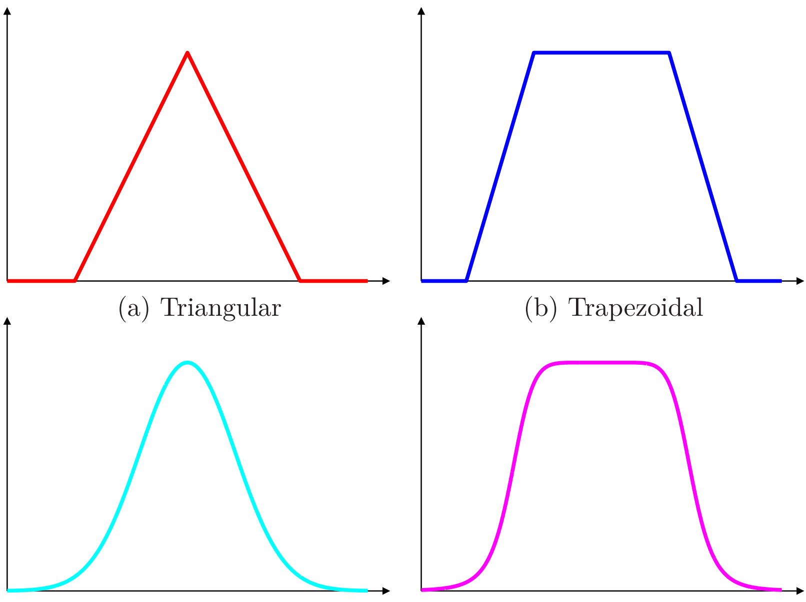

(a) Triangular (b) Trapezoidal

(c) Gaussian (d) Bell

Figure 40 – Typical membership functions

It is interesting to emphasize again, that the optimal local models, for OPs that are not equilibrium points of the systems, cannot be obtained by linearization using Taylor series. This is due to the fact that Taylor linearizes the model in terms of the variations of the variables, and not in their original values, thus yielding an affine model for each OP that is not an equilibrium point.

Example - Approximate T-S Fuzzy Modeling: Consider the problem of balancing an inverted pendulum on a cart represented by (TANAKA; WANG, 2001):

$$\begin{aligned}
\dot{x}_{(1)} &= x_{(2)} \\
\dot{x}_{(2)} &= \frac{\mathfrak{g}\sin(x_{(1)}) - \mathfrak{a}\mathfrak{m}\mathfrak{l}x_{(2)}^2\sin(2x_{(1)})/2 - \mathfrak{a}\cos(x_{(1)})u}{4\mathfrak{l}/3 - \mathfrak{a}\mathfrak{m}\mathfrak{l}\cos^2(x_{(1)})}
\end{aligned}$$

where $x_{(1)}$ denotes the angle (in radians) of the pendulum from the vertical; $x_{(2)}$ is the angular velocity (in radians/s); $\mathfrak{g} = 9.8(m/s^2)$ is the gravity acceleration; $\mathfrak{m}$ is the mass of the pendulum (in kg); M is the mass of the cart (in kg); $2\mathfrak{l}$ is the length of the pendulum (in m); and u is the force applied to the cart (in newtons). It is defined $\mathfrak{a} = 1/(\mathfrak{m} + M)$.

For this example it is considered the following data: $\mathfrak{m} = 2.0kg$, $M = 8.0kg$ and $2\mathfrak{l} = 1.0m$. So, the constant $\mathfrak{a}$ can be computed. Furthermore, it is assumed that the desired interval of operation is about $|x_{(1)}| \leq \pi/3$ and $|x_{(2)}| \leq 1.5$. Then, the OPs are arbitrarily chosen (which will influence the model accuracy by the amount and positioning of the points), as shown in Figure 41.

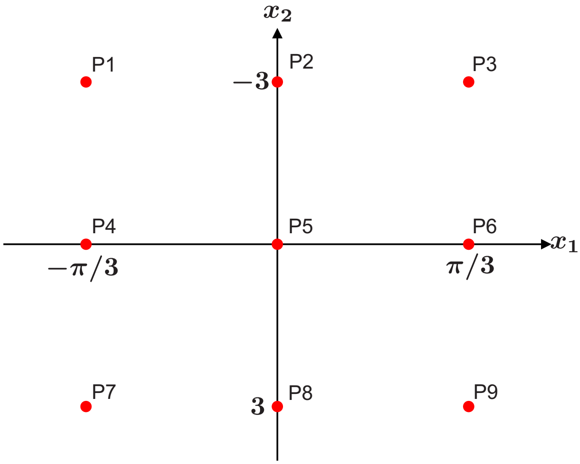

Figure 41 – Operation points

Thus, by applying the equations (A.2), it is computed the T-S fuzzy model as follows

$$\dot{\boldsymbol{x}} = \sum_{i=1}^{9} \boldsymbol{h}_{(i)} \left\{ \boldsymbol{A}_i \boldsymbol{x} + \boldsymbol{B}_i \boldsymbol{u} \right\}$$

where the functions $\boldsymbol{h}_{(i)}$ are chosen with one of the shapes defined in Figure 40, and the matrices that compose the submodels are given by:

$$\boldsymbol{A}_1 = \begin{bmatrix} \mathbf{0} & \mathbf{1} \\ \mathbf{7.3487} & \mathbf{-1.6412} \end{bmatrix}, \quad \boldsymbol{B}_1 = \begin{bmatrix} \mathbf{0} \\ \mathbf{-0.0779} \end{bmatrix},$$

$$\boldsymbol{A}_2 = \begin{bmatrix} \mathbf{0} & \mathbf{1} \\ \mathbf{15.7059} & \mathbf{0} \end{bmatrix}, \quad \boldsymbol{B}_2 = \begin{bmatrix} \mathbf{0} \\ \mathbf{-0.1765} \end{bmatrix},$$

$$\boldsymbol{A}_3 = \begin{bmatrix} \mathbf{0} & \mathbf{1} \\ \mathbf{7.3487} & \mathbf{1.6412} \end{bmatrix}, \quad \boldsymbol{B}_3 = \begin{bmatrix} \mathbf{0} \\ \mathbf{-0.0779} \end{bmatrix},$$

$$\boldsymbol{A}_4 = \begin{bmatrix} \mathbf{0} & \mathbf{1} \\ \mathbf{12.6304} & \mathbf{0} \end{bmatrix}, \quad \boldsymbol{B}_4 = \begin{bmatrix} \mathbf{0} \\ \mathbf{-0.0779} \end{bmatrix},$$

$$\boldsymbol{A}_5 = \begin{bmatrix} \mathbf{0} & \mathbf{1} \\ \mathbf{9.3600} & \mathbf{0} \end{bmatrix}, \quad \boldsymbol{B}_5 = \begin{bmatrix} \mathbf{0} \\ \mathbf{-0.0052} \end{bmatrix},$$

$$\boldsymbol{A}_6 = \begin{bmatrix} \mathbf{0} & \mathbf{1} \\ \mathbf{12.6304} & \mathbf{0} \end{bmatrix}, \quad \boldsymbol{B}_6 = \begin{bmatrix} \mathbf{0} \\ \mathbf{-0.0779} \end{bmatrix},$$

$$\boldsymbol{A}_7 = \begin{bmatrix} \mathbf{0} & \mathbf{1} \\ \mathbf{7.3487} & \mathbf{-1.6412} \end{bmatrix}, \quad \boldsymbol{B}_7 = \begin{bmatrix} \mathbf{0} \\ \mathbf{-0.0779} \end{bmatrix},$$

$$\boldsymbol{A}_8 = \begin{bmatrix} \mathbf{0} & \mathbf{1} \\ \mathbf{15.7059} & \mathbf{0} \end{bmatrix}, \quad \boldsymbol{B}_8 = \begin{bmatrix} \mathbf{0} \\ \mathbf{-0.1765} \end{bmatrix},$$

$$\boldsymbol{A}_9 = \begin{bmatrix} \mathbf{0} & \mathbf{1} \\ \mathbf{7.3487} & \mathbf{-1.6412} \end{bmatrix}, \quad \boldsymbol{B}_9 = \begin{bmatrix} \mathbf{0} \\ \mathbf{-0.0779} \end{bmatrix}.$$

APPENDIX B – Examples of Fuzzy Models

B.1 EXAMPLES OF T-S FUZZY MODELS

In the sequel are presented some examples of nonlinear systems modeled using classical and/or N-fuzzy approaches, as described in subsection 2.2.2, and that will be used in order to demonstrate the performance of the proposed controllers in Chapters **3**, **4** and **5**.

B.2 DYNAMIC SYSTEM 1

Consider the following discrete-time nonlinear system (KLUG; CASTELAN; COUTINHO, 2013):

$$\begin{aligned}
x_{(1)}(k+1) &= -\frac{13}{20}x_{(1)}(k)+\frac{11}{20}x_{(2)}(k)+\frac{9}{40}x^2_{(1)}(k)+\frac{3}{40}x_{(1)}(k)x_{(2)}(k) \\
&\quad +\frac{3}{10}x_{(2)}(k)(1+\sin(x_{(2)}(k))) \\
x_{(2)}(k+1) &= \frac{1}{5}x_{(1)}(k)+\frac{6}{5}x_{(2)}(k)+\frac{1}{5}x^2_{(1)}(k)+\frac{1}{20}x_{(1)}(k)x_{(2)}(k) \\
&\quad +\frac{5}{4}u(k)+\frac{1}{40}x_{(1)}(k)u(k)+\frac{51}{100}w(k)+\frac{39}{400}x_{(1)}(k)w(k) \\
z(k) &= x_{(1)}(k)+\frac{23}{20}u(k)+\frac{7}{40}x_{(1)}(k)u(k)
\end{aligned} \tag{B.1}$$

Assume that the domain of validity $\mathcal{X}$ as given in (2.17) is defined by means of

$$N = \begin{bmatrix} 1 & 0 \\ 0 & 1 \end{bmatrix} \quad \text{and} \quad \phi = \begin{bmatrix} 2 \\ 1.5 \end{bmatrix}.$$

Additionally, defining the premise variable $\nu(k) = x_{(1)}(k)$, and the sector nonlinearity $\varphi(k)=\varphi(Lx(k))=\frac{3}{10}x_{(2)}(k)(1+\sin(x_{(2)}(k)))$, with $L = \begin{bmatrix} 0 & 1 \end{bmatrix}$, the system dynamics in (B.1) can be cast as follows:

$$\begin{aligned}
x(k+1) = {} & \left\{ \begin{bmatrix} -\frac{13}{20} & \frac{11}{20} \\ \frac{1}{5} & \frac{6}{5} \end{bmatrix} + \nu(k) \begin{bmatrix} \frac{9}{40} & \frac{3}{40} \\ \frac{1}{5} & \frac{1}{20} \end{bmatrix} \right\} x(k) + \begin{bmatrix} 1 \\ 0 \end{bmatrix} \varphi(k) \\
& + \left\{ \begin{bmatrix} 0 \\ \frac{5}{4} \end{bmatrix} + \nu(k) \begin{bmatrix} 0 \\ \frac{1}{40} \end{bmatrix} \right\} u(k) + \left\{ \begin{bmatrix} 0 \\ \frac{51}{100} \end{bmatrix} + \nu(k) \begin{bmatrix} 0 \\ \frac{39}{200} \end{bmatrix} \right\} w(k) \\
z(k) = {} & x_{(1)}(k) + \left(\frac{23}{20} + \frac{7}{40}\nu(k) \right) u(k)
\end{aligned} \tag{B.2}$$

where $x(k) = \begin{bmatrix} x_{(1)}(k) & x_{(2)}(k) \end{bmatrix}'$.

Note that the nonlinearity $\varphi(k)$ can be globally encompassed into a sector bounded nonlinearity, i.e., $\varphi(k) \in S[0, 0.7]$, as shown in Figure 42.

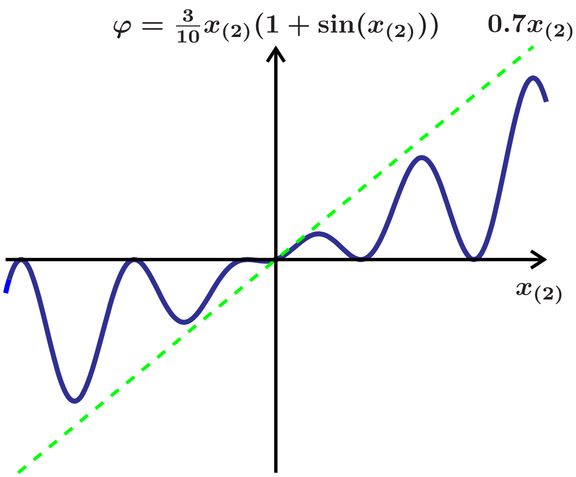

Figure 42 – Global sector for $\varphi = \frac{3}{10}x_{(2)}(1 + \sin(x_{(2)}))$

Also, it can be observed that $\nu(k) \in [d_1, d_2]$, with $d_1 = -2$ and $d_2 = 2$ being the extremum points of $\nu(k)$ for the domain $\mathcal{X}$. Thus, the system in (B.2) can be exactly described by the following N-fuzzy model:

$$
\begin{aligned}
x(k+1) &= \sum_{i=1}^{2} h_{(i)}(k)\{A_i x(k)+B_i u(k)+B_{wi} w(k)+G_i \varphi(k)\}\\
z(k) &= \sum_{i=1}^{2} h_{(i)}(k)\{C_{zi} x(k)+B_{zi} u(k)+B_{zwi} w(k)+G_{zi} \varphi(k)\}
\end{aligned}
\tag{B.3}
$$

with $h_{(1)}(k) = \dfrac{d_2 - \nu(k)}{d_2 - d_1}$, $h_{(2)}(k) = \dfrac{\nu(k) - d_1}{d_2 - d_1}$, and the following system matrices, for $i = 1, 2$:

$$
A_i = \begin{bmatrix} -\frac{13}{20} + \frac{9}{40} d_i & \frac{11}{20} + \frac{3}{40} d_i \\ \frac{1}{5} + \frac{1}{5} d_i & \frac{6}{5} + \frac{1}{20} d_i \end{bmatrix}, \ B_i = \begin{bmatrix} 0 \\ \frac{5}{4} + \frac{1}{40} d_i \end{bmatrix}
$$

$$
B_{wi} = \begin{bmatrix} 0 \\ \frac{51}{100} + \frac{39}{200} d_i \end{bmatrix}, \ G_i = G = \begin{bmatrix} 1 \\ 0 \end{bmatrix}
$$

$$
C_{zi} = C_z = \begin{bmatrix} 1 & 0 \end{bmatrix}, \ B_{zi} = \frac{23}{20} + \frac{7}{40} d_i, \ B_{zwi} = 0 \text{ and } G_{zi} = 0.
$$

B.3 DYNAMIC SYSTEM 2

Consider the control problem of backing-up a truck-trailer as studied in (FENG; MA, 2001; LO; LIN, 2003; KLUG; CASTELAN; COUTINHO, 2015b). The state space representation of the system is described by

$$
\begin{aligned}
x_{(1)}(k+1) &= x_{(1)}(k) - \frac{vT}{\mathcal{L}} \sin(x_{(1)}(k)) + \frac{vT}{l} u(k)\\
x_{(2)}(k+1) &= x_{(2)}(k) + \frac{vT}{\mathcal{L}} \sin(x_{(1)}(k)) + 0.2 w(k)\\
x_{(3)}(k+1) &= x_{(3)}(k) + vT \cos(x_{(1)}(k)) \sin(x_{(2)}(k)\\
&\qquad + \frac{vT}{2\mathcal{L}} \sin(x_{(1)}(k))) + 0.1 w(k)\\
z(k) &= 7 x_{(1)}(k) - vT x_{(2)}(k) + 0.03 x_{(3)}(k) - \frac{vT}{l} u(k)
\end{aligned}
\tag{B.4}
$$

where $x_{(1)}(k)$ represents the angle between the truck and the trailer, $x_{(2)}(k)$ denotes the angle of the trailer, $x_{(3)}(k)$ is the vertical position of the rear, and l and $\mathcal{L}$ represent the length of the vehicle and of the trailer, respectively. T is the sampling time, and v the constant reverse speed. In particular, we consider $l = 2.8m$, $\mathcal{L} = 5.5m$, $v = -1.0m/s$ and $T = 2.0s$. Due to physical limitations and/or to guarantee a safe operation of the system, such as preventing the *jack-knife* effect that occurs when $x_{(1)}(k) = \pm\pi/2$, the considered domain of validity $\mathcal{X}$ in (2.17) is defined as follows (LO; LIN, 2003)

$$N = \begin{bmatrix} 1 & 0 & 0 \\ 0 & 1 & 0 \end{bmatrix} \text{ and } \phi = \begin{bmatrix} \dfrac{\pi}{3} & \dfrac{170\pi}{180} \end{bmatrix}'.$$

Then, by defining the premise variables

$$\nu_{(1)}(k) = \frac{\sin(x_{(1)}(k))}{x_{(1)}(k)},\ \nu_{(2)}(k) = \frac{\cos(x_{(1)}(k))}{x_{(1)}(k)},\ \nu_{(3)}(k) = \frac{\sin(\rho(k))}{\rho(k)},$$

with $\rho = x_{(2)}(k) + \frac{vT}{2\mathcal{L}}\sin(x_{(1)}(k))$, and observing that $\nu_{(1)}(k) \in [b_1, b_2]$, $\nu_{(2)}(k) \in [d_1, d_2]$ and $\nu_{(3)}(k) \in [g_1, g_2]$ for the considered domain $\mathcal{X}$, with $b_1 = 1$, $b_2 = 0.827$, $d_1 = 1$, $d_2 = 0.5$, $g_1 = 1$ and $g_2 = 10^{-2}/\pi$, it is obtained the following classical T-S model of the system (B.4) with eight linear local rules

$$\begin{aligned} x(k+1) &= \sum_{i=1}^{8} h_{(i)}(k)\left(A_i x(k) + B_i u(k) + B_{wi} w(k)\right) \\ z(k) &= C_z x(k) + B_z u(k) + B_{zw} w(k) \end{aligned} \tag{B.5}$$

where

$$A_i = A_{jkl} = \begin{bmatrix} 1 - \dfrac{vT}{\mathcal{L}} b_j & 0 & 0 \\ \dfrac{vT}{\mathcal{L}} b_j & 1 & 0 \\ \dfrac{v^2T^2}{2\mathcal{L}} b_j d_k g_l & vT d_k g_l & 1 \end{bmatrix},$$

$$B_i = B = \begin{bmatrix} \dfrac{vT}{l} \\ 0 \\ 0 \end{bmatrix},\ B_{wi} = B_w = \begin{bmatrix} 0 \\ 0.2 \\ 0.1 \end{bmatrix},$$

$$C_z = \begin{bmatrix} 7 & -2 & 0.03 \end{bmatrix},\ B_z = -\frac{vT}{l},\ \text{and}\ B_{zw} = 0,$$

with $i = l + 2(k-1) + 4(j-1)$, for $j, k, l = \{1, 2\}$. The membership functions $h_{(i)}(k)$, $i = 1, ..., 8$, are the binary product between functions M_j^i, $j = \{1, 2\}$ and $i = \{1, 2, 3\}$, defined as:

$$M_1^1 = \begin{cases} \dfrac{\sin(x_{(1)}(k)) - b_2 x_{(1)}(k)}{x_{(1)}(k)(b_1 - b_2)}, & x_{(1)}(k) \neq 0 \\ 1, & x_{(1)}(k) = 0 \end{cases},\ M_2^1 = 1 - M_1^1,$$

$$M_1^2 = \frac{\cos(x_{(1)}(k)) - d_2}{d_1 - d_2},\ \ M_2^2 = 1 - M_1^2\ \text{ and}$$

$$M_1^3 = \begin{cases} \dfrac{\sin(\rho) - g_2 \rho}{\rho(g_1 - g_2)}, & \rho \neq 0 \\ 1, & \rho = 0 \end{cases},\ M_2^3 = 1 - M_1^3.$$

B.4 DYNAMIC SYSTEM 3

Consider the following discrete-time nonlinear system (KLUG; CASTELAN; COUTINHO, 2015):

$$\begin{aligned} x_{(1)}(k+1) = {} & \frac{3}{10}x_{(1)}(k) - \frac{1}{2}x_{(2)}(k) - \frac{1}{10}x_{(1)}^2(k) + \frac{1}{4}x_{(1)}(k)x_{(2)}(k) \\ & + \frac{3}{10}x_{(2)}(k)(1 + \sin(x_{(2)}(k))) + \frac{7}{10}u(k) + \frac{1}{20}x_{(1)}(k)u(k) \\ & - \frac{1}{2}w_{(1)}(k) - \frac{1}{4}x_{(1)}(k)w_{(1)}(k) - \frac{11}{20}w_{(2)}(k) + \frac{7}{40}x_{(1)}(k)w_{(2)}(k) \\ x_{(2)}(k+1) = {} & \frac{1}{20}x_{(1)}(k) - \frac{3}{10}x_{(2)}(k) + \frac{9}{40}x_{(1)}^2(k) - \frac{1}{10}x_{(1)}(k)x_{(2)}(k) \\ & - \frac{1}{20}u(k) + \frac{1}{40}x_{(1)}(k)u(k) + \frac{9}{10}w_{(1)}(k) + \frac{9}{20}x_{(1)}(k)w_{(1)}(k) \\ & + \frac{1}{20}w_{(2)}(k) + \frac{19}{40}x_{(1)}(k)w_{(2)}(k) \end{aligned} \tag{B.6}$$

Assume that the domain of validity $\mathcal{X}$ as given in (2.17) is defined by means of

$$N = \begin{bmatrix} 1 & 0 \\ 0 & 1 \end{bmatrix}\ \text{ and }\ \phi = \begin{bmatrix} 2 \\ 1.5 \end{bmatrix}.$$

i) Classical T-S Modeling: Defining the premise variables $\nu_{(1)}(k) = x_{(1)}(k)$ and $\nu_{(2)}(k) = \sin x_{(1)}(k)$, the system dynamics in (B.6) can be cast as follows:

$$x(k+1) = \left\{ \begin{bmatrix} -\frac{1}{2} & -\frac{11}{20} \\ \frac{9}{10} & \frac{1}{40} \end{bmatrix} + \nu_{(1)}(k) \begin{bmatrix} -\frac{1}{4} & \frac{7}{40} \\ \frac{9}{20} & \frac{19}{40} \end{bmatrix} \right\} w(k)$$
$$+ \left\{ \begin{bmatrix} \frac{3}{10} & -\frac{1}{5} \\ \frac{1}{20} & -\frac{3}{10} \end{bmatrix} + \nu_{(1)}(k) \begin{bmatrix} -\frac{1}{10} & \frac{1}{4} \\ \frac{9}{40} & -\frac{1}{10} \end{bmatrix} + \nu_{(2)}(k) \begin{bmatrix} 0 & \frac{3}{10} \\ 0 & 0 \end{bmatrix} \right\} x(k)$$
$$+ \left\{ \begin{bmatrix} \frac{7}{10} \\ -\frac{1}{20} \end{bmatrix} + \nu_{(1)}(k) \begin{bmatrix} \frac{1}{20} \\ \frac{1}{40} \end{bmatrix} \right\} u(k). \tag{B.7}$$

where $x(k) = \begin{bmatrix} x_{(1)}(k) & x_{(2)}(k) \end{bmatrix}'$ and $w(k) = \begin{bmatrix} w_{(1)}(k) & w_{(2)}(k) \end{bmatrix}'$.

In the domain $\mathcal{X}$, the maximum and minimum values of the premise variables are such that $\nu_{(1)}(k) \in [d_1, d_2]$, with $d_1 = -2$ and $d_2 = 2$, and $\nu_{(2)}(k) \in [e_1, e_2]$, with $e_1 = -0.998$ and $e_2 = 0.998$. Thus, the system in (B.6) can be exactly described by the following classical T-S fuzzy model:

$$x(k+1) = \sum_{i=1}^{4} h_{k(i)} \left(A_i x(k) + B_i u(k) + B_{wi} w(k) \right) \tag{B.8}$$

where, for $j, l = 1, 2$ and $i = l + 2(j-1)$:

$$A_i = \begin{bmatrix} \frac{3}{10} - \frac{1}{10} d_j & -\frac{1}{5} + \frac{1}{4} d_j + \frac{3}{10} e_l \\ \frac{1}{20} + \frac{9}{40} d_j & -\frac{3}{10} - \frac{1}{10} d_j \end{bmatrix},$$

$$B_i = \begin{bmatrix} \frac{7}{10} + \frac{1}{20} d_j \\ -\frac{1}{20} + \frac{1}{40} d_j \end{bmatrix}, \; B_{wi} = \begin{bmatrix} -\frac{1}{2} - \frac{1}{4} d_j & -\frac{11}{20} + \frac{7}{40} d_j \\ \frac{9}{10} + \frac{9}{20} d_j & \frac{1}{40} + \frac{19}{40} d_j \end{bmatrix}.$$

The membership functions $h_{(i)}(k)$, $i = 1, ..., 4$, are the binary product between functions $\tilde{M}_j^i$, $j = \{1,2\}$ and $i = \{1,2\}$, defined as:

$$\tilde{M}_1^1 = \frac{d_2 - \nu_{(1)}(k)}{d_2 - d_1},\ \tilde{M}_2^1 = \frac{\nu_{(1)}(k) - d_1}{d_2 - d_1},$$
$$\tilde{M}_1^2 = \frac{e_2 - \nu_{(2)}(k)}{e_2 - e_1},\ \tilde{M}_2^2 = \frac{\nu_{(2)}(k) - e_1}{e_2 - e_1}.$$

ii) N-Fuzzy Modeling: Considering the sector nonlinearity $\varphi(k) = \varphi(Lx(k)) = \dfrac{3}{10}x_{(2)}(k)(1+\sin(x_{(2)}(k)))$, and by defining the premisse variable $\nu(k) = x_{(1)}(k)$, the system dynamics in (B.6) can be cast as follows:

$$\begin{aligned} x(k+1) = &\left\{\begin{bmatrix} \frac{3}{10} & -\frac{1}{2} \\ \frac{1}{20} & -\frac{3}{10} \end{bmatrix} + \nu(k)\begin{bmatrix} -\frac{1}{10} & \frac{1}{4} \\ \frac{9}{40} & -\frac{1}{10} \end{bmatrix}\right\} x(k) + \begin{bmatrix} 1 \\ 0 \end{bmatrix} \varphi(k) \\ &+\left\{\begin{bmatrix} -\frac{1}{2} & -\frac{11}{20} \\ \frac{9}{10} & \frac{1}{40} \end{bmatrix} + \nu_{(1)}(k)\begin{bmatrix} -\frac{1}{4} & \frac{7}{40} \\ \frac{9}{20} & \frac{19}{40} \end{bmatrix}\right\} w(k) \\ &+\left\{\begin{bmatrix} \frac{7}{10} \\ -\frac{1}{20} \end{bmatrix} + \nu(k)\begin{bmatrix} \frac{1}{20} \\ \frac{1}{40} \end{bmatrix}\right\} u(k) \end{aligned} \tag{B.9}$$

where $x(k) = \begin{bmatrix} x_{(1)}(k) & x_{(2)}(k) \end{bmatrix}'$ and $w(k) = \begin{bmatrix} w_{(1)}(k) & w_{(2)}(k) \end{bmatrix}'$.

Notice that the nonlinearity $\varphi(k)$ is the same as that presented in the dynamic system 1, therefore it can be globally encompassed into a sector bounded nonlinearity, i.e., $\varphi_k \in S[0, 0.7]$, as well as $\nu(k) \in [d_1, d_2]$, with $d_1 = -2$ and $d_2 = 2$ being the extremum points for $\nu(k)$ in the domain $\mathcal{X}$. Thus, the system in (B.9) can be exactly described by the following N-fuzzy model:

$$x(k+1) = \sum_{i=1}^{2} h_{k(i)} \left(A_i x(k) + B_i u(k) + B_{wi} w(k) + G_i \varphi_k\right) \tag{B.10}$$

where, for $i = 1, 2$:

$$A_i = \begin{bmatrix} \frac{3}{10} - \frac{1}{10}d_i & -\frac{1}{2} + \frac{1}{4}d_j \\ \frac{1}{20} + \frac{9}{40}d_i & -\frac{3}{10} - \frac{1}{10}d_i \end{bmatrix}, G_i = G = \begin{bmatrix} 1 \\ 0 \end{bmatrix},$$

$$B_i = \begin{bmatrix} \frac{7}{10} + \frac{1}{20}d_i \\ -\frac{1}{20} + \frac{1}{40}d_i \end{bmatrix}, B_{wi} = \begin{bmatrix} -\frac{1}{2} - \frac{1}{4}d_i & -\frac{11}{20} + \frac{7}{40}d_i \\ \frac{9}{10} + \frac{9}{20}d_i & \frac{1}{40} + \frac{19}{40}d_i \end{bmatrix},$$

and $h_{(1)}(k) = \dfrac{d_2 - \nu(k)}{d_2 - d_1}$, $h_{(2)}(k) = \dfrac{\nu(k) - d_1}{d_2 - d_1}$.

APPENDIX C – Mesh Transformation

C.1 TRANSFORMATION $\bar{\varphi} \in [\boldsymbol{\Omega_1}, \boldsymbol{\Omega_2}]$ IN $\varphi \in [\mathbf{0}, \boldsymbol{\Omega}]$

This appendix demonstrates a transformation process with sector nonlinearities which is required to compatibilize the representation given in (2.6) with the condition (2.3).

Let $\bar{\varphi}(\boldsymbol{k}) = \bar{\varphi}(\boldsymbol{Lx}(\boldsymbol{k}))$ a vector of nonlinearities belonging to the bounded sector condition $\bar{\varphi}(.) \in [\boldsymbol{\Omega_1}, \boldsymbol{\Omega_2}]$, i.e. for the matrices $\boldsymbol{\Omega_1}$ and $\boldsymbol{\Omega_2}$ the following condition is satisfied

$$[\bar{\varphi}(\boldsymbol{k}) - \boldsymbol{\Omega_1 Lx}(\boldsymbol{k})]^{'} \boldsymbol{\Delta}^{-1} [\bar{\varphi}(\boldsymbol{k}) - \boldsymbol{\Omega_2 Lx}(\boldsymbol{k})] \leq \mathbf{0}, \quad \bar{\varphi}(\mathbf{0}) = \mathbf{0}. \tag{C.1}$$

Defining $\varphi(\boldsymbol{k}) = \bar{\varphi}(\boldsymbol{k}) - \boldsymbol{\Omega_1 Lx}(\boldsymbol{k}) \Rightarrow \bar{\varphi}(\boldsymbol{k}) = \varphi(\boldsymbol{k}) + \boldsymbol{\Omega_1 Lx}(\boldsymbol{k})$ and replacing in (C.1), leads to

$$\varphi^{'}(\boldsymbol{k}) \boldsymbol{\Delta}^{-1} [\varphi(\boldsymbol{k}) - (\boldsymbol{\Omega_2} - \boldsymbol{\Omega_1}) \boldsymbol{Lx}(\boldsymbol{k})] \leq \mathbf{0}.$$

If $\boldsymbol{\Omega} = \boldsymbol{\Omega_2} - \boldsymbol{\Omega_1}$, then the mesh transformation $\bar{\varphi} \in [\boldsymbol{\Omega_1}, \boldsymbol{\Omega_2}]$ in $\varphi \in [\mathbf{0}, \boldsymbol{\Omega}]$ is computed by

$$\begin{cases} \varphi^{'}(\boldsymbol{k}) \boldsymbol{\Delta}^{-1} [\varphi(\boldsymbol{k}) - \boldsymbol{\Omega Lx}(\boldsymbol{k})] \leq \mathbf{0}, \quad \bar{\varphi}(\mathbf{0}) = \mathbf{0}, \\ \boldsymbol{\Omega} = \boldsymbol{\Omega_2} - \boldsymbol{\Omega_1} \quad \text{e} \quad \varphi(\boldsymbol{k}) = \bar{\varphi}(\boldsymbol{k}) - \boldsymbol{\Omega_1 Lx}(\boldsymbol{k}) \end{cases} \tag{C.2}$$

Example 1 - Sector nonlinearity $\bar{\varphi} = \boldsymbol{sin}(\boldsymbol{x})$, $\boldsymbol{L} = \mathbf{1}$: It is possible to verify the for the region $|\boldsymbol{x}| \leq \boldsymbol{d}$, with $\boldsymbol{d} = \mathbf{2\pi/3}$, the nonlinearity is encompassed into the bounded sector

$$\bar{\varphi}(.) \in [\boldsymbol{\Omega_1}, \boldsymbol{\Omega_2}], \quad \boldsymbol{\Omega_1} = \frac{\boldsymbol{sin}(\mathbf{2\pi/3})}{\mathbf{2\pi/3}} \text{ and } \boldsymbol{\Omega_2} = \mathbf{1}.$$

Applying the mesh transformation elucidated in (C.2), it is obtained $\varphi = \boldsymbol{sin}(\boldsymbol{x}) - \dfrac{\boldsymbol{sin}(\mathbf{2\pi/3})}{\mathbf{2\pi/3}} \boldsymbol{x}$, belonging to the bounded sector

$$\varphi(.) \in [\mathbf{0}, \boldsymbol{\Omega}], \quad \boldsymbol{\Omega} = \boldsymbol{\Omega_2} - \boldsymbol{\Omega_1}, \quad \text{for} \quad |\boldsymbol{x}| \leq \boldsymbol{d}.$$

A graphic description of the transformation process can be seen in Figure 43.

Example 2: - Effect upon the system matrices: Let the subsystems described by:

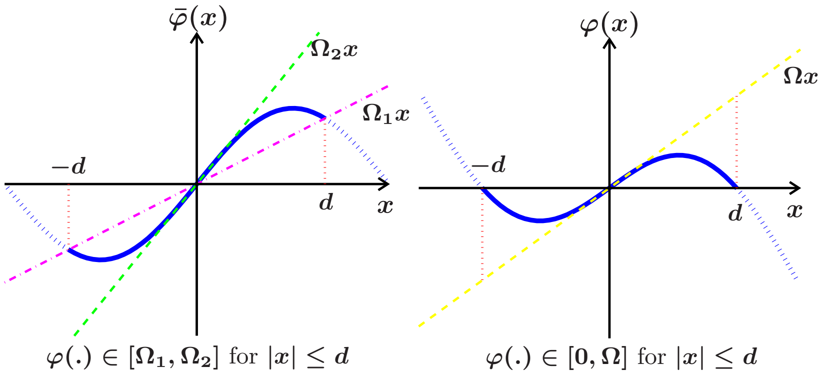

Figure 43 – Mesh transformation

$$\bar{\Sigma}_i = \begin{cases} x(k+1) &= \bar{A}_i x(k) + \bar{B}_i u(k) + \bar{B}_{wi} w(k) + \bar{G}_i \bar{\varphi}(k) \\ y(k) &= \bar{C}_i x(k) \\ & \bar{\varphi}(.) \in [\Omega_1, \Omega_2] \end{cases}$$

Applying the mesh transformation elucidated in (C.2), the modified subsystem is given by

$$\Sigma_i = \begin{cases} x(k+1) &= A_i x(k) + B_i u(k) + B_{wi} w(k) + G_i \varphi(k) \\ y(k) &= C_i x(k) \\ & \varphi(.) \in [0, \Omega] \end{cases}$$

with the new matrices computed as $\Omega = \Omega_2 - \Omega_1$, $\varphi(k) = \bar{\varphi}(k) - \Omega_1 L x(k)$, $A_i = \bar{A}_i + G_i \Omega_1 L$, $B_i = \bar{B}_i$, $B_{wi} = \bar{B}_{wi}$, $G_i = \bar{G}_i$ and $C_i = \bar{C}_i$.

APPENDIX D – Conditions of Literature and Numerical Complexity Analysis

D.1 CONDITIONS OF LITERATURE

In the following, stabilization conditions for nonlinear systems represented by T-S fuzzy models deriving from literature works are presented. The structure of this appendix is as follows: conditions in Sections D.2.1 and D.2.2 deals with state feedback problem and were used to perform a Numerical Complexity Analysis in Section D.2.3, also generating the comparative Tables 6 and 7. Section D.3 deals with the dynamic output feedback problem and their conditions were used in the Illustrative Example 2.3.

D.2 NUMERICAL COMPLEXITY

It is noteworthy that the numerical complexity for the solution of LMI-based optimization problems is related to the number of scalar decision variables, $\mathscr{K}$, and the number of rows, $\mathfrak{L}$, of the considered LMIs. The number of floating point operations (FLOP) or the time required to solve a problem, using interior point methods, is proportional to $\mathscr{K}^3\mathfrak{L}$ (GAHINET et al., 1995; LEITE et al., 2004).

For comparison purposes, the following conditions, associated with literature control laws, are considered:

D.2.1 Adapted conditions of Klug & Castelan (2011)

The results presented below are stabilization conditions based in the work Klug & Castelan (2011). For this case are considered nonlinear systems that can be represented by N-fuzzy models, as described in (2.5). The proposed control law is based on the feedback of states and sector nonlinearities, given by

$$\boldsymbol{u(k) = K(h(k))x(k) + \Gamma(h(k))\varphi(k).} \tag{D.1}$$

It is interesting to note that these conditions effectively do not guarantee the closed-loop stability when applied to the original nonlinear system, since the additional condition that deal with the regional validity issue is not taken into consideration. Such factor is required to exist a fair comparison regarding the techniques from literature.

Proposition 2 in Klug & Castelan (2011) - Adapted: *Given a real scalar* $\boldsymbol{\lambda \in (0,1]}$, *suppose that there exists symmetric positive defi-*

nite matrices $\boldsymbol{Q_i} \in \Re^{n_x \times n_x}$, *a positive diagonal matrix* $\boldsymbol{\Delta} \in \Re^{n_\varphi \times n_\varphi}$ *and matrices* $\boldsymbol{U} \in \Re^{n_x \times n_x}$, $\boldsymbol{Y_{1i}} \in \Re^{n_u \times n_x}$ *and* $\boldsymbol{Y_{2i}} \in \Re^{n_u \times n_\varphi}$, *satisfying the following conditions:*

$$\begin{bmatrix} -Q_j & A_iU + B_iY_{1i} & G_i\Delta + B_iY_{2i} \\ \star & \lambda(Q_i - U - U') & U'\Omega \\ \star & \star & -2\Delta \end{bmatrix} < 0 \tag{D.2}$$
$$\forall\, i, j = 1, \ldots, 2^{n_s - n_\varphi}$$

$$\begin{bmatrix} -2Q_j & \Pi_{i1}^1 & (G_i + G_q)\Delta + B_iY_{2q} + B_qY_{2i} \\ \star & \Pi_{i1}^2 & 2U'\Omega \\ \star & \star & -4\Delta \end{bmatrix} < 0 \tag{D.3}$$
$$\forall\, j = 1, \ldots, 2^{n_s - n_\varphi}, \forall\, i = 1, \ldots, 2^{n_s - n_\varphi} - 1 \;\; \textit{and}$$
$$\forall\, q = i + 1, \ldots, 2^{n_s - n_\varphi}$$

with

$$\Pi_{i1}^1 = (A_i + A_q)U + B_iY_{1q} + B_qY_{1i},$$
$$\Pi_{i1}^2 = \lambda(Q_i + Q_q - 2U - 2U').$$

Then, the controller matrices in (D.1) computed by

$$K_i = Y_{1i}U^{-1} \;\textit{and}\; \Gamma_i = Y_{2i}\Delta^{-1},$$

are such that the origin of the closed-loop system composed by the interconnection of the fuzzy model (2.5) and the controller (D.1) is globally asymptotically stable.

D.2.2 Adapted conditions of Tanaka & Wang (2001)

The results presented below are stabilization conditions based in the work Tanaka & Wang (2001). For this case are considered the nonlinear systems that can be represented by the following T-S fuzzy model

$$\begin{aligned} x(k+1) &= A(h(k))x(k) + B(h(k))u(k) \\ y(k) &= Cx(k) \end{aligned} \tag{D.4}$$

and the control law by states feedback proposed as

$$u(k) = K(h(k))x(k). \tag{D.5}$$

Theorem 8 in Tanaka & Wang (2001) - Adapted: *Given a real scalar* $\boldsymbol{\lambda} \in (\mathbf{0},\mathbf{1}]$, *suppose that there exists symmetric positive definite matrices* $\boldsymbol{Q_i} \in \Re^{n_x \times n_x}$, *and matrices* $\boldsymbol{U} \in \Re^{n_x \times n_x}$ *and* $\boldsymbol{Y_i} \in \Re^{n_u \times n_x}$, *satisfying the following conditions:*

$$\begin{bmatrix} -Q_j & A_iU + B_iY_i \\ \star & \lambda(Q_i - U - U') \end{bmatrix} < 0 \qquad \text{(D.6)}$$
$$\forall\, i, j = 1, \ldots, 2^{n_s}$$

$$\begin{bmatrix} -2Q_j & (A_i + A_q)U + B_iY_q + B_qY_i \\ \star & \lambda(Q_i + Q_q - 2U - 2U') \end{bmatrix} < 0$$
$$\forall\, j = 1, \ldots, 2^{n_s}, \forall\, i = 1, \ldots, 2^{n_s} - 1 \;\; \text{and} \;\; \forall\, q = i+1, \ldots, 2^{n_s} \qquad \text{(D.7)}$$

Then, the controller matrices in (D.5) computed by

$$K_i = Y_{1i}U^{-1}$$

are such that the origin of the closed-loop system composed by the interconnection of the fuzzy model (D.4) and the controller (D.5) is globally asymptotically stable.

D.2.3 Complexity Analysis

Based on the aforementioned conditions, the following cases are considered:

- Case **1**: $\boldsymbol{u(k) = K(h(k))x(k)}$ → Conditions (D.6) and (D.7) → Applied to classical T-S fuzzy models - linear rules;
- Case **2**: $\boldsymbol{u(k) = K(h(k))x(k) + \Gamma(h(k))\varphi(k)}$ → Conditions (D.2) and (D.3) → Applied to N-fuzzy models - nonlinear rules;

It should be highlighted that special precautions should be taken into consideration by control engineers when using the obtained control gains in the original nonlinear system, with the possibility of the loss of performance or even instability, since the regional validity of the T-S fuzzy model was not considered.

Tables 6 and 7 show, respectively, the values of $\mathscr{K}$ and $\mathfrak{L}$ for the Cases **1** and **2**, being $\boldsymbol{n_x}$ the number of states, $\boldsymbol{n_u}$ the number of inputs, $\boldsymbol{n_y}$ the number of outputs, $\boldsymbol{n_s}$ the number of nonlinearities handled in a classical way and $\boldsymbol{n_\varphi}$ the number of nonlinearities handled by sector.

Table 6 – Numerical complexity parameters for Case **1**

Param.:	$u(k) = K(h(k))x(k)$
$\mathscr{K}$	$n_x^2 + 2^{n_s} n_x \left[n_u + \dfrac{n_x + 1}{2} \right]$
$\mathfrak{L}$	$2^{n_s} n_x \left[3(2^{n_s}) - 1 \right]$

Table 7 – Numerical complexity parameters for Case **2**

Param.:	$u(k) = K(h(k))x(k) + \Gamma(h(k))\varphi(k)$
$\mathscr{K}$	$n_x^2 + n_\varphi^2 + 2^{n_s - n_\varphi} \left[n_u(n_x + n_\varphi) + \dfrac{n_x(n_x + 1)}{2} \right]$
$\mathfrak{L}$	$2^{n_s - n_\varphi}(2n_x + n_\varphi) \dfrac{\left[3(2^{n_s - n_\varphi}) - 1\right]}{2}$

Figure 44 shows a graph of the relative complexity, i.e. the ratio $\mathscr{K}^3\mathfrak{L}$ between the Cases **1** and **2**, considering $n_x = 2$, $n_u = 1$, $n_y = 1$ and $n_\varphi = 1, \ldots, 4$. It should be noted that the use of N-Fuzzy

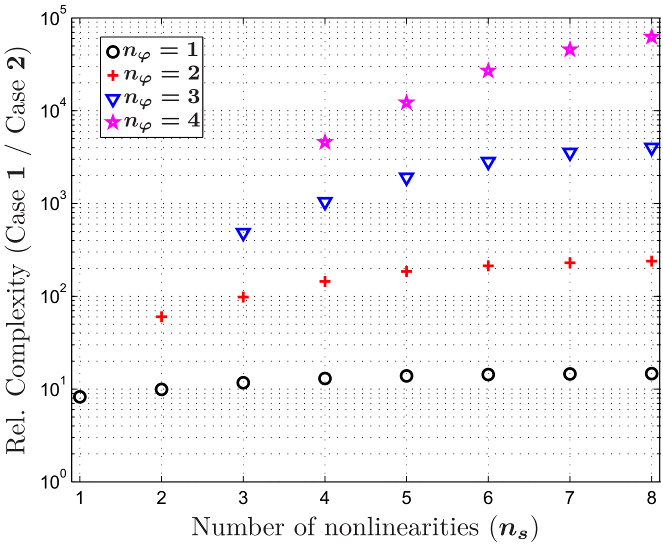

Figure 44 – Comparison of numerical complexity

models (Case **2**) provides a meaningful numerical complexity reduction compared to classical T-S fuzzy models (Case **1**), which becomes more pronounced with an increase in $\boldsymbol{n_{\varphi}}$. This characteristic is explained by the rule reduction provided by the nonlinear approach, dominant over the generation of new decision variables, such as $\boldsymbol{\Delta}$ and $\boldsymbol{Y_{2i}}$.

D.3 ADAPTED CONDITIONS OF FENG (2010)

The results presented below are stabilization conditions based in the work Feng (2010). For comparison purposes, the conditions were adapted to handle with the stabilization problem, considering the following fuzzy representation of the nonlinear system (2.1)

$$\begin{array}{rcl} \boldsymbol{x(k+1)} & = & \boldsymbol{A(h(k))x(k) + B(h(k))u(k)} \\ \boldsymbol{y(k)} & = & \boldsymbol{C(h(k))x(k)} \end{array} \tag{D.8}$$

in which the definition of variables and functions are identical as those established in equation (3.1). The dynamic output feedback controller is defined by

$$\begin{array}{rcl} \boldsymbol{x_c(k+1)} & = & \boldsymbol{\hat{A}(h(k))x_c(k) + \hat{B}(h(k))y(k)} \\ \boldsymbol{u(k)} & = & \boldsymbol{\hat{C}(h(k))x_c(k)} \end{array} \tag{D.9}$$

where it should be emphasized that the matrix structure of $\boldsymbol{A_c(h(k))}$, $\boldsymbol{B_c(h(k))}$ and $\boldsymbol{C_c(h(k))}$ are not the same as in (3.7). The candidate fuzzy Lyapunov function is

$$\boldsymbol{V(\xi(k)) = \xi'(k) \left(\sum_{i=1}^{n_r} h_{(i)}(k) X_i^{-1} \right) \xi(k).} \tag{D.10}$$

Theorem 8.10 in Feng (2010) - Adapted: *The closed-loop system, formed by the T-S fuzzy model (D.8) and the controller (D.9), is globally exponentially stable if exists the positive definite matrices*

$$\boldsymbol{\bar{X}_i = \begin{bmatrix} \bar{X}_{i1} & \star \\ \bar{X}_{i2} & \bar{X}_{i3} \end{bmatrix}, \quad \forall i = 1, ..., n_r,}$$

and matrices $\boldsymbol{G_1}$, $\boldsymbol{U_1}$, $\boldsymbol{M}$, $\boldsymbol{\bar{A}_i}$, $\boldsymbol{\bar{B}_i}$, $\boldsymbol{\bar{C}_i}$, $\forall \boldsymbol{i = 1, ..., n_r}$, *such that the following LMIs are verified:*

$$\begin{bmatrix} \bar{X}_{i1} - G_1 - G_1' & \star & \star & \star \\ \bar{X}_{i2} - M - I & \bar{X}_{i3} - U_1 - U_1' & \star & \star \\ A_i G_1 + B_{1i} \vec{C}_j & A_i & -\bar{X}_{l1} & \star \\ \vec{A}_i & U_1 A_i + \vec{B}_r C_i & -\bar{X}_{l2} & -\bar{X}_{l3} \end{bmatrix} \leq 0$$
$$\forall\ i, j, r, l = 1, ..., n_r$$

Furthermore, the controller gains can be computed by

$$\begin{aligned} \hat{A}(h(k)) &= \Big(\vec{A}(h(k)) - U_1 A(h(k)) G_1 - \vec{B}(h(k)) C(h(k)) G_1 \\ &\quad - U_1 B_1(h(k)) \vec{C}(h(k))\Big) (M - U_1 G_1)^{-1}, \\ \hat{B}(h(k)) &= \vec{B}(h(k)), \\ \hat{C}(h(k)) &= \vec{C}(h(k)) (M - U_1 G_1)^{-1}, \end{aligned}$$

with

$$\left[\vec{A}(h(k))\ \ \vec{B}(h(k))\ \ \vec{C}(h(k))\ \ A(h(k))\ \ B(h(k))\ \ C(h(k))\right] = \sum_{i=1}^{n_r} h_{(i)}(k) \left[\vec{A}_i \quad \vec{B}_i \quad \vec{C}_i \quad A_i \quad B_i \quad C_i\right].$$

Proof *The procedures used for determining the conditions of the above theorem can be found in Chapter* **8** *of the work Feng (2010).*

APPENDIX E – Projections

E.1 PROJECTION OF AN ELLIPSOID

Consider $\boldsymbol{\mathcal{E}(P)}$ a ellipsoid such that $\boldsymbol{\xi}'\boldsymbol{P\xi} \leq \mathbf{1}$, with $\boldsymbol{\xi} = \begin{bmatrix} \boldsymbol{x} \\ \boldsymbol{x_c} \end{bmatrix}$. It is desired to obtain the projection of this ellipsoid over, for example, the subspace of $\boldsymbol{x}$. Thus, for a given $\boldsymbol{\mathcal{E}(P)}$, it has the following decomposition

$$\boldsymbol{P} = \begin{bmatrix} \boldsymbol{P_{11}} & \boldsymbol{P_{12}} \\ \boldsymbol{P_{12}'} & \boldsymbol{P_{22}} \end{bmatrix} > \mathbf{0}$$

and the definition

$$\boldsymbol{\xi} = \begin{bmatrix} \boldsymbol{x} \\ \boldsymbol{x_c} \end{bmatrix} = \begin{bmatrix} \boldsymbol{I} & \mathbf{0} \\ -\boldsymbol{P_{22}^{-1}P_{12}'} & \boldsymbol{I} \end{bmatrix} \begin{bmatrix} \boldsymbol{x} \\ \boldsymbol{\breve{x}_c} \end{bmatrix}.$$

Notice that $\boldsymbol{P_{22}^{-1}}$ exists, because $\boldsymbol{P} > \mathbf{0}$. Hence, $\boldsymbol{\xi}'\boldsymbol{P\xi} \leq \mathbf{1}$ can be rewritten as

$$\begin{bmatrix} \boldsymbol{x}' & \boldsymbol{\breve{x}_c'} \end{bmatrix} \begin{bmatrix} \boldsymbol{I} & -\boldsymbol{P_{12}P_{22}^{-1}} \\ \mathbf{0} & \boldsymbol{I} \end{bmatrix} \begin{bmatrix} \boldsymbol{P_{11}} & \boldsymbol{P_{12}} \\ \boldsymbol{P_{12}'} & \boldsymbol{P_{22}} \end{bmatrix} \begin{bmatrix} \boldsymbol{I} & \mathbf{0} \\ -\boldsymbol{P_{22}^{-1}P_{12}'} & \boldsymbol{I} \end{bmatrix} \begin{bmatrix} \boldsymbol{x} \\ \boldsymbol{\breve{x}_c} \end{bmatrix} \leq \mathbf{1} \Rightarrow$$

$$\begin{bmatrix} \boldsymbol{x}' & \boldsymbol{\breve{x}_c'} \end{bmatrix} \begin{bmatrix} \boldsymbol{P_{11}} - \boldsymbol{P_{12}P_{22}^{-1}P_{12}'} & \mathbf{0} \\ \mathbf{0} & \boldsymbol{P_{22}} \end{bmatrix} \begin{bmatrix} \boldsymbol{x} \\ \boldsymbol{\breve{x}_c} \end{bmatrix} \leq \mathbf{1}. \qquad \text{(E.1)}$$

Since $\boldsymbol{x}$ and $\boldsymbol{\breve{x}_c}$ are decoupled in equation (E.1), the associated projection can be defined by

$$Proj\,[\boldsymbol{\mathcal{E}(P)}]_{\text{over } \boldsymbol{x}} = \left\{ \boldsymbol{x} : \boldsymbol{x}'(\boldsymbol{P_{11}} - \boldsymbol{P_{12}P_{22}^{-1}P_{12}'})\boldsymbol{x} \leq \mathbf{1} \right\}. \qquad \text{(E.2)}$$

In this way, the Schur complement of $\boldsymbol{P}$ in relation to $\boldsymbol{P_{22}}$ provides the orthogonal projection of $\boldsymbol{\mathcal{E}(P)}$ over the portion of space relative to $\boldsymbol{x}$.

Example - Projection of an ellipse: Let the ellipse given by:

$$[\boldsymbol{x} \;\; \boldsymbol{y}]\,\boldsymbol{P}\,[\boldsymbol{x} \;\; \boldsymbol{y}]' \leq \mathbf{1}, \qquad \boldsymbol{P} = \begin{bmatrix} \mathbf{0.3} & -\mathbf{0.4} \\ -\mathbf{0.4} & \mathbf{1} \end{bmatrix}, \qquad \text{(E.3)}$$

to which it is desired to obtain the orthogonal projections over the axes $\boldsymbol{x}$ and $\boldsymbol{y}$. Using the definition in (E.2), the projections are equivalent to:

$$\begin{cases} Proj\,[\text{Ellipse}]_{\text{over } \boldsymbol{x}} & = \left\{\boldsymbol{x} : \boldsymbol{x}^{'}(\boldsymbol{P_{11}} - \boldsymbol{P_{12}}\boldsymbol{P_{22}^{-1}}\boldsymbol{P_{12}^{'}})\boldsymbol{x} \leq \mathbf{1}\right\} \\ & \Rightarrow |\boldsymbol{x}| \leq \mathbf{2.6726} \\ Proj\,[\text{Ellipse}]_{\text{over } \boldsymbol{y}} & = \left\{\boldsymbol{y} : \boldsymbol{y}^{'}(\boldsymbol{P_{22}} - \boldsymbol{P_{12}^{'}}\boldsymbol{P_{11}^{-1}}\boldsymbol{P_{12}})\boldsymbol{y} \leq \mathbf{1}\right\} \\ & \Rightarrow |\boldsymbol{y}| \leq \mathbf{1.4639} \end{cases} \tag{E.4}$$

The graphics of the ellipse (represented by a continuous line) and its projections obtained by (E.4) (where the projections over $\boldsymbol{x}$ and $\boldsymbol{y}$ are represented by a dashed and dashed-dotted lines, respectively) are shown in Figure 45.

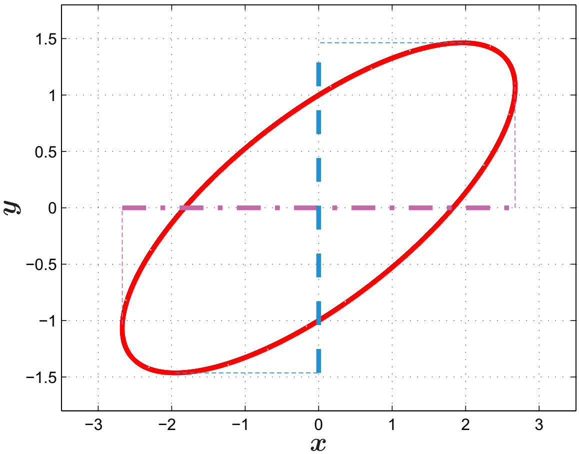

Figure 45 – Projection of an ellipse

Example - Projection of an Ellipsoid: Let the generic ellipsoid $\boldsymbol{\xi}^{'}\boldsymbol{P}\boldsymbol{\xi} \leq \mathbf{1}$, with $\boldsymbol{\xi} \in \Re^{\mathbf{3}}$. The Figure 46 represents the ellipsoid translated from the state space origin (for the sake of better visualization), as well as its projection (green ellipse) over a plane formed by the green and red axes, and the respective intersection over the same plane (red ellipse).

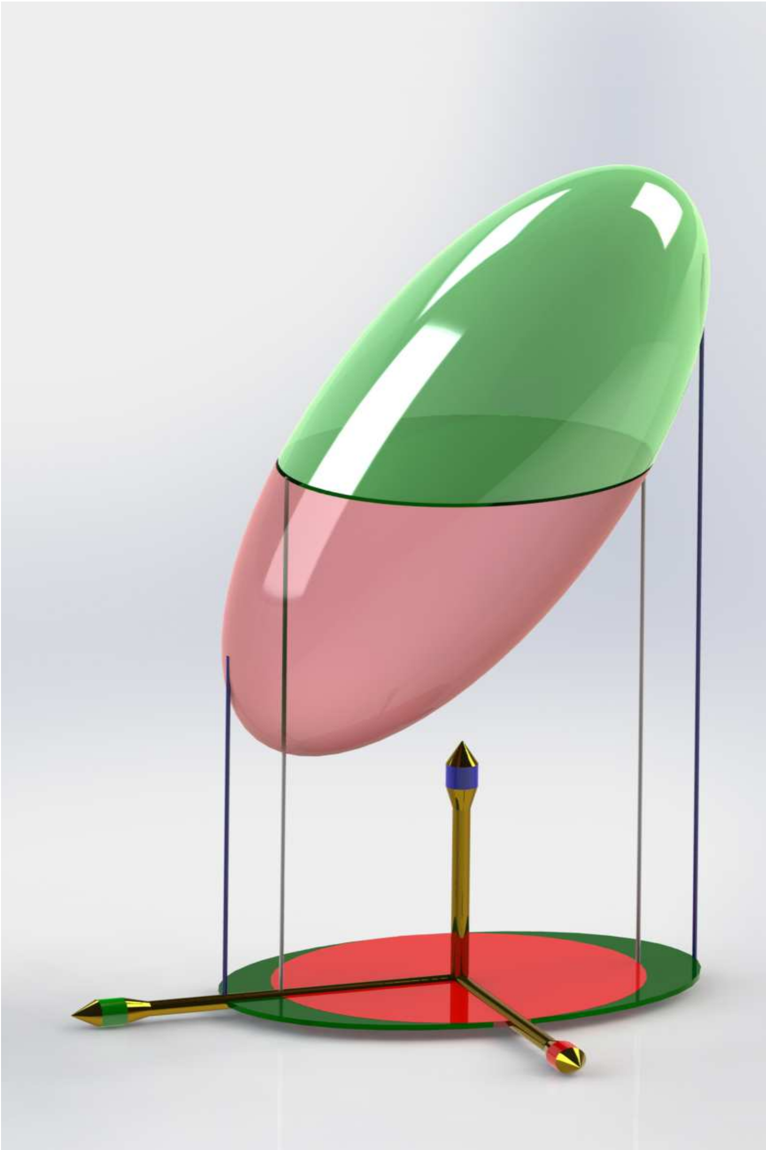

Figure 46 – Projection of an ellipsoid